ABSTRACT

Title of Thesis: OPTIMAL PROPULSION SYSTEM DESIGN FOR A MICRO QUAD ROTOR

Aaron M. Harrington, Masters of Science 2011

Thesis directed by: Professor Inderjit Chopra
Department of Aerospace Engineering

Currently a 50 gram micro quad rotor vehicle is being developed in collaboration with Daedalus Flight Systems. Optimization of the design at this scale requires a systematic study to be carried out to investigate the factors that affect the vehicles performance. Endurance of hovering vehicles at this scale is severely limited by the low efficiencies of their propulsion systems and rotor design and optimization has been performed in the past in an attempt to increase endurance, but proper coupling of the rotor with the motor has been lacking. The current study chose to investigate the factors that had the greatest effect on the vehicle's endurance through analysis of the propulsion system. Therefore, a coupled aerodynamic and structural analysis was carried out that incorporated low Reynolds number airfoil table lookup in order to predict micro rotor performance. A parametric study on rotor design was performed further determine the effect of different rotor designs on hover performance. The experiments performed showed that airfoil camber had the biggest impact on rotor efficiency and other factors such as leading edge shape, number of blades, max camber location, and blade planform taper only had negligible influence on performance. Systematic studies of the interactions between micro rotor blades operating in close proximity to each other were performed in order to

determine the changes in rotor efficiency that might occur in a compact quad rotor design. Tests done on the effect of rotor separation demonstrated that there is a negligible interaction between rotors operating near each other. Brushless motors were also tested systematically and characterized by their torque, rpm, and efficiency. It was found that the maximum efficiency of the motors tested was only 60%, which has significant effects on the efficiency of the coupled system. A method for rotor and motor coupling was also established that utilized the motor efficiency curves and the known torque and rotational speed of the rotors at their operating thrust. Through this, it was found that propulsion system efficiency could be increased by 10% by simply using the proper motor and rotor combination. Further, coupled design would have additional benefits and could increase vehicle efficiency further.

OPTIMAL PROPULSION SYSTEM DESIGN FOR A MICRO QUAD ROTOR

by

Aaron M. Harrington

Thesis submitted to the Faculty of the Graduate School of the
University of Maryland, College Park in partial fulfillment
Of the requirements for the degree of
Master of Science
2011

Advisory Committee:
Professor Inderjit Chopra, Chair/Advisor
Professor James D. Baeder
Professor J. Sean Humbert

Acknowledgement

I would like to sincerely thank everyone that has made this thesis possible. First, I would like to thank Dr. Inderjit Chopra for taking me on as his grad student and guiding me throughout my study. He has always pushed me to work hard and has taught me to go beyond my comfort zone and try new things. Second, I would like to thank Dr. Stephen Wilkerson, Christopher Kroninger, Dr. Mark Bundy, and all of those at the Army Research Laboratory that have helped me in my research and for providing me opportunities to learn though research. Thanks to Paul Samuel for his help and guidance on rotor design and motor characterization. I am sincerely grateful to Dr. V. T. Nagaraj for all the help he has provided me. His door was always open to me and he was my first stop whenever I had a quick question on just about anything. I would also like to thank Dr. James Baeder and Dr. Sean Humbert for serving on my thesis committee.

Additionally, I would like to thank all of the graduate students who I have worked with and have been there to help me answer questions. Sincere thanks to Moble Bennedict for helping me think though problems with research and for helping me edit my thesis. I would also like to thank Cyrus Abdollahi for teaching me the importance of critically reading technical papers and asking tough questions.

Most importantly, the greatest thanks go to my family. My mom, Bonnie Harrington, dad, Michael Harrington, and brother David Harrington, for being there when I thought I might not succeed and helping keep my spirits high. My future wife, Shannon Sullivan, who has also been there listening to me, and encouraging and motivating me. For all of their prayers, encouragement, and love, I would not have been able to do it without them.

Table of Contents

List of Figures

Nomenclature

AR	aspect ratio of the blades, b/c
b	blade span
c	blade chord
C_d	drag coefficient
C_l	lift coefficient
$C_{l\alpha}$	lift curve slope
C_P	power coefficient, $P/\rho A(\Omega R)^3$
C_Q	torque coefficient, $Q/\rho A(\Omega R)^3$
C_T	thrust coefficient, $T/\rho A(\Omega R)^2$
D	diameter
DL	disk loading, T/A
EI	bending stiffness
F	tip loss factor
F_x, F_z	blade chordwise and normal force
FM	figure of merit
GJ	torsional stiffness
H	hermite polynomial
K	stiffness matrix
k_{ij}	elemental stiffness matrix
l	length
M	mass matrix
m_{ij}	elemental mass matrix
N_b	number of blades
Q	torque
R	blade radius
Re	Reynolds number
T	thrust
v	velocity
y	blade radial location

Greek Symbols

α	blade section angle of attack

θ	blade pitch angle
λ	inflow velocity
λ_c	climb inflow velocity
ρ	air density
σ	rotor solidity, $N_b bc/2\pi R$
Ω	rotational speed

Abbreviations

AOA	Angle of Attack
ARL	Army Research Laboratory
BEMT	Blade Element Momentum Theory
BET	Blade Element Theory
CAD	Computer Aided Design
CFD	Computational Fluid Dynamics
CNC	Computer Numerically Controlled
CSD	Computational Structural Dynamics
CTA	Collaborative Technology Alliance
DARPA	Defense Advanced Research Projects Agency
DFS	Daedalus Flight Systems
DoD	Department of Defense
FEA	Finite Element Analysis
FEM	Finite Element Model
GPS	Global Positioning System
LSB	Laminar Separation Bubble
MAST	Micro Autonomous Systems and Technology
MAV	Micro Air Vehicle
PIV	Partical Image Velocimetry
PWM	Pulse Width Modulation
SL	Stereolithography
SLAM	Simultaneous Localization and Mapping
UAV	Unmanned Aerial Vehicle

Chapter 1

1.1 Introduction

Within the past decade, there has been a large growth in the use of unmanned aerial vehicles (UAVs), specifically by the military, which has made them an indispensible tool for soldiers. Many of these UAVs such as the Predator and Global Hawk are as large as manned aircraft and offer a large coverage of the battlefield. UAVs such as the Shadow are smaller and are carried and flown by soldiers on the ground with a minimal interaction with a ground station. However, recently, special interest has been placed on development of even smaller vehicles called micro aerial vehicles (MAVs).

The term MAV has been used earlier to describe vehicles from 20 grams to 20 pounds but in 1997 DARPA created a formal definition that MAVs were aircraft, that would have no dimension larger than 15 cm and weigh less than 100 g [1]. DARPA envisioned that MAVs would be man portable aircraft for the purpose of increasing the soldier's situational awareness while minimizing his/her exposure [2]. MAVs can have many specialized applications that range from surveillance, reconnaissance, search and rescue, and even terrain and environment mapping, and because of their size, can covertly fly into areas that are inaccessible by traditional means of surveillance such as inside of buildings or caves. These vehicles have a small footprint and require little or no infrastructure as they can be piloted by the soldier or flown autonomously. One of the biggest advantages of these small vehicles is their mechanical simplicity, which makes them more robust, useful, and practical.

Table 1.1: Design and performance parameters of various MAV designs [3]

Vehicle Properties	Black Widow (Aerovironment)	Hummingbird (Aerovironment)	Microbat (CalTech)	MICOR (UMD)
GTOW, g	80	19	10.5	103
Cruise Speed, m/s	13.4	5	5	2
Wing span/rotor diameter, cm	15.24	16	15.24	15.24
Endurance, min	30	11	2	10
Power Source	Lithium-ion batteries	Lithium-ion batteries	NiCad N-50 cells	Lithium-ion batteries
Hover Power, W	N/A	Unknown	N/A	11
Hover FM	N/A	Unknown	N/A	0.65

There are many different types of MAVs including fixed wing, rotary wing, and flapping wing. Table 1 shows the design and performance parameters of some of the representative MAV designs. The Aerovironment Black Widow, is an example of a fixed wing MAV weighing 80 grams and having an endurance of 30 minutes [3]. Fixed wing designs are advantageous since they are more efficient (longer endurance), relatively simple, have excellent stability characteristics, can be easily controlled, have higher forward speeds and carry larger payloads. However, fixed wing MAVs, such as BlackWidow, cannot hover and because of their minimum cruise speed, would not be ideally suited for many scenarios, such as indoors. CalTech's flapping wing MAV design, the Microbat, emulates birdlike flight allowing it to fly at much lower speeds with nearly the same wing loading and wing span as the Black Widow but only 13% the weight. However, the Microbat also cannot hover and is highly inefficient with an endurance of only 2 min and therefore could not be used for any practical mission.

Another type of flapping wing MAV is Aerovironment's Nano Hummingbird. This is an example of a flapping wing MAV designed to hover [4]. Hummingbird is a highly advanced design with superior flight stability but requires sophisticated onboard stabilization. The Hummingbird can fly indoors as well as outdoors, but can only handle wind speeds of 5 mph which would be a limitation to outdoor operation on windy or gusty days. Another example of a hover-capable MAV design is the rotary-wing MICOR, developed at UMD [5]. MICOR is a coaxial micro-helicopter designed for hover. Extensive research towards rotor optimization went into this design to increase its hover endurance. However this design is larger than the previously described MAVs with a mass of 103 grams and although it has a highly optimized rotor design, its 10 minute hover endurance is relatively low.

These MAVs are representative of a few of the many configurations. However, rotary wing MAVs tend to be more useful for most of the missions because of their hover and low-speed flight capabilities. The simplest rotary-wing design is the single main rotor with tail rotor configuration or conventional helicopter design, which is essentially a scaled down version of a full scale helicopter. However, these are not always well suited for use as MAVs due to the large power requirements for having a tail rotor that does not contribute to the thrust. Ducted fan designs, however, have been extensively studied where the thrust is augmented by enclosing the rotor in a duct [6]. The duct helps to accelerate the flow causing a region of low pressure along the duct inlet, which results in the duct itself generating a component of the thrust. These designs are advantageous for hover, but are quite sensitive to gust perturbations as the duct can create a high pitching/rolling moment, which makes the vehicle difficult to control. Another feature

that makes ducted rotors unattractive is the large momentum drag experienced in forward flight. A revolutionary cycloidal-rotor (cyclorotor) MAV design utilizes a completely new configuration where the rotational axis is now parallel to the ground and the rotors cyclicly pitch to produce thrust [7]. This new concept has the distinct advantage of thrust vectoring, where the component of thrust can be pointed in any direction providing the vehicle high maneuverability and agility. This MAV design, however, tends to require complex mechanisms and also has a lowered payload capacity. Another type of rotary-wing MAV that has been the subject of much research recently, is the quad rotor helicopter. Quad rotors offer a wide range of benefits as these vehicles have large operational envelopes, having both high agility and thrust to weight ratios as well as superior flight stability [8]. Most of the previous studies on quad rotors also place high emphasis on dynamics and controls. Quad rotors are inherently neutrally stable and the small quad rotors tend to have very fast dynamics that can make them difficult to control. Therefore, many studies focus on accurate dynamics modeling so that better control schemes can be implemented [9].

1.2 Technical Challenges

The proposed missions for MAVs lead to tight constraints being placed upon their design. In order to effectively perform these missions, emphasis has been placed on the compactness of these vehicles, and there has been always a drive for them to be smaller, lighter, and with longer endurance. These objectives can become difficult to achieve simultaneously as important components such as batteries, motors, and rotors are

constrained by their size, weight, capabilities, and efficiency. Therefore, most of these challenges center on issues related to power storage, propulsion system design, aerodynamics, and stability and control. Each of these different MAV configurations discussed in the previous section has numerous technical barriers that needs to be overcome.

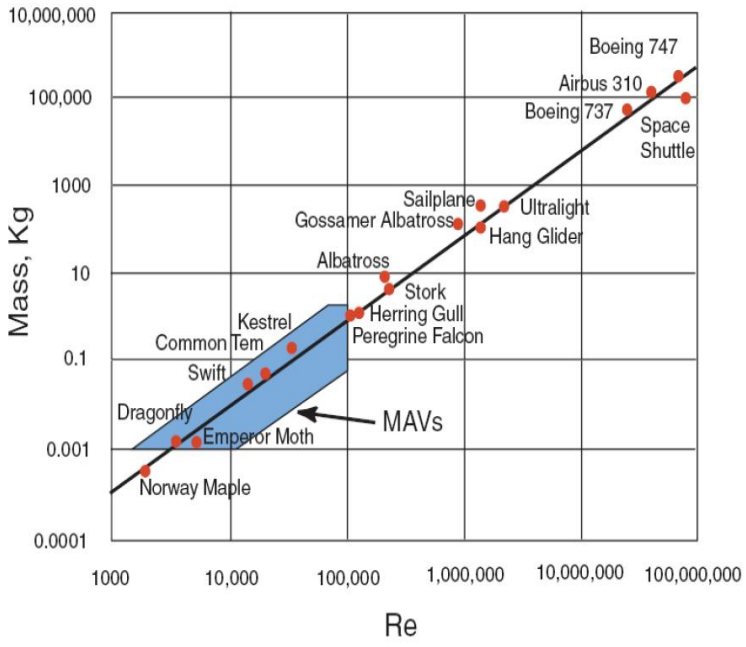

Figure 1.1: Vehicle size showing mass versus Reynolds number [2]

The biggest challenge facing MAV designs, therefore, pertains to their aerodynamics. As the size of these vehicles decreases, the Reynolds numbers at which they operate also becomes low (see Figure 1.1). Reynolds number is the ratio of inertia forces to viscous forces and is given by the relation:

$$Re = \frac{\rho v c}{\mu}$$

where the ρ is the air density, v is the flow velocity, c is the characteristic length, and μ is the dynamic viscosity. The Reynolds number is often used in fluid dynamics as a non-dimensional parameter to describe the flow regime. At high Reynolds number, the inertial forces dominate, while at low Reynolds numbers, the flow is more affected by the viscous forces. Large transport category aircrafts operate at Reynolds numbers in millions while MAVs operate in a regime two or three orders of magnitude lower (10,000 – 70,000). There have been many interesting discoveries as to the aerodynamic behavior of wings and rotors at these low Reynolds numbers specifically in the region in which MAVs operate. This is mainly due to the flow being dominated by viscous effects making the flow highly sensitive to pressure gradients. This flow regime is also characterized by larger regions of laminar flow which results in an increase in skin friction drag and can also result in boundary layer thickening and the formation of laminar separation bubbles, that can lead to flow separation. Therefore, thin airfoils such as flat plate and circular arc airfoils tend to have better performance than conventional airfoil designs used at higher Reynolds numbers.

One of the earliest studies on low Reynolds number aerodynamics was done by Schmitz in 1941 [10]. Schmitz conducted wind tunnel tests on airfoils of model airplanes, sailplanes, and birds at Reynolds numbers between 20,000 and 170,000. He found that flow around airfoils at Reynolds numbers below 100,000 exhibited very poor lift-to-drag ratios as a result of laminar boundary layers and laminar separation which resulted in increases in drag. Schmitz distinguished his tests as being in two regimes he called “subcritical” and “supercritical” as he noticed a sharp decrease in airfoil lift-to-drag ratios at Reynolds numbers below 70,000. He characterized the subcritical region as having a

high sensitivity to Reynolds number as viscous forces became highly dominant. He demonstrated his finding though experiments on a sphere were the subcritical flow would cause separation ahead of the sphere's equator and the supercritical flow would separate behind the equator.

Schmitz also found that airfoil leading edges played a crucial role in the sensitivity of the airfoil to low Reynolds number flows. He determined that rounded leading edges experienced a higher sensitivity to low Reynolds numbers as the boundary layer would separate from the surface of the airfoil much earlier than "sharp-nosed" airfoils. A sharp leading edge creates a series of leading edge vortices. These vortices roll along the top surface of the airfoil and keep the boundary layer energized helping it to stay close to the upper surface. A blunt leading edge can cause the flow to separate at the leading edge and results in higher drag, thus increasing the rotor's power requirements.

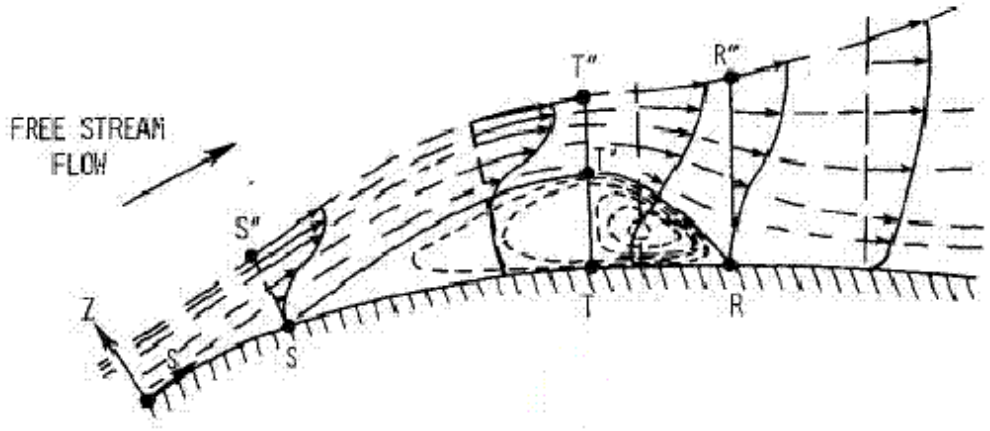

Figure 1.2: Formation of a laminar separation bubble [10]

A laminar separation bubble (Figure 1.2) is formed when the boundary layer meets an adverse pressure gradient which is caused by the lowering of the pressure on the upper surface of the airfoil which produces lift. This suction on the upper surface causes the boundary layer to separate and change from laminar to turbulent in a region known as the transition region. The turbulent boundary layer, when fully developed then re-attaches to the airfoil. The region between where the boundary layer separates and reattaches is referred to as a laminar separation bubble. Boundary layers on low Reynolds number airfoils are therefore very sensitive to perturbations and can easily be caused to separate. Schmitz found the airfoil's sensitivity to Reynolds number could be reduced through artificial creation of turbulence by sharpening the airfoil leading edge, roughing the leading edge, "tripping" it with a thin wire, or though noise excitation. Schmitz's experiments provided great insight into low Reynolds number flows for the first time. However, the accuracy of some of these experiments at Reynolds numbers below 70,000 was brought into question by Laitone.

Studies correlated by Laitone on airfoils operating at Reynolds numbers below 70,000 attempted to provided more accurate data on low Reynolds number flows [11]. His experiments provide lift and drag measurements for a NACA0012 airfoil and compared them to measurements of flat and cambered plate airfoils. The study found that traditional airfoil shapes such as the NACA0012 had relatively poor performance compared to circular arc (cambered plate) profiles with sharp LE, as seen in Figure 1.3. Laminar flow was found to be the reason why low Reynolds number airfoils are plagued with relatively low maximum lift coefficients, rounded lift and moment curves, and lower lift to drag ratios. A 5% cambered plate airfoil had the best performance and the flat plate airfoil

even had a 10% greater lift-to-drag ratio over the NACA 0012 profile. Laitone confirmed Schmitz's findings by demonstrating that laminar separation was a big issue and airfoil leading edges played a significant role in the sensitivity to the flow. He identified that the sharp leading edge created a series of small leading edge vortices that would roll along the surface of the airfoil, helping to keep the flow from separating. He also found that turbulence in the flow greatly reduced the lift-to-drag ratio of the NACA 0012 profile but did not significantly affect the cambered or flat plate airfoils. Aerodynamics of low Reynolds number airfoils (below 70,000) has also been extensively modeled using Computational Fluid Dynamics (CFD) techniques and some studies have incorporated these results into small-scale rotor design and optimization [12].

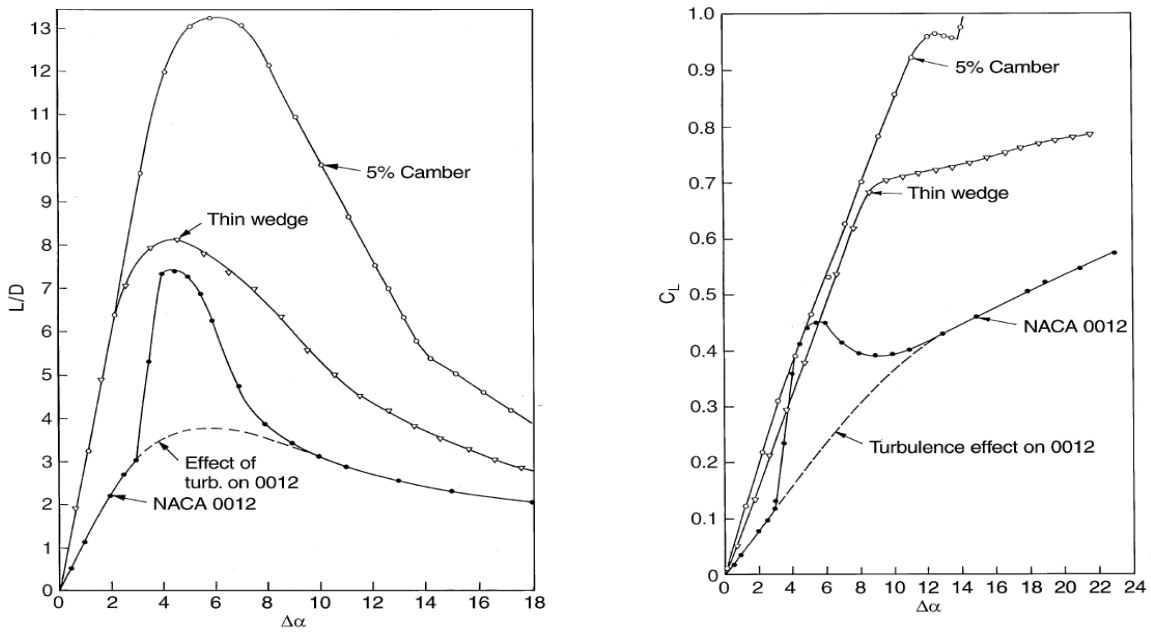

Figure 1.3: a) Lift-to-drag ratio and b) lift coefficient versus angle of attack for 5% cambered circular arc, thin wedge (flat plate), and NACA 0012 airfoils [11]

Because of these reasons, propulsion system design is extremely challenging at the low Reynolds environments in which these vehicles operate. Propulsion system design focuses mainly on rotor design and optimization in an attempt to increase payload, endurance, and/or maneuverability. Bohorquez did a comprehensive experimental study of isolated rotors having representative MAV-scale Reynolds numbers around 60,000 [12]. Bohorquez also used CFD to obtain 2D airfoil tables at low Reynolds numbers to be used in a Blade Element Momentum Theory (BEMT) analysis to predict the performance of micro rotors. He then used this analysis as an optimization tool to determine the best rotor plan form and twist distribution for a microrotor to be used on a micro coaxial helicopter. He found that the rotor efficiency is largely determined by the airfoil characteristics, including the magnitude and location of camber, thickness ratio, leading edge shape, and also the taper ratio of the blade planform. Figure 1.4 shows the lift and drag characteristics of circular arc airfoils with different amounts of camber.

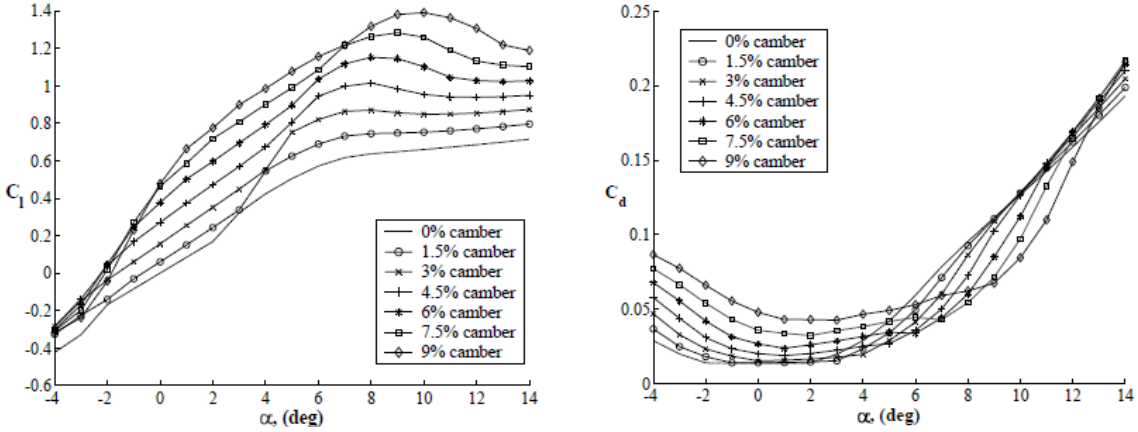

Figure 1.4: Lift and drag coefficients for various circular arc airfoils with different amounts of camber [12].

The rotors exhibiting the best performance generally utilized circular arc airfoils with camber between 6% and 9%. Bohorquez also found that a modest taper ratio of 2:1 starting at 80% of the radius generally increased the figure of merit of the rotors by reducing the induced and profile power. Also, it was suggested that figure of merit is not the best measure of the rotor's performance as the goal is to minimize the power and thus power loading (thrust/power) should be used as the design driver. The analysis was validated by the experimental data, showing that BEMT was a reliable method for predicting rotor performance as long as accurate airfoil tables were used for the table lookup portion of the analysis. Bohorquez's rotors had the capability to change pitch and, therefore, all the rotors were tested at different angles of attack. The goal of his research was to develop efficient rotors for a coaxial helicopter configuration that used collective and cyclic pitch of the lower rotor for control.

Bohorquez also suggested that the combined motor-rotor performance was as important as rotor performance alone and he developed a method for measuring motor performance using an eddy current brake. However, calibration, verification, and validation of his method were lacking and the results of his motor tests were limited.

Another key area of research focuses on new methods of navigation, sensing, and control. Accurate modeling of vehicle dynamics is essential for designing stability augmenting control algorithms. The dynamics often includes linear system models of the motor dynamics and some include rotor dynamics as well. The state space models are often used in conjunction with system identification techniques [13]. Some of these vehicles will be operated in GPS denied environments and in areas where the terrain and obstacles are unknown. These MAVs often lack human in-the-loop control and, therefore, must

navigate on their own. Vision based methods of sensing such as optic flow and navigation techniques that require simultaneous localization and mapping (SLAM) are popular topics in the research community [14]. As far as quad rotors are concerned, most of the research effort has gone into dynamics, controls, sensing, and navigation; therefore, the key design aspects such as aerodynamic performance and propulsion system design have not been thoroughly studied. However, because of the low Reynolds numbers at which these vehicles operate, their aerodynamic efficiency can be a key design driver because it directly affects the vehicle endurance, which has become the key limiting factor in their ability to effectively carry realistic missions.

1.3 Motivation and Goals

The Objective of the Army's Micro Autonomous Systems and Technology (MAST) Collaborative Technology Alliance (CTA) is to enhance the situational awareness of the soldier in urban and complex environments [15]. This is accomplished by the use of autonomous operation of mobile Microsystems, which are defined as being on a scale of 30 cm in length or less and weighing less than 500 grams. Therefore, a 50 gram micro quad rotor vehicle is being developed in collaboration with Daedalus Flight Systems [16] to meet requirements set forth by the Army. The vehicle under investigation was designed to be extremely small and lightweight so that it can be operated in constrained environments and indoors. Specifically, the primary constraint placed on the current design is that the platform must fit within a 150 mm by 150 mm (6 in by 6 in) square box, including the rotors (Figure 1.5).

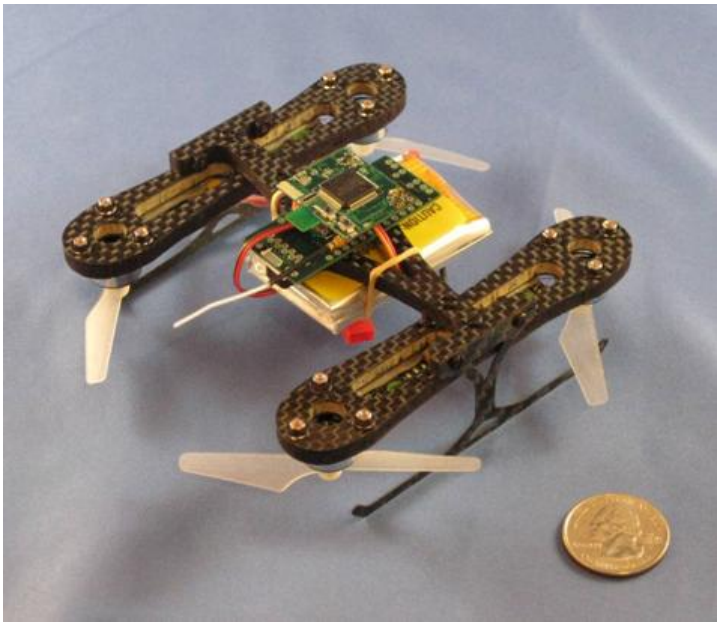

Figure 1.5: DFS/UMD Micro Quad

Three operational scenarios have been proposed for an MAV, which include operations in an urban dwelling, in a collapsed building or cave, and in a perimeter defense of environment. These scenarios present a unique set of challenges that must be overcome. In particular this needs a vehicle that can precisely maneuver autonomously and have a long endurance. Advances in remote sensing with and without GPS are now allowing these vehicles to navigate in these environments successfully. However, a major hurdle that needs to be overcome is the endurance of these small platforms. Lithium polymer batteries are providing lightweight power sources for these vehicles, but the limitations of the propulsion system are the primary drivers affecting endurance.

As discussed in the previous section, most of the studies on quad rotors have been focused on the control and dynamics and not on the efficiency of the vehicle itself. The goal of the present study is to improve the overall efficiency of the micro quad rotor design by systematically investigating the performance affecting the efficiency of the two

key systems that forms the heart of the vehicle – the motor and the rotor. This coupled rotor-motor design is the unique difference between the present study and all the previous research, which only focused on rotor aerodynamic design and not on the propulsion system as a whole. The previous studies on rotor design provide a strong starting point for the current study and examining the efficiency of the electric brushless motors will be shown to be as important as investigative studies related to rotor design.

The current analysis examines the problems associated with using small brushless motors at this scale and focuses on the reasons why these motors have low efficiencies, and what design features are desired when choosing motors for a vehicle of this size. It is difficult to design highly efficient micro motors and therefore designing custom motors does not provide a beneficial, economical, or practical solution to the problem. However, through understanding what motor parameters, such as number of magnets, coils, winding style, etc, affect torque, speed, and power, proper motor selection can be performed so that the motors are operating at their peak efficiency for the particular rotors being used on the vehicle.

The current study chooses to use brushless outrunner direct drive motors. Brushless motors are more efficient and supply higher torque than brushed motors of the same size. However, their efficiency, the ratio of the mechanical power output by the motor to the electrical power input, is highly dependent upon their operating conditions [17]. This is what makes proper motor and rotor coupled design difficult, as the brushless motors are more efficient at higher rpm and the rotors may be more efficient when running at lower rpm. Use of a gearbox can help both motor and rotor to operate at their optimum rpm, however, gearboxes are noisy, add weight, introduce losses, and greatly increase

complexity. The quad rotor would need a separate gearbox for each rotor and gearboxes would introduce complexity into the propulsion system where significant power could be wasted. Due to these added factors, the use of a gearbox was eliminated as a viable option for the design of the micro quad rotor.

Proper selection of rotors for the vehicle is also a primary concern because there is few off-the-shelf rotors exist at the desired size (3 inch diameter) as well as a lack of both right-handed and left-handed rotors which are required by the quad rotor. Therefore, specific rotors must be designed.

The current study's main focus is to determine the parameters that go into proper motor and rotor coupling in an effort to increase the quad rotor's propulsive efficiency. As part of this study, there are four main goals:

1. Determine the most efficient, fixed pitch rotor design in terms of power loading (thrust/power) to minimize the power per unit thrust.
2. Examine how rotor spacing affects rotor performance and determine the optimal rotor spacing, if any, to provide the greatest benefits in thrust and power.
3. Characterize the efficiency of the micro brushless motors and determine the driving factors that influence motor efficiency.
4. Develop a method to determine the proper rotor selection for use on different types of brushless motors.

This thesis will detail the design and analysis of the micro quad rotor propulsion system and develop a methodology for proper rotor/motor coupling. In Chapter 2, the quad rotor

design and fabrication will be discussed. This chapter will give an overview of the quad rotor design and include details as to the method used for control. It will also detail the basic design of the propulsion system and discuss the aspects of brushless motor design and control through pulse width modulation. Design of micro rotors will also be described and the problems relating to low Reynolds number effects and how they affect the design will be discussed. The method used for blade fabrication will also be detailed in Chapter 2. In Chapter 3, the method used for analysis of the micro-rotors will be discussed. A modified blade element code that incorporated flexibility through a beam based finite element analysis as well as Reynolds tabulated airfoil table lookup was used for initial rotor design. Validation of the analysis will be discussed as well as the applicability and limitations of the analysis. Experiments conducted on the rotors and motors will be the focus of Chapter 4. This chapter will cover the experimental setup used and will include a brief study of different rotor designs and will also cover experiments done on rotor blade separation and its effect on propulsive efficiency. Experiments done on brushless motors will also be presented and there will be a discussion on the factors that affect motor efficiency. Finally, couple rotor/motor tests will be presented to show how propulsion system efficiency as a whole is affected by the selection of the rotor for a particular motor. In conclusion, Chapter 5 will give a summary of the topics covered, the conclusions found, and areas of research that are open for future work.

Chapter 2

Quad Rotor Design and Fabrication

2.1 Introduction

In this chapter, the different aspects of the quad rotor's design will be introduced and discussed. This will include the methods used for control of the vehicle and the role of the propulsion system for both hover and maneuvering flight. The theory and design of brushless DC motors and the factors that affect torque, rpm, power, and efficiency will be presented. The method for manufacture of the rotors will also be discussed. A description of the problems associated with rotor design including an explanation of the effects of low Reynolds number flows on micro rotors will also be discussed.

2.2 Vehicle Configuration

For the types of missions desired by the Army, the quad rotor platform offers the widest operational envelope. As with any design, there are inherent advantages and disadvantages that must be carefully considered. For the quad rotor configuration, the increased number of motors is a significant contributor to the vehicle's low endurance as each rotor must now power its own rotor. However, the quad rotor offers many more advantages than other designs, which helps offset its inherently low endurance. Quad rotor designs generally have a higher payload capability, greater maneuverability, and better handling in gusty environments which also stems from the use of four rotors .

The quad rotor under investigation was designed to be extremely small and lightweight since it has to maneuver in confined environments and indoors [18,19]. Specifically, the primary constraint placed on the design is that the planform must fit within a 15 cm by 15 cm (6 in by 6 in) square, including the rotors. The overall dimensions of the quad rotor are shown in figure 1. Hence, an initial rotor diameter of 70 mm was selected to provide some tip clearance between each rotor, and the primary frame design specification was defined to provide an 80 mm ceter-to-center rotor separation.

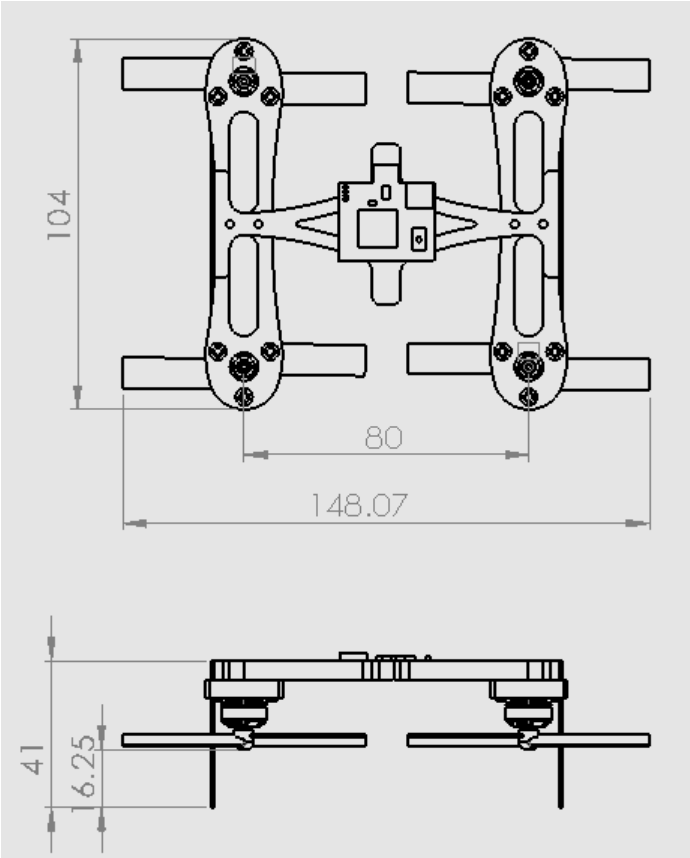

Figure 2.1: General Dimensions of DFS/UMD Microquad v3

Based on these constraints, vehicle components including brushless motors and electronic speed controllers (ESCs) were selected. For an inherently unstable platform such as a

quadrotor helicopter, an active control algorithm must be implemented. Thus, in addition to ESCs, the electronics must include a 3 axis gyro, and a processor to enable implementation of the attitude control algorithms onboard. Finally, wireless communication is required. For the micro quad rotor helicopter under consideration, the GINA Mote, an open source wireless sensor board developed at the University of California, Berkeley, was selected as the primary electronics board [20]. This board includes wireless 802.15.4 communication, an MSP430 processor, 3 gyros and 3 accelerometers.

Table 2.1: Mass Breakdown of the DFS/UMD Microquad v3

Component	Qty	Unit Mass (grams)	Total Mass (grams)
Airframe	1	12	12
Motor	4	3.15	12.6
Motor Mount Hardware	4	1	4
ESC	4	2	8
Breakout Board	1	1.65	1.65
Mote	1	1.8	1.8
Misc wiring	1	2.15	2.15
Vicon Dot	4	0.6	2.4
Vicon Dot Mount	4	0.4	1.6
Rotor	4	0.45	1.8
Landing Gear	2	0.6	1.2
Battery (350mAh)	1	10.4	10.4
Empty Mass (w/o Battery)			49.2
Total Vehicle Mass			59.6

Once the components were specified, the frame was designed. The frame is constructed out of a light-weight carbon-fiber/balsa sandwich structure. The rotor arms are separate from the center frame, enabling a Sorbothane vibration damping layer to be installed. This layer helps to reduce the transmission of vibration from the motor/rotor to the sensors [18]. Overall, the vehicle was designed using the ultra light materials and lightweight avionics and weighs 49.2 grams without a payload. The current mass breakdown of the micro-quad is shown in Table 2.1.

2.3 Quad Rotor Control

The mechanically simple design of quad rotors also makes them easier to control as collective and cyclic control of the rotors is eliminated and there is no tail rotor. Complete vehicle control can be accomplished though differential increase or decrease in rotor rpm. This method is used for pitch, roll, and yaw control of the vehicle. On the quad rotor, diagonally opposite rotors spin in the same direction and adjacent rotors spin in opposite directions as shown in Figure 2.2. This ensures that the torque reactions of each motor are countered by the adjacent motors so the vehicle does not spin around the yaw axis.

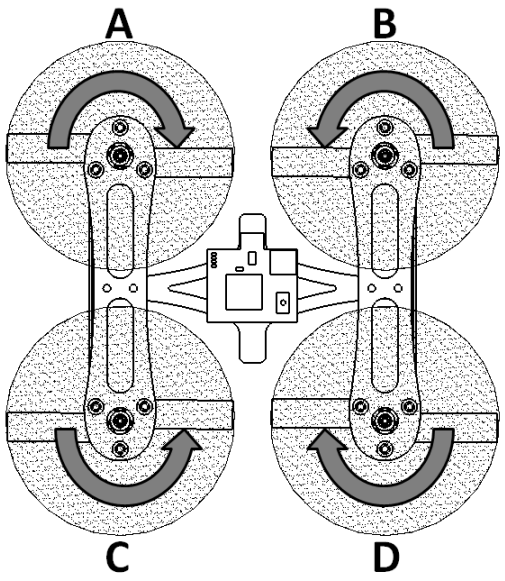

Figure 2.2: Direction of rotation of rotors on a quad rotor.

There are a few different control schemes for quad rotors, but the simplest scheme involves symmetric rpm changes which help to minimize control mixing or the need for collective control of the rotors. Two main methods exist: the plus style and the X style. Plus style control is the simplest form of control and is thus used on lower level vehicles [13]. In this style of control, the vehicle is oriented like a plus sign where the front, rear, left, and right side each have a rotor. Forward/back pitching is accomplished through a combination of increase and decrease of the forward and rear rotor rpm. In much the same way, lateral banking or roll control is done through differential rpm of the left and right rotors. Yaw or heading control is achieved by creating a torque imbalance by increasing rpm for rotors that spin in the same direction and decreasing rpm for the opposite pair of rotors.

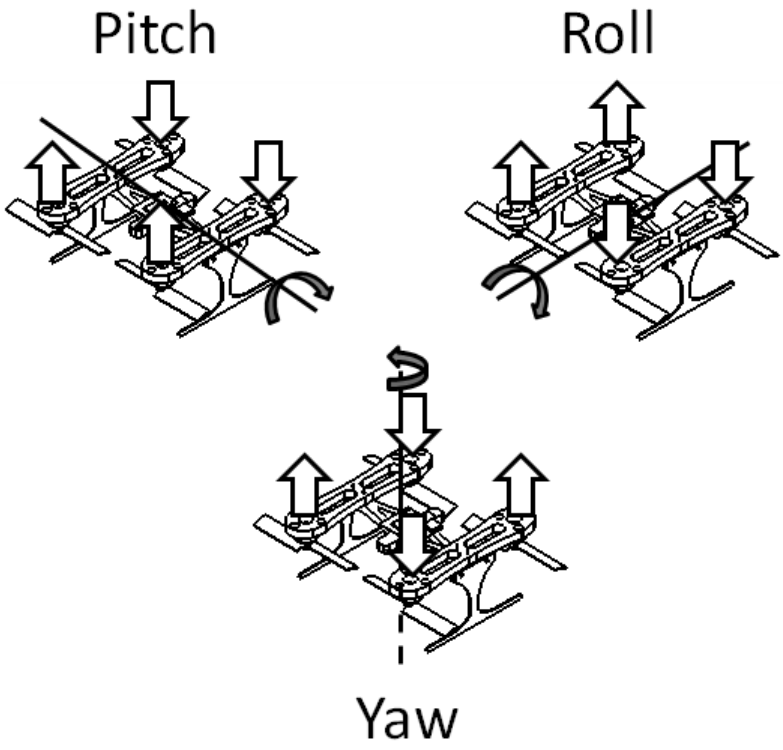

Figure 2.3: X style control mixing scheme used for the current micro quad rotor study

The quad rotor used in the current study utilizes an X style control method which is shown in Figure 2.3. This method is only slightly more involved than the plus style, but offers benefits as any forward facing cameras mounted on the vehicle are no longer obstructed by rotors. In this style, the rotors are oriented along the arms of a letter X. In order to pitch the vehicle forward, the two motors in the rear increase rpm while the two motors in the front decrease rpm. This creates a lift imbalance which induces a pitching moment, tilting the vehicle forward while maintaining torque equilibrium so it does not yaw. The same method is used for rolling the vehicle. Heading control is still accomplished using the same methodology as in the plus style control method. Two opposite motors increase rpm while the other two decrease rpm creating an induced yawing moment on the vehicle and it will thus, change its heading. Although these two

styles of control are not the only methods, they are the easiest to implement and, therefore, used by nearly all quad rotors.

2.4 Brushless Outrunner Motors

The micro quad rotor uses small brushless motors to power the rotors. These motors must efficiently spin the rotors at the required torque in hover. Electric motors use permanent magnets and electromagnets to convert electrical power to a rotating mechanical power. There are two main classes of electric motors – brushed and brushless. Brushed motors generally use direct current (DC) signal and motor speed is varied by varying the voltage. This signal is used to activate half the coils within the motor, turning them into an electromagnet that is attracted to permanent magnets that lie within the casing of the motor. The motor then rotates and two brushes, or slip rings, which cause the opposite coils to magnetize, thus repeating the process. Brushed motors have the advantage of simplicity but they require a variable voltage to operate and the brushes increase noise, decrease efficiency, and can wear out over time.

Brushless motors are slightly more sophisticated but, have the added advantages of reduced noise and increased torque and efficiency with no brushes to wear out. They are also easier to keep cool, and offer more precise rpm control [21]. Brushless motors utilize a series or permanent magnets attached to the rotating portion of the motor, called the rotor, and multiple phases of coils on the stationary portion of the motor called stators as seen in Figure 2.4. When the rotor is on the outside surrounding the stators, this is called an outrunner brushless motor, while a rotor surrounded by stators is called an inrunner.

There are normally only three phases of stators for either inrunner or outrunner brushless motors.

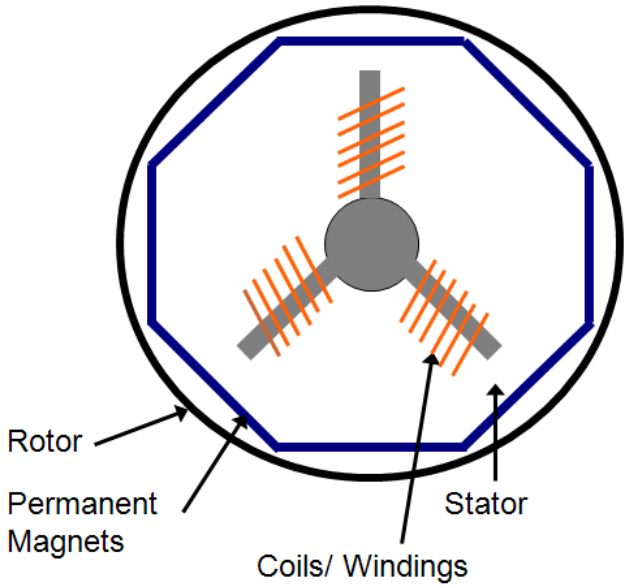

Figure 2.4: Outrunner brushless motor configuration

There are many factors that affect the performance of brushless motors. These factors include:

I. Number of permanent magnets
II. Number of electromagnets
III. Rotor/stator air gap
IV. Wire gauge
V. Permanent magnet coverage
VI. Number of coil windings
VII. Phase winding style
VIII. Core material

Many of these factors are interrelated or are influenced by the inherent design of the brushless motor. The two main factors that must be properly designed include the number of permanent magnets (poles) and the number of electromagnets (stators.) The number of stators must always be a multiple of three because of the number of phases being equal to three. This then places a constraint on the number of poles as they must now be an even number and also must not be a multiple of the number of stators. This is to prevent the motor from being in magnetic equilibrium, which would cause rotor to lock as each rotor magnet would be attracted to its paired stator. Thus, a motor with three stators, would generally have either two or four poles.

The choice of the number of poles and stators determines if the motor will operate at high rpm and low torque or at a low rpm and high torque [17]. Increasing the number of stators has the effect of increasing the torque of the motor. Reducing the number of poles will result in higher rpm but will reduce torque. Changing the number of stators or poles can sometimes be constrained by space due to the size of the motor or the size and availability of magnets. Therefore, the operational torque and rpm of the motor can also be influenced by the number of coil windings around each stator. Two motors with the same number of rotors and stators will operate at different speeds if one motor has more coil windings per stator. The motor with more stator windings will decrease the operational rpm of the motor while increasing its torque output.

Phase winding style can also have an effect on the motors performance. Two main winding styles exist – delta winding and star winding. These configurations are named after their circuit diagram as shown in Figure 2.5. The star winding style provides higher

torque over the delta winding style. This is also the preferred winding style as it is easiest to manufacture.

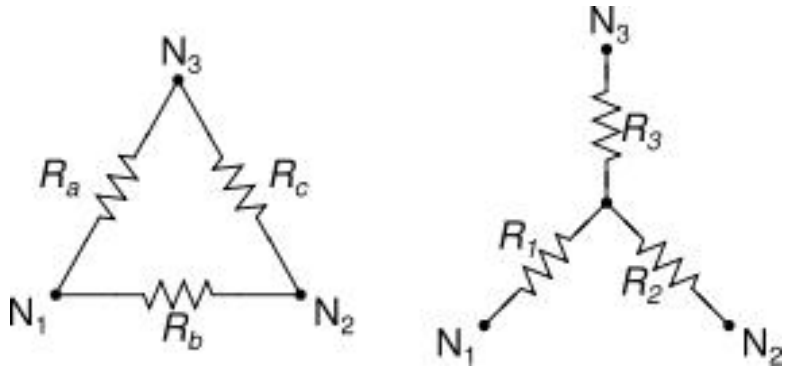

Figure 2.5: a) Star winding and b) delta winding configuration

A brushless motor operates through the application of a voltage over two of the three phases of the motor at any given time [21]. This causes the stators associated with that phase to create an electric field. The permanent magnets then cause the rotor to move as the magnets are attracted to the electromagnetic coils. This process occurs over and over again with the rotor progressively "chasing" the magnetic field created by the sequentially active stators. The movement of the magnets over the coils also creates a back electro-motive force (EMF), which is sensed by the speed controller. As seen in Figure 2.6, the current is applied as sequential square waves. On top of the square wave, the back EMF creates a trapezoid pattern. The speed controller measures this back EMF and uses it to determine the speed of the motor. Thus, if the motor slows down due to an applied torque, the speed controller will adjust to provide the motor more power. Therefore, the EMF and the torque are closely related.

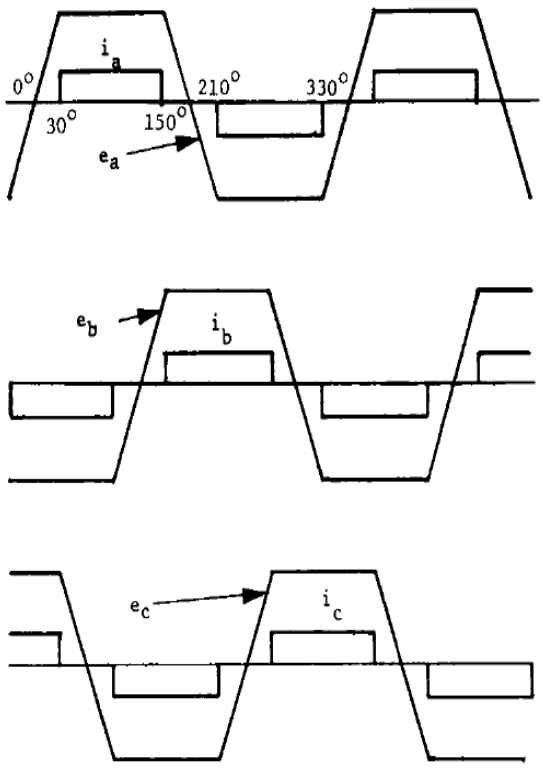

Figure 2.6: Current and back EMF waveforms for a brushless motor [17]

To control the brushless motor, a pulse width modulated (PWM) current controller is used. The PWM signal is a square wave where the pulse width is adjusted to have a delay between 1000 ms and 2000 ms. This corresponds to either closed throttle or open throttle respectively. The speed controller then decodes this signal and correspondingly controls the motor.

Currently there is a limited availability of brushless motors at this small scale. Therefore, the study analyzed two different outrunner brushless motors with 9 stators and 12 poles with the star winding style. The only difference between the two motors is the number of coil windings per stator and the gauge of the wire.

Estimation of the efficiency of brushless motors at this scale appears difficult to determine without experiments. Large brushless motors are designed with tight tolerances and efficiencies are generally very high. However, micro sized brushless motors are much more difficult to manufacture and are generally hand wound. Therefore, coil winding is highly inconsistent and magnet spacing and coverage can vary. This is expected to result in decreased efficiency from larger brushless motors. Also, peak efficiency is expected to occur at only one point corresponding to a certain torque and rpm. To measure this, the current study will use a dynamometer to measure the torque, rpm, and efficiency of the brushless motors. The results of these experiments will be discussed further in Chapter 4.

2.5 Micro Rotor Design

The rotors form the heart of the quad rotor propulsion system. The rotors have a length of 34 mm and chord of 9.4 mm and nominally operate near 10,000 rpm. Therefore, they have a nominal tip Reynolds number of 21,600 in hover. As previously discussed in Chapter 1, traditional airfoils have been shown to have poor performance at Reynolds numbers below 100,000 [10,11]. Therefore, the present investigation utilizes the research in low Reynolds number aerodynamics and small-scale rotor optimization (discussed in Chapter 4). The choice of airfoil is fundamental to the success of any aircraft including MAVs. When deciding on an airfoil for use on micro rotors, the same characteristics that are desired for full scale helicopters are desired at the MAV scale. However, at very low Reynolds numbers, this is difficult to achieve. Many studies have shown to date, that at these very low Reynolds numbers, flat plate and circular arc (cambered plate) airfoils provide better performance than traditional airfoils such as the NACA airfoils [22].

However, obtaining lift, drag, and moment data at these low Reynolds numbers presents a serious challenge as it is very difficult to design test setups sensitive enough to measure the extremely small forces with sufficient accuracy. Muller [23] performed water tunnel experiments of thin flat and cambered plate airfoils at Reynolds numbers between 60,000 and 200,000. His tests were on 4% cambered airfoils and flat plate airfoils for different aspect ratio wings. In his experiments, he found separated flow occurring at nearly all angles of attack with the region of separation increasing to near 50% of the chord at angles of attack around 8 deg.

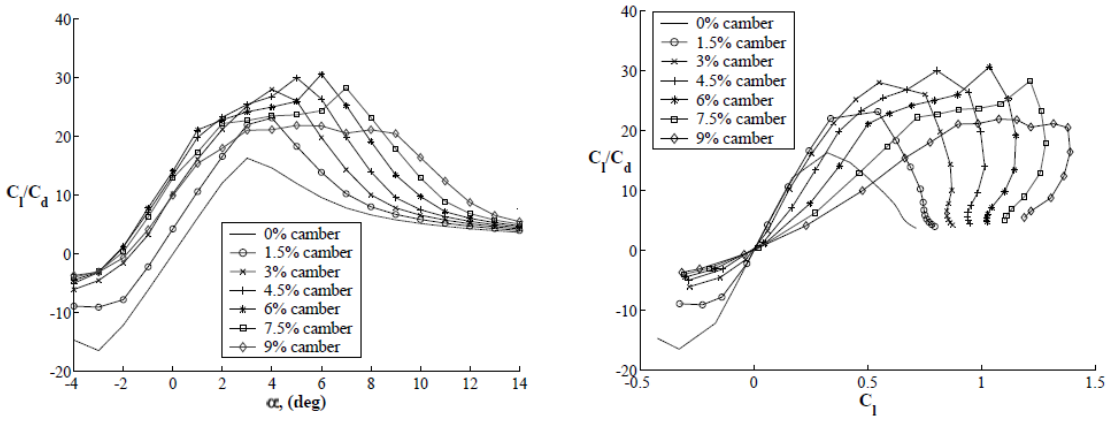

Figure 2.7: a) C_l/C_d versus angle of attack and b) C_l/C_d versus C_l for a range of different circular arc airfoils with different camber and a thickness-to-chord of 2.5% [12]

CFD techniques are often used to obtain the data for these airfoils but this process can become very time consuming as convergence, especially at very low Reynolds numbers, can be slow. As a result, there is not an abundance of 2D data for airfoils at these Reynolds number regimes as compared to traditional airfoils, and wind tunnel data is even harder to find. This critically limits the ability to analytically predict the behavior of micro rotors using different airfoils through simple analysis. However, a database of low

Reynolds number results for airfoils with different amounts of camber was obtained through Bohorquez as shown in Figure 2.7. [12].

This data shows that camber has a beneficial effect on the lift-to-drag ratio for thin cambered plate airfoils. However, the amount of camber is beneficial only to a point, as further increasing camber causes the lift-to-drag curves to round out at lower values. This result can be seen when camber becomes greater than 6%. This data suggests that in order to have the most efficient MAV rotor, a camber of between 4.5% and 7.5% would be most beneficial. This airfoil data was used in a simple blade element analysis to predict the behavior of the micro rotors.

2.5.1 Blade Fabrication

The current study examined rotors with a maximum radius of 34 mm. The current availability of commercial off-the-shelf (COTS) rotors at this scale is limited and all rotors of this size are made with flat plate airfoils. This radius was chosen to provide the largest rotor diameter possible while still meeting the size constraints for the vehicle. Quad rotors need two different rotor designs – right handed and left handed. A right handed rotor, when viewed from above, will appear to rotate clockwise while a left handed rotor will rotate counterclockwise. Although there is no aerodynamic or mechanical advantage of a right handed versus left handed rotor, by tradition, most rotors are manufactured as left handed rotors. At the current scale of 34 mm radius, there are no right handed rotors available, therefore, it was necessary to manufacture these rotors in house.

The initial goal was to manufacture metal rotors where the collective could be adjusted. However, to quickly and efficiently manufacture identical pairs of both left and right handed rotors needed for the quad rotor, precluded this method of manufacture and, therefore, other techniques were examined. The method of composite molding, a method used by Pereira [2], exhibited similar challenges to metal rotor blade construction, making it very difficult to manufacture multiple identical blades. CNC milling, although a highly accurate way of producing multiple identical rotors, was found to be time consuming and was, therefore, not a viable option either. The plastic injection molding and the rapid prototyping methods showed the greatest promise as they are both highly consistent and the actual processes take relatively lesser time to complete. Ultimately the rapid prototyping process was chosen as multiple different rotor designs could be made simultaneously along with their identical left and right handed pairs, thus, reducing manufacture time and increasing accuracy and consistency beyond what has been used by previous researchers.

The micro rotors were first designed using a CAD software. This allowed the rotors to be designed to a high degree of accuracy so they could be manufactured in nearly any shape. This process ensured that all dimensions, planform, and airfoil shapes were accurately modeled. Drawings could easily and quickly be changed and then exported for rapid prototyping manufacture.

2.5.2 Stereolithography Rapid Prototyping Process

The micro rotors were manufactured using the stereolithography (SL) rapid prototyping process. The SL process, commonly known as 3D printing, is an additive technique

where the part is manufactured one layer at a time. An ultraviolet (UV) curable polymer is extruded through printer heads that move back and forth like an inkjet printer to form the pattern of the part. A UV light is then focused on the liquid layer which causes it to cure in place. A gel-like support material is also extruded through adjacent heads to surround the part during manufacture [24]. This process is shown in Figure 2.8. Once the part is complete, it is fully cured and the support material can be washed off with water jet or removed by hand. This study utilized an Objet Eden 350V 3D printing system for all rotor manufacture. This ensured a high degree of accuracy as the machine has a print resolution of 42 microns in the *x* and *y* directions and extruded layers 16 microns thick in the *z* direction [24].

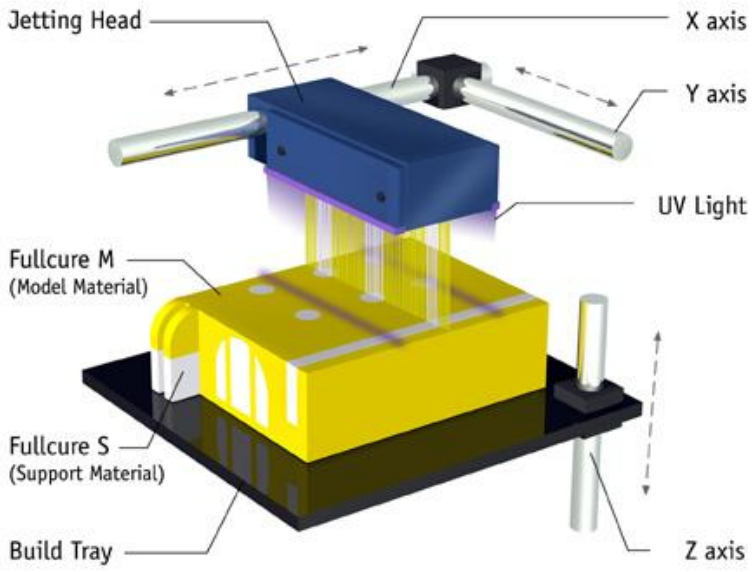

Figure 2.8: The Objet Polyjet™ stereolithography rapid prototyping process [24]

The stereolithography process is a highly accurate efficient method for manufacturing many different blade designs simultaneously. However, for micro rotor manufacture, this

method presented some shortcomings. The main shortcoming in this process is that the rotors are highly sensitive to heat. When the rotors are heated, either by the air in the surrounding environment, or through heat conduction from the motor, deformation of the material can occur. Subsequent cooling of the material will "freeze" the deformation into shape. Similarly, it is important to store the rotors flat on the table as they will also start to sag or droop over a period of weeks if left unsupported. For the current study, all rotor tests were performed within a couple of days after initial manufacture to ensure the rotors were tested in their original shape. Rotors were also periodically checked for signs of deformation before and after testing.

Although the SL rapid prototyping process used had an *x-y* accuracy of 42 microns and a *z* direction accuracy of 16 microns, the practical thickness of the rotors had to be greater than 0.4 mm or 400 microns. Initial rotor designs were manufactured with a thickness of 0.4 mm and bending and torsional deformations occurred during testing. To ensure against these deformations, a rotor thickness of 0.6 mm was used for all rotor testing which minimized blade deformations.

2.6 Summary

The micro quad rotor was developed to meet the requirements of the Army's MAST CTA [15]. The vehicle's compact design, being less than 6 inches by 6 inches and weighing less than 50 grams without a payload makes it ideally suited for the indoor and outdoor environments. Brushless motors were used as they offer a powerful alternative to traditional brushed style motors and do not require the use of gear boxes helping to keep the weight of the vehicle to a minimum. The efficiency of the brushless motors is not

expected to remain constant over a range of rpm and it is predicted that it will be much lower than larger brushless motors (around 50%). A three phase power analyzer and micro dynamometer will be used to measure the power input and output of the motors to determine their efficiency. Details of these experiments will be described in later chapters. Because of the vehicle's small size, rotors must be used that operate efficiently at low Reynolds numbers. The vehicle requires identical pairs of both left and right handed rotors. To quickly and precisely manufacture custom rotors, the stereolithography rapid prototyping process was used, which allowed the manufacture of many different blade designs simultaneously. Aerodynamic analysis of these rotors will provide insight into their efficiency in terms of their ability to produce a given thrust for the minimum power. A simple blade element based analysis will be presented in the next chapter and details of rotor experiments will be presented in Chapter 4.

Chapter 3

Analysis

3.1 Introduction

In this chapter, the methods used for the rotor analysis will be discussed. The blade element momentum theory (BEMT) used for analysis will be described as well as a discussion on the applicability of the blade element analysis to low Reynolds number flows. A beam based finite element analysis (FEA) that included bending and torsional degrees of freedom for the analysis of the rotors will also be discussed. The structural analysis (FEA) is coupled to the aerodynamic analysis (BEMT) to capture the effect of blade deformation on thrust and power. Finally, the analysis was systematically validated with test data.

3.2 Blade Element Momentum Theory

The mathematical model used for predicting rotor performance known as the blade element theory (BET) is a classical technique that had been developed as early as 1900 by a Frenchman by the name of Stefan Drzewiecki and was originally used to analyze aircraft propellers [25]. The technique was later expanded to utilize momentum theory and was combined with the blade element theory, which now forms the basis for many modern analysis tools used for predicting rotor performance. BET assumes that the rotor can be divided into individual blade sections where each airfoil section is assumed to

experience 2-D flow. The aerodynamic forces and moments are then calculated and integrated along the blade span and used to provide estimates of thrust, torque, and power for the rotor.

When BET is combined with the momentum theory, it is called the blade element momentum theory (BEMT), which takes into account the effects of blade geometry along with the inflow distribution to obtain the angle of attack distribution, which is used to calculate rotor thrust, torque, and power. The present BEMT methodology utilizes an airfoil table lookup scheme, and the methodology is described below.

The BEMT works through an iterative process that converges on an inflow and then calculates the desired parameters (i.e. thrust, torque, power, etc). This is done by first obtaining an estimate of the local flow velocity and aerodynamic angle of attack at each of the blade sections. The thrust, torque, and power of the rotor can then be obtained by integrating along the span of the rotor and non-dimensionalized (eqns 3.1).

$$dT = N_b dF_z \qquad dQ = N_b dF_x r \qquad dP = N_b dF_x \Omega r \qquad (3.1)$$

$$dC_T = \frac{dT}{\rho(\pi R^2)(\Omega R)^2} \qquad dC_Q = \frac{dQ}{\rho(\pi R^2)(\Omega R)^2 R} \qquad dC_p = \frac{dP}{\rho(\pi R^2)(\Omega R)^3}$$

In order to determine the induced inflow of the rotor, it is assumed that the thrust is constant on the annular ring of the rotor disk. The differential thrust (*dT*) obtained from the momentum theory is equated to the thrust from BET to obtain the inflow equation (eqn. 3.2) which can be used to find the inflow velocity along the span of the blade as well as the aerodynamic angle of attack

$$\lambda = \sqrt{\left(\frac{\sigma C_{l_\alpha}}{16F} - \frac{\lambda_c}{2}\right)^2 + \frac{\sigma C_{l_\alpha}}{8F}\theta y} - \left(\frac{\sigma C_{l_\alpha}}{16F} - \frac{\lambda_c}{2}\right) \qquad (3.2)$$

This formulation is typically used for analysis of larger scale rotors where the airfoil lift curve slopes remain mostly linear and are not strongly dependent on Reynolds number. Results from Harrington's experiments [26] on full scale rotors that had a tapered planform and symmetric NACA 0015 airfoil sections were used to validate the current analysis as shown in Figure 3.1.

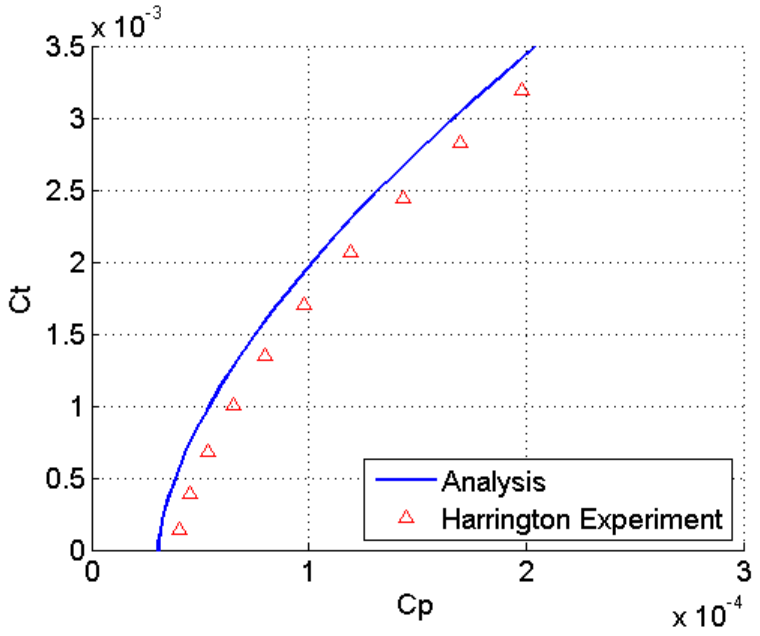

Figure 3.1: Validation of BEMT analysis with experimental data

The analysis clearly shows good correlation with experimental results at these larger scales and results in only a slight over prediction of the power at a given C_T. The analysis was then used to model the low Reynolds number rotors. The analysis was compared to low Reynolds number experiments (below 80,000) to show correlation (Figure 3.2).

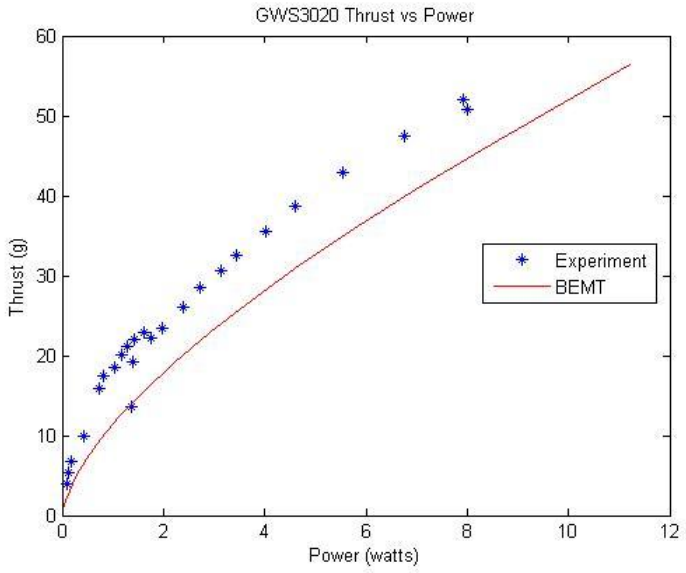

Figure 3.2: Thrust versus power for a micro rotor with a radius of 42 cm.

Although the analysis follows the same trend as the experimental results, the power was overpredicted for the same thrust. It therefore, became obvious that in order to get better agreement with experiments, the analysis required the addition of airfoil data table lookup for thin flat and cambered plates [12]. Linear $C_L(\alpha)$ was originally used to validate the code against full scale rotor tests, however low Reynolds number airfoils do not generally exhibit linear behavior. The addition of table lookup increased the predictive accuracy of the analysis to within 5% of experimental data for the flat plate blades. These results will be shown in the validation section of this chapter. This is satisfactory for the purposes of predicting performance of rotors at these small scales without performing a more in-depth analysis.

In the derivation of C_T, C_Q, and C_P, and the inflow λ, the lift and drag coefficients C_L and C_D appear. Both of these values are obtained through the airfoil table lookup. However, it proved difficult to find a single source that provided a complete set of coefficient data at

all the desired Reynolds numbers. The table lookup functionality uses Lagrangian interpolation to find lift, drag, and moment coefficients at particular angles of attack and Reynolds numbers where experimental airfoil data was not available. The solution to the Lagrangian interpolation problem is defined:

$$P(t) = p_0(x)P_0 + \cdots + p_n(x)P_n \tag{3.3}$$

$$p_i(x) = \frac{\prod_{i \neq j}(x - x_j)}{\prod_{i \neq j}(x_i - x_j)} = \prod_{i \neq j} \frac{x - x_j}{x_i - x_j} \tag{3.4}$$

where *p* represents the polynomial in *x* where each of the coordinates used to solve the function *P* lie. Each time the airfoil table lookup function is called within the BEMT analysis, a Lagrangian interpolation is performed first between angles of attack for all available Reynolds numbers to find the coefficients at the desired angle of attack. These resulting lift, drag, and moment coefficients are then interpolated again between the Reynolds numbers to find the coefficients at the desired Reynolds number. Since the Lagrangian interpolation functions used are quadratic, a minimum of three Reynolds tabulated tables must be available for a single airfoil. This method effectively allows contour plots to be created for lift, drag, and moment coefficients as a function of both Reynolds number and angle of attack as shown in Figure 3.3.

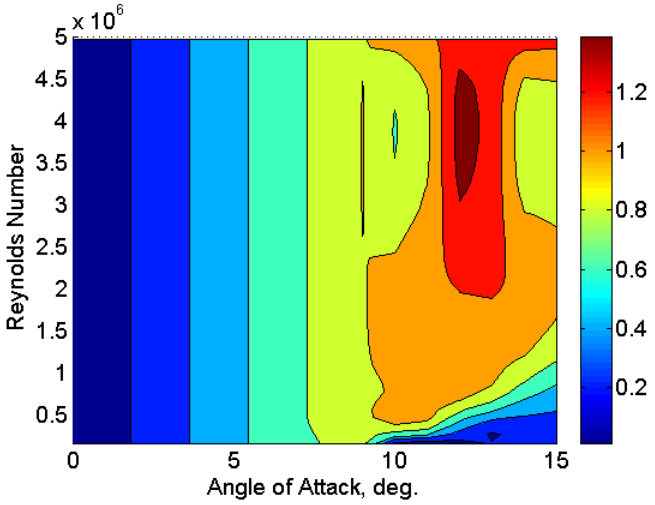

a)

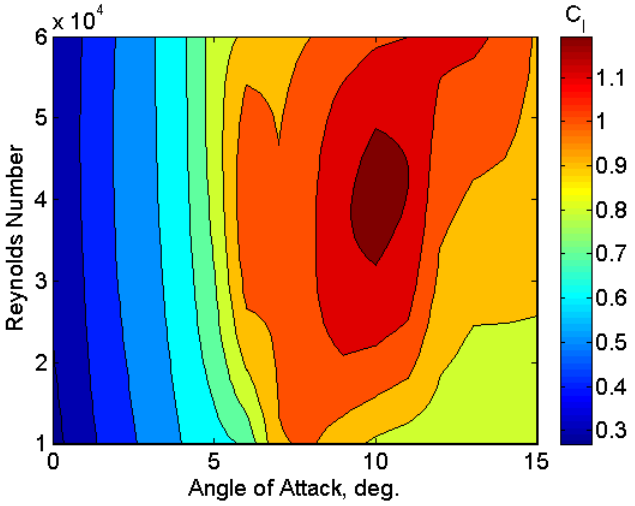

b)

Figure 3.3: Contour plots showing interpolation between angle of attack and Reynolds number for a) NACA0012 and b) 6% cambered plate airfoil

Using this methodology, the blade element momentum theory appears attractive as a design tool because of its inherent flexibility for expansion into more advanced analysis. As shown before, the present analysis provides good agreement with experimental data for large scale rotors [26], but the analysis needed to be validated for MAV-scale rotors. Systematic validation of the analysis will be discussed towards the end of the chapter.

3.3 Effect of Blade Deformations

During the initial validation of the code against currently available rotors, an interesting phenomenon emerged. For stiff rotors, the analysis had good correlation with experiments at all operating conditions, but for rotors with thin flexible blades, the analysis correlated well for lower rotational speeds but then started to diverge from experimental results at higher rotation rates as seen in figure 4.

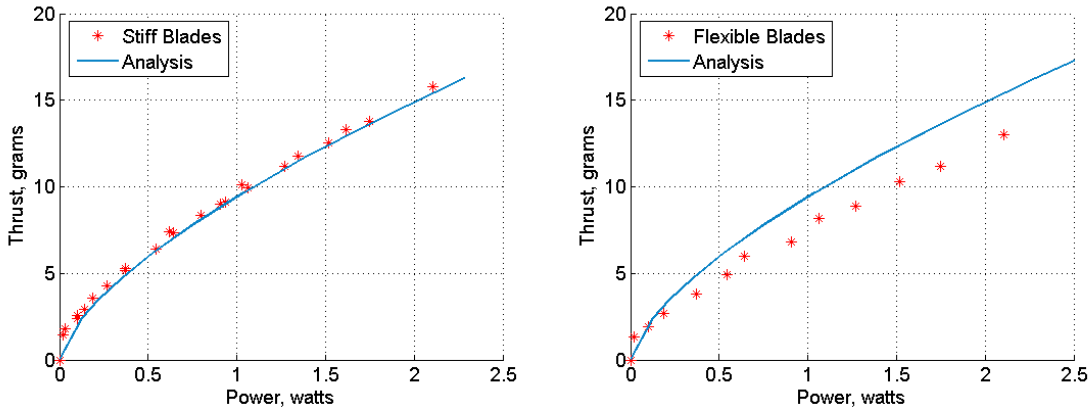

a) Stiff Blades *b) Flexible Blades*

Figure 3.4: Effect of blade deformation and correlation with rigid blade analysis

Accurate predictions of thrust and power at these high rotational speeds are limited by the fact that some rotors of this scale are very thin and flexible. Low torsional and bending stiffness causes undesired elastic deformations. Large bending and torsional deformations have been observed when testing small rotor blades which causes a significant drop in the thrust. These deformations were further verified by using a photo-gate circuit to trigger a strobe light so that the deformations could be observed. A photograph of the observed deformations using this technique is shown in Figure 3.5.

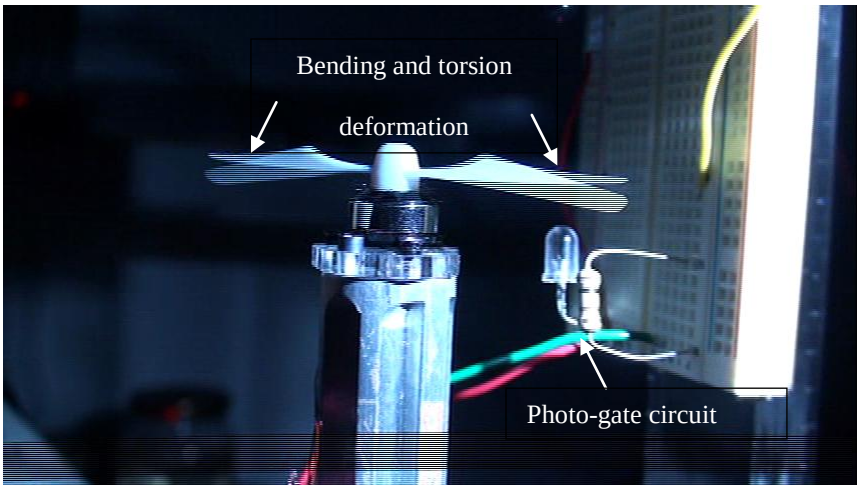

Figure 3.5: Blade deformation resulting in decreased thrust of a 34 mm radius rotor

This elastic deformation can be caused by a variety of reasons. The current rotors rotate at high rpm (near 10,000 rpm) and the propeller moment due to the centrifugal force can flatten the pitch angle of the blade. This may be the most significant contributor. The airfoils at this scale also have relatively high negative pitching moments which also has the potential of twisting the blade down decreasing its overall thrust production. The offset distance between the blades pitching axis and the center of pressure may also have an effect. If the center of pressure is aft of the pitch axis, this will further compound the negative pitching moment. A center of pressure ahead of the pitch axis will cause a positive pitching moment [25]. Therefore, it is evident that a structural model of the blade is required along with the aerodynamic model to predict the blade deformations, which would play a significant role in the accurate thrust and power prediction

3.4 Finite Element Analysis

The structural model used for the present analysis is a beam-based FEM analysis with bending and torsion degrees of freedom. The FEM model calculates the bending and

torsion deformations along the span of the blade due to the aerodynamic and inertial loads.

In the FEM analysis, each element is formulated into two torsional rotations θ_1, θ_2, and two bending displacements and slopes, w_1, w_2 and w_1', w_2'. These are the displacements and are located at node points within each element. Interpolation functions are then chosen to represent the assumed shape of the deformed elements. These shape functions are first and third order Hermite polynomials for torsion and bending respectively [25].

The stiffness and mass matrices are derived from the potential and kinetic energy expressions respectively. The stiffness matrix and mass matrix are given by the expressions:

$$\boldsymbol{K} = \int_0^1 GJH'^T H' ds \quad (3.5) \qquad \boldsymbol{M} = \int_0^1 mH^T H ds \quad (3.6)$$

There is also a component of the stiffness matrix due to centrifugal stiffening of the blade represented in equation 3.5.

$$k_{ij} = \sum_{j=2}^{N} \frac{m_j \Omega^2}{2} \left(x_{j+1}^2 - x_j^2\right) \int_0^l H_i' H_j' \, ds - m_i \Omega^2 \int_0^l \left(x_i s + \frac{1}{2} s^2\right) H_i' H_j' \, ds \quad (3.5)$$

The elemental mass and stiffness matrices are assembled to obtain the global matrices and the cantilevered boundary condition was applied. The blade bending and torsional stiffness (*EI* and *GJ)* distribution was obtained from the blade geometry and the material properties supplied by the manufacture.

3.5 Combined BEMT and FEM

The FEM analysis was then coupled with the BEMT analysis to obtain accurate performance prediction. The coupling works by first calculating the lift, drag, and moment at each element along the span of the blade. These values are then used to assemble the forcing vector and the FEM analysis is carried out to determine the blade displacements. The torsional displacement is then used to modify the twist distribution along the span of the blade. The blade element analysis is then performed with the modified twist distribution to obtain the modified force vector. This iterative process is continued until the bending and torsional displacements of the rotor blade converge. The lift distribution along the span of the blade is then modified to reflect tilting of the lift vector caused by the blade bending deformation. The resulting thrust vector is then integrated to determine the thrust of the rotor.

For a quad rotor, in order to change the amount of thrust produced by each blade, the rotor rpm is varied. As a result, the BEMT analysis must be executed over a range of operating rpms so that an accurate picture of how thrust and power vary with rotor speed can be obtained.

3.6 Validation of Analysis

The augmented BEMT method with table lookup and beam based finite element analysis was presented as a means of predicting the performance of the micro rotors. However, the analysis needs to be extensively validated with experimental results to determine if rotor design at these low Reynolds numbers could be performed using the predictions from the analysis rather than through the laborious process of experimentation. To validate the

final blade element aerodynamic analysis combined with the finite element structural analysis, tests were performed using un-twisted, rectangular planform rotor blades with flat plate and cambered airfoils. The analysis was validated using the test data obtained on a rotor having a radius of 34 mm, a chord of 9.4 mm and a collective set at 18 degrees. This blade design was chosen for simplicity so that the aerodynamics due to twist and taper do not influence the performance and the rotor stiffness remains constant along the span of the blades. This rotor design was also chosen to produce the desired amount of thrust required for hover for the actual micro quad rotor. The rotors were also carefully designed so that the bending/torsional deformations were small and they remain within the linear range. The correlations between the experiment and the analysis are discussed below.

The key limiting factor in the analysis is the lack of reliable airfoil tables. The analysis utilizes a quadratic Lagrangian interpolation between Reynolds numbers within the airfoil tables to obtain lift and drag coefficients. This type of interpolation requires a minimum of three points to create a curve for the interpolation. Some airfoils for cambered plates only had data available for one or two Reynolds numbers and many did not have data within the desired Reynolds number regime at all. For airfoils where data for only two Reynolds numbers was available, linear interpolation was used. However, it is important to note that this may result in a reduced accuracy of prediction for certain rotors.

Figure 3.6 shows the correlation of analytical predictions with experimental results for rectangular rotors with a flat plate airfoil and 7.5% cambered plate airfoil. Here the flat plate airfoil tables have data for three different Reynolds numbers, while the 7.5% cambered plate airfoil tables only have data at two Reynolds numbers (15,000 and

60,000). It can be seen that the analysis accurately captures the thrust versus power requirements of the rotor with a flat plate airfoil, while it over predicts the thrust and power slightly for the rotor with the 7.5% cambered plate. The power for the 7.5% airfoil is the same for the flat plate airfoil. However, in both cases, the analysis accurately captures the trends. This shows that with the proper airfoil tables, the analysis is capable of not only predicting the performance trends of rotors with different airfoils, but is able to reasonably predict the magnitude of thrust and power for the micro rotors.

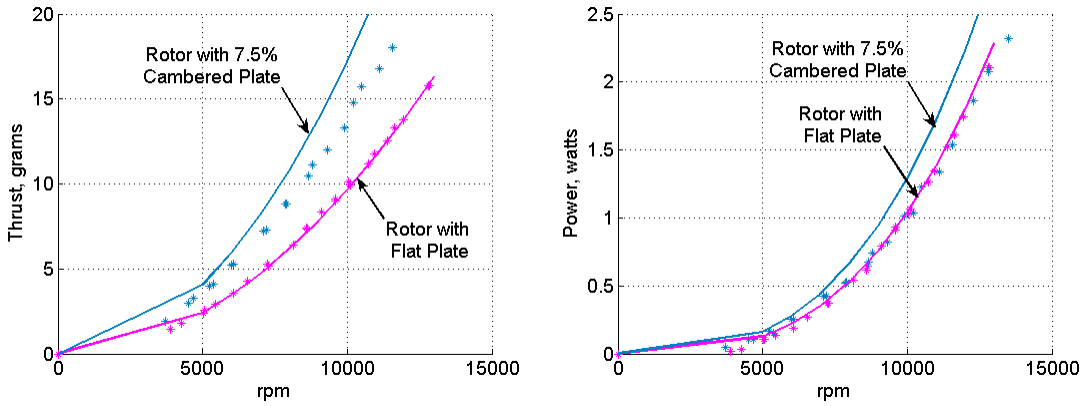

a) Thrust versus rpm *b) Power versus rpm*

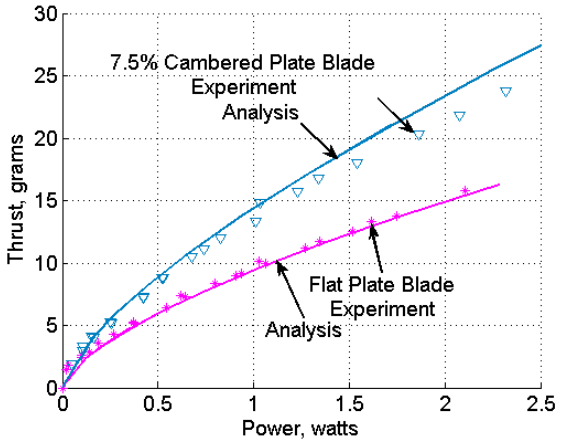

b) Thrust versus power

Figure 3.6: Correlation of analysis and experiments for rotors with two different airfoils

The rotor with the flat plate airfoil was then made thinner so that the bending and torsional deformations would have a greater effect on the thrust and power prediction as was seen previously. Comparison between the rigid BEMT analysis and the coupled aerodynamic and structural analysis was then shown for the flexible rotor as seen in Figure 3.7. Here the flexible blade analysis shows much better agreement with the experimental results than the rigid blade analysis.

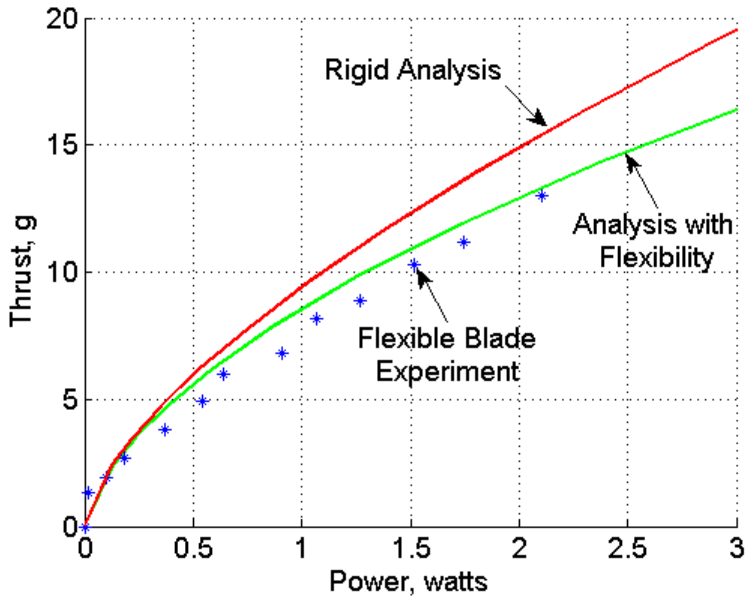

Figure 3.7: Correlation of coupled aerodynamic and structural analysis for flexible rotors

The validation for rectangular, non-twisted rotors shows good agreement between the analysis and experiment. This shows that for simple rectangular blades, the blade element analysis is a useful design tool and is capable of predicting rotor performance for rotors operating at different rpms.

The analysis was also performed to validate rotors with tapered blades. However, this proved difficult as tapered rotors have a continuous variation of camber along the tapered portion of the blade. This required an additional step where further interpolation between the different airfoil tables was necessary. Figure 3.8 shows the analysis results for rotors that have taper and no twist and the correlation with experiment.

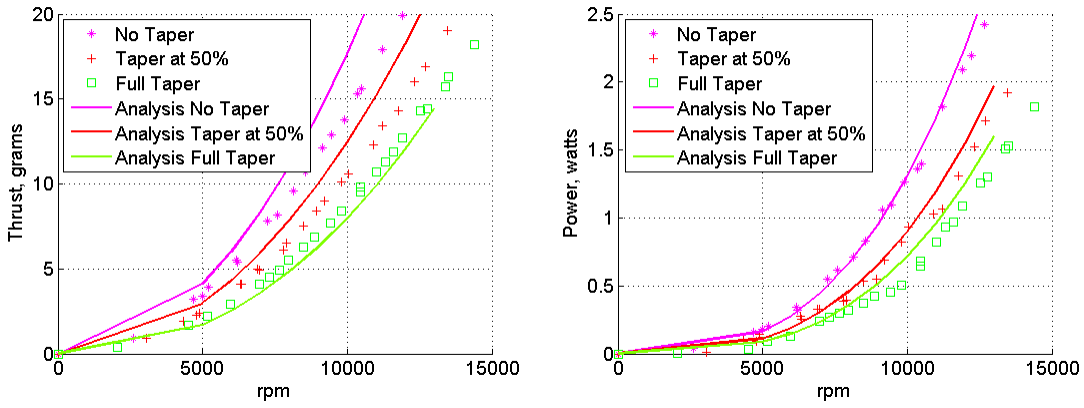

a) Thrust versus rpm *b) Power versus rpm*

Figure 3.8: Correlation of analysis with experiment for symmetrically tapered blades

In the correlation of the analysis with experiments for rotors with symmetric taper starting at various spanwise locations along the blade, it can be seen that the analysis is once again able to capture the trends seen in the experiments. Both thrust and power reduce with the addition of taper at a given root collective and rpm which is reflected in the analysis. Due to the limited amount of airfoil data available at these Reynolds numbers, the table lookup functionality is interpolating not only between angles of attack and Reynolds numbers, but between different airfoil tables and the three fold combination of this interpolation could be resulting in the over prediction of thrust seen for two of the three analysis cases. Another reason correlation is off for these rotors could be coming from 3-D effects. The rectangular rotors have an aspect ratio of 3.6 while the

tapered rotors have an aspect ratio of 4.8. Although the aerodynamic analysis takes into account tip losses, the 3-D effects for rotors with these very low aspect ratios may have a greater influence on the trust and power at low Reynolds numbers. However, the analysis is capable of capturing the correct trends, which are important for rotors at this scale.

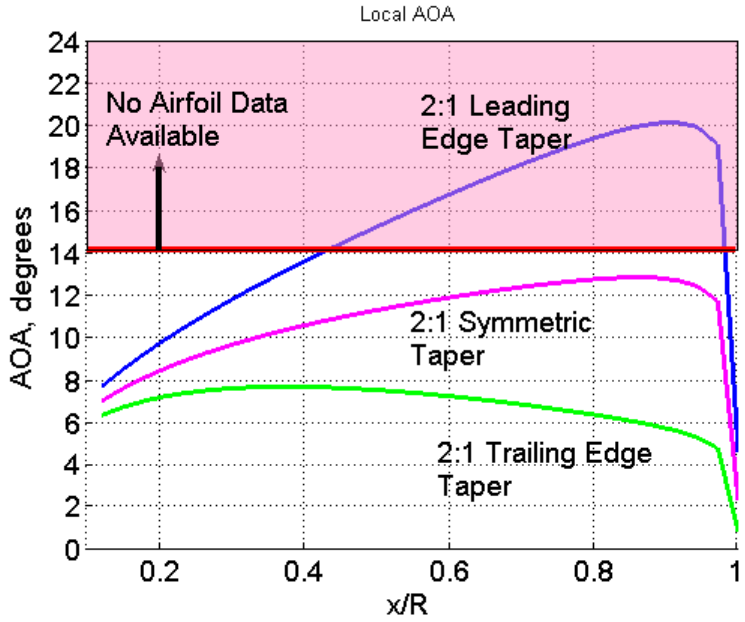

Figure 3.9: Local AOA along blade for symmetric and asymmetrically tapered blades

Comparison of the experimental results with analysis for rotors with asymmetric taper was also performed. Asymmetrically tapered rotors not only have a variation of camber and chord along the span of the blade, but are also twisted. As will be discussed in Chapter 4, blades with leading edge taper exhibit a wash-in or positive twist towards the tip of the blade. This case could not be correlated as the aerodynamic angle of attack predicted by the analysis far exceeded the range of available angles of attack in the table lookup, as well as exceeded stall over the outer 50% of the blade. Figure 3.9 shows the predicted AOA of the rotors where the line at 14 degrees represents the upper limit of the

available data in the airfoil tables. Interpolation within the airfoil tables is only valid over the range at which data is available but extrapolation beyond the available data was assumed to be invalid as the behavior of low Reynolds number airfoils in deep stall is non-linear.

For the case of trailing edge taper, which results in a negative 10 degree twist of the blade, the analysis once again follows the trends of the experimental data but prediction of the magnitude of thrust and power are not necessarily reliable for design purposes. Correlation of this analysis is shown in Figure 3.10. This is most likely because of the lack of airfoil data at the different Reynolds numbers and different cambers along the blade as was seen previously in Figure 3.8.

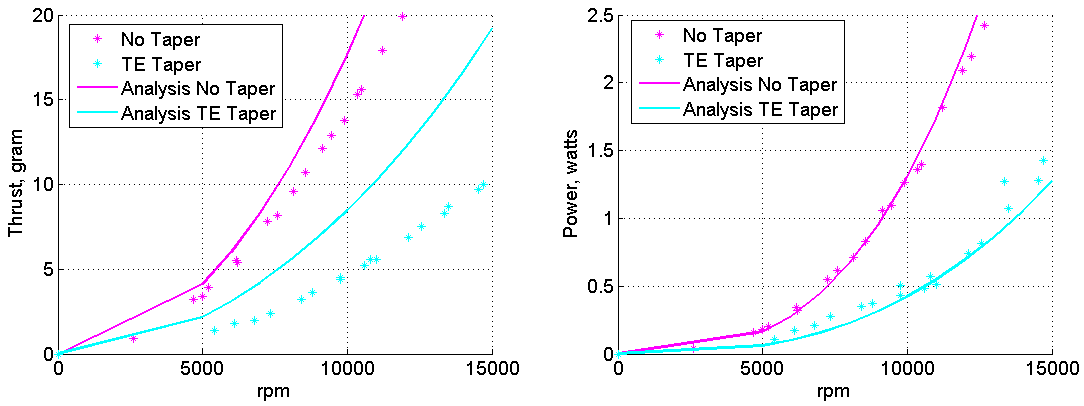

a) Thrust versus rpm *b) Power versus rpm*

Figure 3.10: Correlation of analysis with asymmetric trailing edge tapered blades

In Figure 3.10, analysis of the power at different rotor speeds seem to be predicted well but thrust is over predicted. This validation case compares two blades with the same root collective and therefore the tapered blade, having a negative 10 degree twist has a much lower collective at 75% span. Blades with varying camber, taper, and twist show the

limits of the analysis where predictions of the thrust is showing to be less reliable for highly twisted and tapered blades.

In all the validation cases, the analysis was able to accurately capture the trends in the effect of airfoil, taper, and twist which suggests that present analysis could be a valuable tool for design but its accuracy is limited by the availability of airfoil tables. As previously mentioned, obtaining reliable and complete airfoil tables at these low Reynolds numbers is not trivial and may require using refined CFD analysis or wind tunnel experiments. The main purpose of these studies was to determine the validity and limitations of the analysis.

3.7 Summary

The low Reynolds number aerodynamic environment at which the micro rotors operate is complex and flows are normally laminar and suffer from viscous effects and separation. In the present study, an analysis based on a combined blade element momentum theory that used airfoil table lookup was developed and validated for the micro rotors. A beam based finite element analysis was developed and coupled with the BEMT to obtain estimates of blade deformations which was used for the accurate prediction of thrust and power. This combined analysis showed good agreement with experimental results for most of the cases, therefore, demonstrating its viability as an analysis tool for micro rotors.

Chapter 4

Experimental Results

This Chapter discusses the experimental setup for the micro rotor parametric measurements, the results from these tests, and the key conclusions drawn from this study. The experiments used custom designed fixed-pitch rotors that were manufactured using a rapid prototyping process described in Chapter 3. An experimental parametric study to investigate the effects of different numbers of blades, airfoil shape, maximum camber location, leading edge shape, and blade taper was conducted to determine the aerodynamic performance of the rotors. The study also includes understanding the interference effects between multiple rotors operating in close proximity to each other, with rotors spinning in same and opposite directions, as would be the case in the micro quad rotor helicopter. An explanation of the motor test setup, and the effect of different motor designs on efficiency and maximum power/torque is also included. Finally, combined motor and rotor tests will be shown to illustrate how rotor-motor coupled design is necessary to increase the vehicle endurance.

4.1 Rotor Stand Test Setup

The test setup for measuring the rotor thrust and power is shown in Figure 4.1. The rotor was directly spun using a small outrunner motor that was mounted on top of a standoff tower. The motor was driven using Castle Thunderbird electronic speed controllers (6 amp or 9 amp) powered by a BK Precision DC Regulated Power Supply and a GWS

multi-servo tester. The standoff tower was connected to a Transducer Techniques Model RTS-5 torque cell which was then mounted to an Ohaus Explorer precision balance. To measure the motor RPM, a reflective marker was placed on the outer casing of the motor and measured by a Monarch Laser Tachometer.

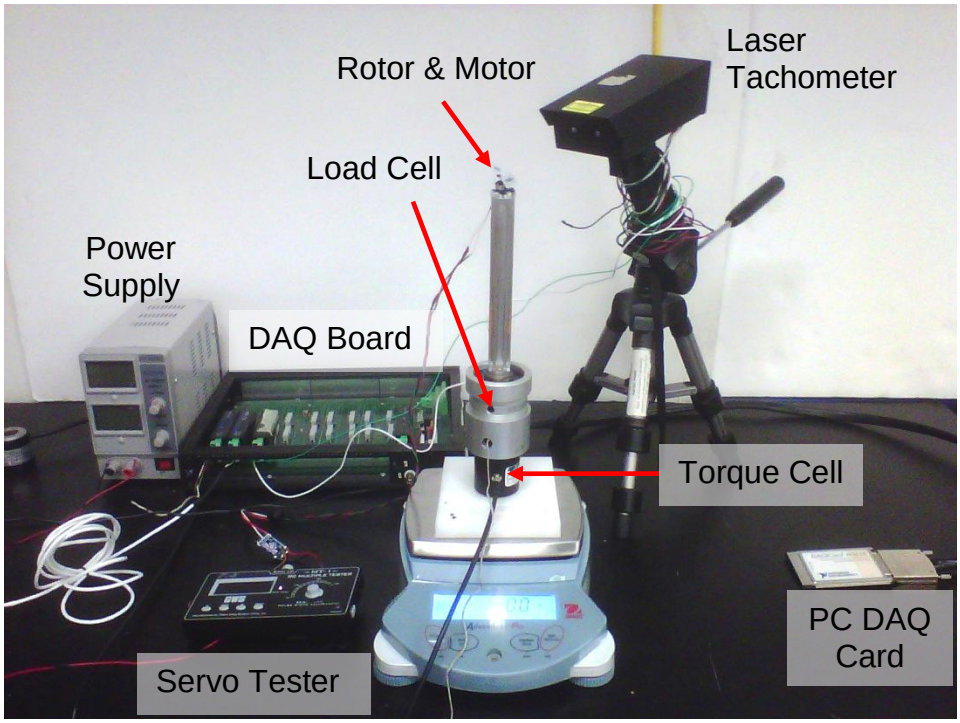

Figure 4.1: Experimental rotor test setup

The signals from the test equipment were connected to a National Instruments SC-2345 Signal Conditioning box through a 12-bit National Instruments DAQCard-6062E capable of 500 kilo samples per second. A custom LabView VI was created that sampled at 1000 samples per second for 3 seconds and then averaged the data. Data was then saved to a file for post processing. Electrical power was also measured from the voltage and current measurement.

In order to prevent the downwash of the rotors from impinging upon the balance, the rotor was mounted inverted so the downwash was directed upwards, which prevented any potential ground effects and also prevented the downwash from being affected by the standoff tower and mounting brackets. This method of testing also mimicked the mounting style of the rotors on the quad rotor as the motors are mounted below the arms of the vehicle and the rotors operate in a “pusher” configuration rather than a “tractor” or pulling configuration.

Error analysis was performed for the test setup and there were three main sources of error. Although the precision balance had an accuracy of 0.01 grams, the varying thrust of the rotors meant the measurements were accurate to 1% of the measured value. The torque cell was also carefully calibrated and periodically checked to ensure the calibration did not change over time. It was seen that the torque cell was highly accurate but with a spinning propeller attached, was accurate to within 5% of the measured value (Figure 4.2).

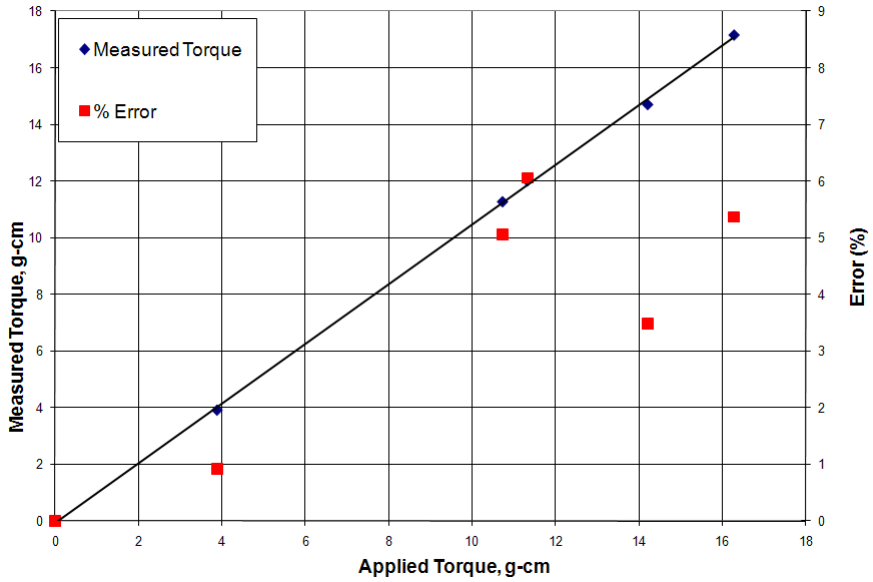

Figure 4.2: Measured torque versus applied torque showing measurement error of torque cell

Since power measurements are a combination of the torque and rotational speed, measured values of the power also incorporated the error from the laser tachometer. The total error in the measured values for power was therefore determined to be about 5% as the laser tachometer was highly accurate. A graph showing thrust versus power is shown with the corresponding error bars in Figure 4.3.

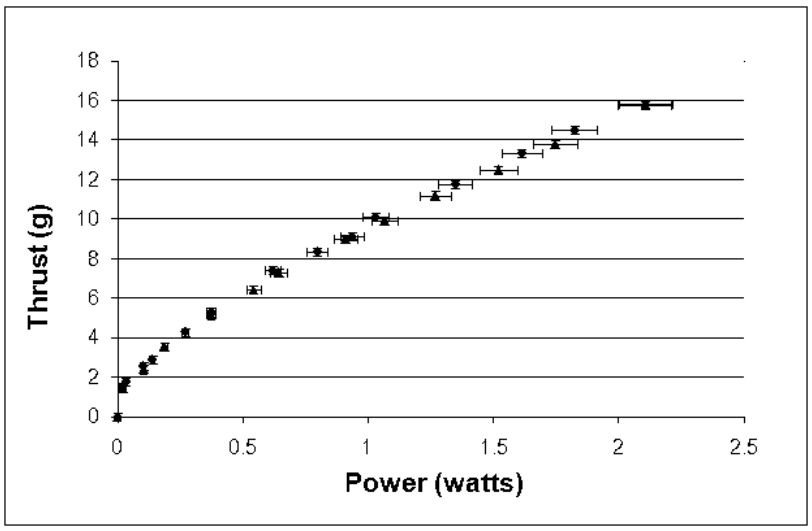

Figure 4.3: Thrust versus power for a rectangular planform rotor showing error bars

4.2 Rotor Blade Testing

.Previous parametric studies on small scale rotors [6,12] formed the starting point for the micro rotors for the quad rotor. The current study chose to examine five different rotor parameters including airfoil shape, max camber location, leading edge shape, number of blades, and taper location. Although this study is not a comprehensive rotor optimization, the goal was to determine how different parameters would affect the overall propulsion system efficiency (rotor and motor) by requiring the motors to operate at different rotational speeds and torques.

There are many parameters that affect the performance of rotors at this scale, which have direct effects on thrust and power requirements. For a micro quad-rotor, the collective angle is fixed and therefore the rotor must operate off design point whenever the vehicle is climbing, descending, or maneuvering as rotor rpm is varied to change the thrust. To understand this, the effect of different rotor parameters on thrust and power were

examined at a fixed collective and varying rpm. Experiments were also carried out for varying pitch angles to ensure the rotors were operating at their best collectivet. Using the BEMT analysis described in Chapter 2, the baseline rectangular rotor configuration was designed to produce 13 – 15 grams thrust operating between 8,000 rpm and 12,000 rpm. This resulted in a baseline collective angle of 18 degrees. Experiments also verified that a collective of 18 degrees was the optimum for a rotor with rectangular un-twisted blades (Figure 4.4).

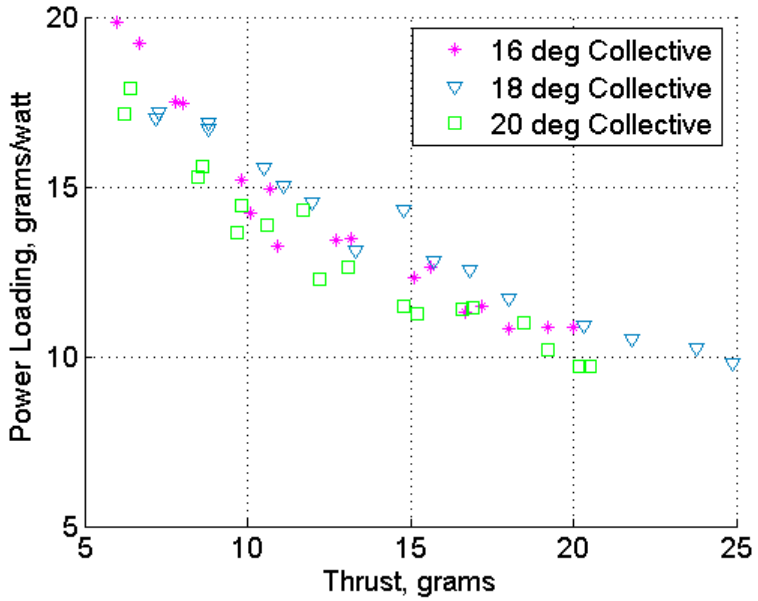

Figure 4.4: Power loading versus thrust for a rectangular blade with 7.5% cambered airfoil at different root collectives

Although the collective angle is high, the aerodynamic angle of attack along the blade is small (below stall) and most of the blade operates near the best lift to drag ratio. Because collective is fixed and rpm is varied, non-dimensional parameters such as C_T and C_P can no longer be used for comparison as the results appear as large clumps of points (shown

in Figure 4.5) rather than smooth lines, which would be the case if angle of attack was varied for a constant rotational speed. However, this plot still provides beneficial information as it can be seen that the 7.5% cambered airfoil rotor has a higher C_T for a given C_P of all the rotors. Further discussion of airfoil shape will be discussed in the following sections.

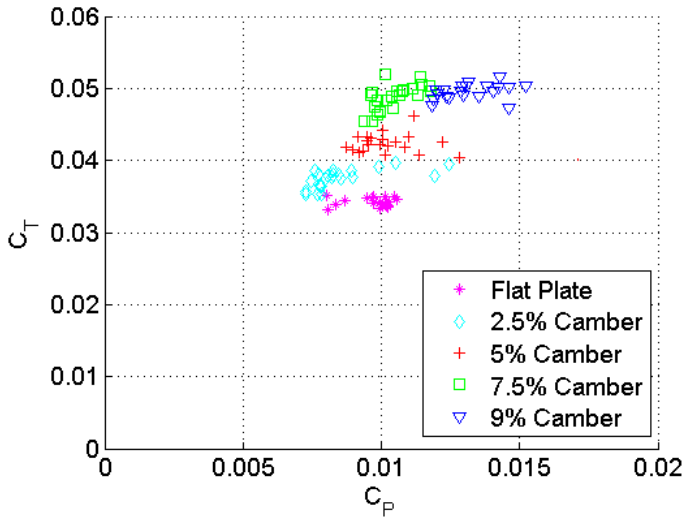

Figure 4.5: C_T and C_P for rectangular bladed rotors with different airfoil shapes

Because the rotors will have a fixed pitch when installed on the micro quad rotor, it is important to understand the variations of thrust and power with respect to varying rpm. Also, the main purpose of this study is not to design rotors with a high power loading, but to determine a method for choosing the best rotor for a particular motor to maximize propulsion system efficiency as a whole. Therefore, dimensional parameters have been used for primary comparison of thrust versus power and parameters such as power loading and figure of merit have been used for efficiency comparison. The most direct method of examining rotor performance is by comparing power loading (*T/P*) at a

constant disk loading (*T/A*). For the purposes of design, the objective is to maximize the thrust for a given power.

4.2.1 Airfoil Shape

As previously discussed in Chapter 2, at Reynolds numbers below 30,000, airfoil shape tends to have the greatest effects on performance. Cambered plate or circular arc airfoils are known to outperform traditional airfoil shapes. For rotors with a 34 mm radius, a study was done to determine the optimal amount of camber using cambered plate airfoils. Five different cambers were examined: flat plate, 2.5%, 5%, 7.5%, and 9% camber. These tests were performed on rotors without twist or taper.

Figure 4.6 shows the flat plate exhibited the poorest performance as power requirements were high at the desired thrust. All other cambers showed a decrease in the power required by more than 30% over the flat plate airfoil for an operating thrust of 15 grams. Even a modest increase in camber of 2.5% significantly improved the performance of the rotor. The rotor with the 7.5% cambered plate airfoil showed the best performance with an approximately 41% reduction in power required to produce 15 grams of thrust. In terms of power loading (thrust/power), as seen in Figure 4.7(a), it is clear that the 7.5% airfoil exhibits the best power loading for a given thrust. It is also interesting to note that the airfoils with 2.5% camber and 9% camber exhibit similar aerodynamic performance. This suggests that the addition of a small amount of camber, from 0% to 2.5%, increases the thrust for a given power but including a high camber, about 9%, results in a significant increase in the power required, having the detrimental effect by reducing the power loading. Figure 4.7(b) shows measurements of the rotor Figure of Merit (FM).

This metric gives the ratio of ideal power to actual power required for different thrusts. The rotor with the flat plate airfoil once again shows poor performance with figures of merit below 0.5 where the rotor with 7.5% cambered airfoil has FM around 0.7.

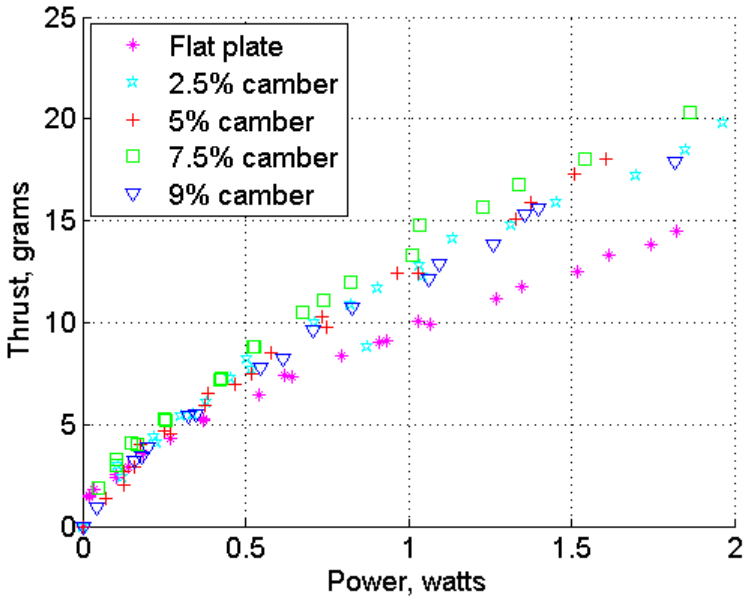

Figure 4.6: Thrust versus power comparison showing the effect of different amounts of camber for rectangular rotor blades

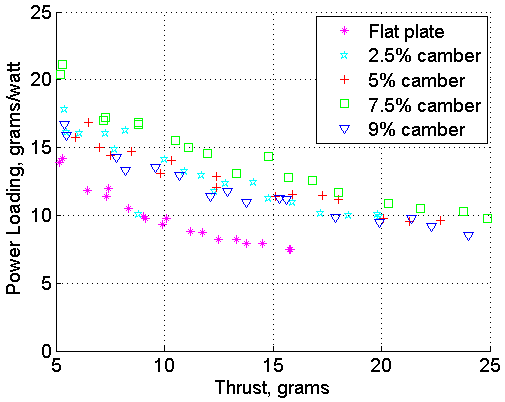

a) Power loading versus thrust

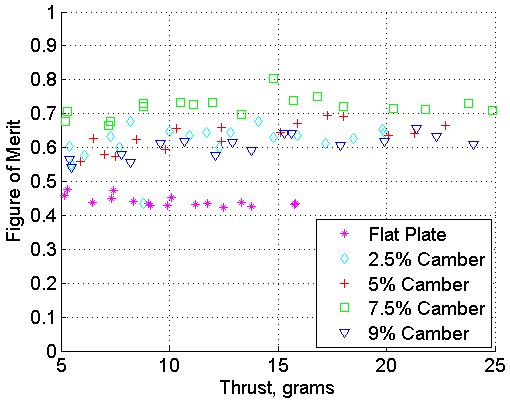

b) Figure of merit versus thrust

Figure 4.7: Comparison showing the effect of different amounts of camber for rectangular rotor blades

However, it is expected that at a constant RPM, increasing the amount of camber will increase the thrust produced. The rotor with the flat plate airfoil produces the lowest thrust at a given rpm and the rotor with the 9% cambered airfoil produces the greatest thrust at the same rpm. Figure 4.8 confirms that for a given rotational speed, increasing the amount of airfoil camber will increase the thrust for the same collective angle.

The results of the airfoil camber study showed that the 9% cambered airfoil rotor produces the most thrust for a given rpm, but the 7.5% cambered airfoil produces the most thrust at a given power. These results agree with previous studies discussed in Chapter 2 where maximum airfoil L/D occurs for cambered plate airfoils between 6% and 9% camber.

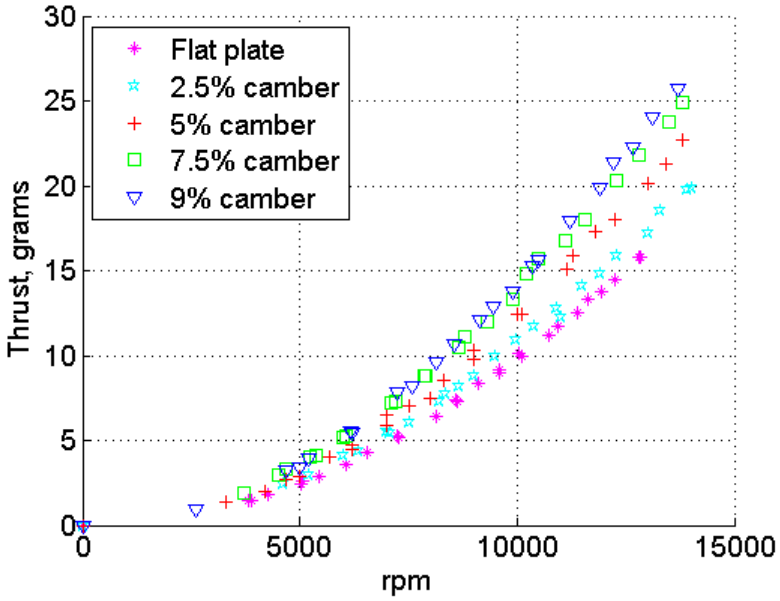

Figure 4.8: Thrust versus rpm comparison showing the effect of different amounts of camber for rectangular rotor blades

4.2.2 Max Camber Location

As previously discussed, for low Reynolds number flows, cambered plate airfoils are often used. However, the maximum camber location for these airfoils is usually placed at the mid chord. The current study examined the effects of maximum camber location by testing rotors with 7.5% cambered airfoils with max camber locations at the quarter chord, mid chord, and three-quarter chord as seen in Figure 4.9.

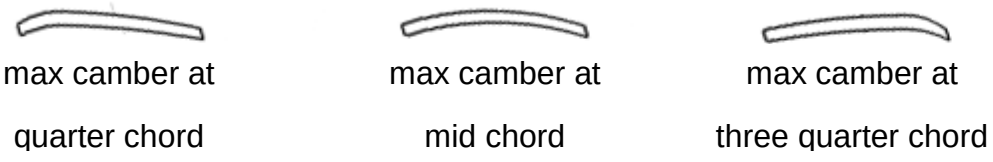

Figure 4.9: 7.5% cambered plate airfoils with maximum camber location at different chordwise locations

The study found that thrust remained constant at a particular rotational speed for all three configurations as seen in Figure 4.10. This indicates that thrust is only a function of magnitude of camber and is not a function of max camber location.

However, camber location did have an effect on power requirements and moving the maximum camber to a location other than the mid chord had a detrimental effect on the performance of the rotor as seen in Figure 4.11. This shows that to achieve the best power loading, max camber occurring at the mid chord is most beneficial.

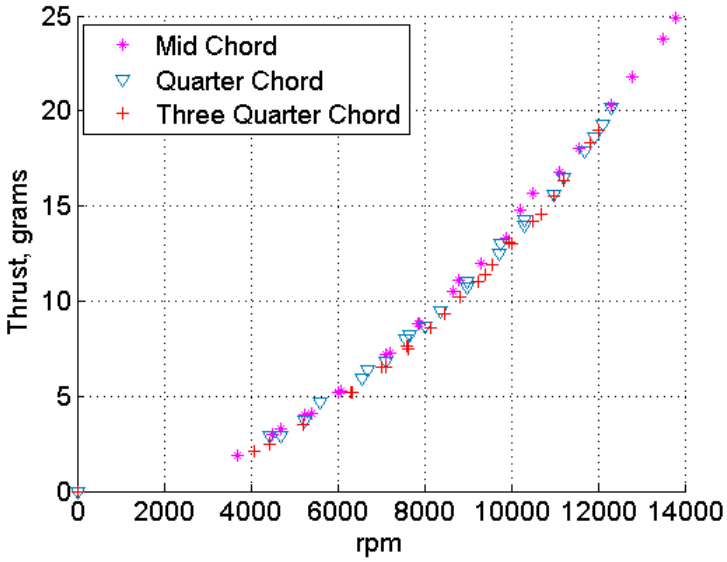

Figure 4.10: Thrust versus rpm for rotors with max camber locations at the mid chord, quarter chord, and three quarter chord

At these very low Reynolds numbers, the flow is highly sensitive to adverse pressure gradients. By placing the max camber at the mid chord, the curvature is more uniform along the chord of the blade and thus the relative strength of the pressure gradient is minimized. However for rotors with max camber at the quarter or three quarter chord, there is a region of high curvature which could result in an increased adverse pressure

gradient. This could be the contributing factor for the increase in power requirements for these rotors. Verification of this theory would require a more in-depth visualization of the flow field along the surface of the airfoil and this could be an area of future work.

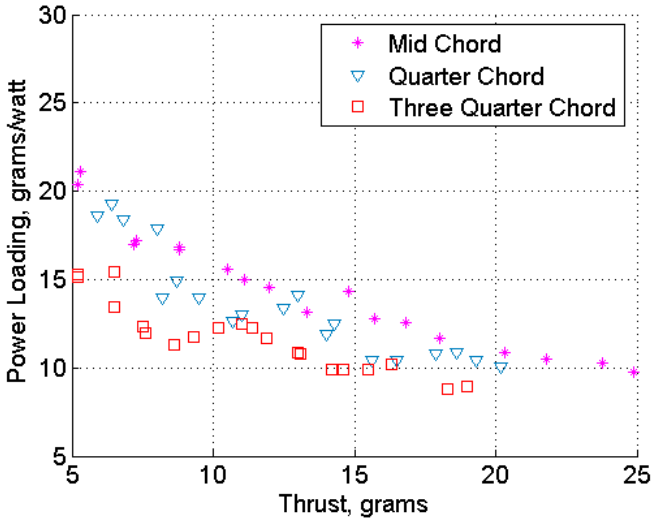

Figure 4.11: Power loading versus thrust for a rotor with max camber location at the mid chord, quarter chord, and three quarter chord

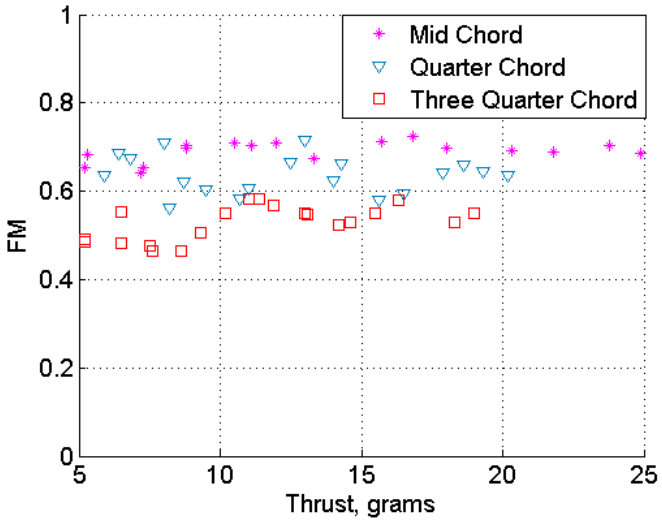

Figure 4.12: Figure of merit versus thrust for a rotor with max camber location at the mid chord, quarter chord, and three quarter chord

Once again, examining the figure of merit (FM) for these three different rotors, the results show a drop in FM from 0.7 to below 0.6 by moving the maximum camber location to either the quarter or three quarter chord (Figure 4.12.)

4.2.3 Number of blades

The current study examined the effect of different numbers of blades. In these experiments, solidity was not held constant because decreasing blade chord below a certain value would cause them to become too flexible and would deform. Therefore, the following results are normalized by solidity and show how thrust and power is changed for four different rotors. A one-bladed rotor was also manufactured and tested but this required a counter-weight to ensure that the rotor was balanced when spun. The experiments show that the one bladed rotor had the poorest performance. This is most likely due to the counter-weight producing drag and not contributing to the thrust causing it to have a very low power loading compared to the other rotor designs. The two bladed rotor had the best performance characteristics while and there was little difference between the three and four bladed rotors.

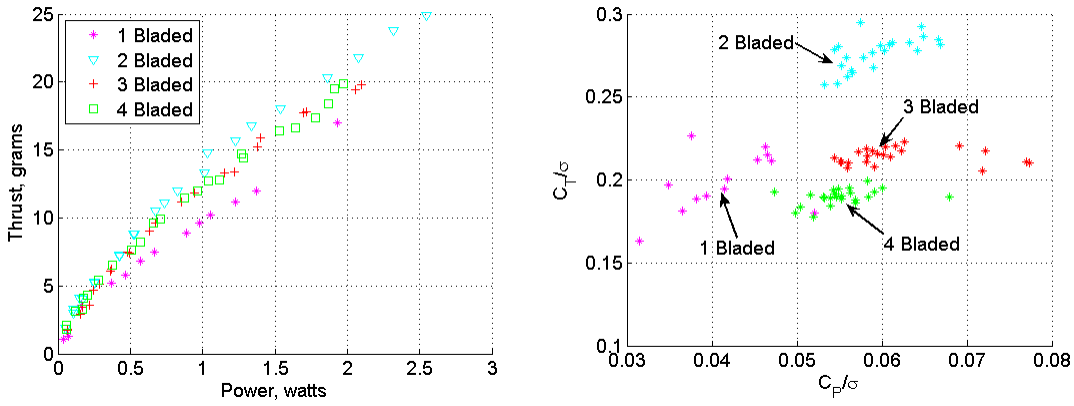

a) Thrust versus power *b)C_T/σ versus C_P/σ*

Figure 4.13: Comparison of different numbers of blades

4.2.4 Leading Edge Shape

Many computational studies using CFD have examined the effects of leading edge shape for rotors and wings operating at these very low Reynolds numbers. As discussed in Chapter 2, leading edge shape can significantly affect the performance of the airfoils at very low Reynolds numbers. A sharp leading edge is expected to have the best performance as the sharpened leading edge is expected to create a leading edge vortex that rolls along upper surface of the airfoil which helps to keep the boundary layer close to the airfoil surface. Experiments were performed for both a rotor with 2.5% camber and a rotor with 9% camber.

From the two tests, it is not easily identifiable whether a sharp or rounded leading edge is beneficial. For both the low camber and high camber rotors, thrust remains roughly the same at a given power for both the sharp and rounded leading edge rotors. Therefore, for these rotors, it can be assumed that there is no added aerodynamic benefit of having a sharp leading edge over a rounded leading edge.

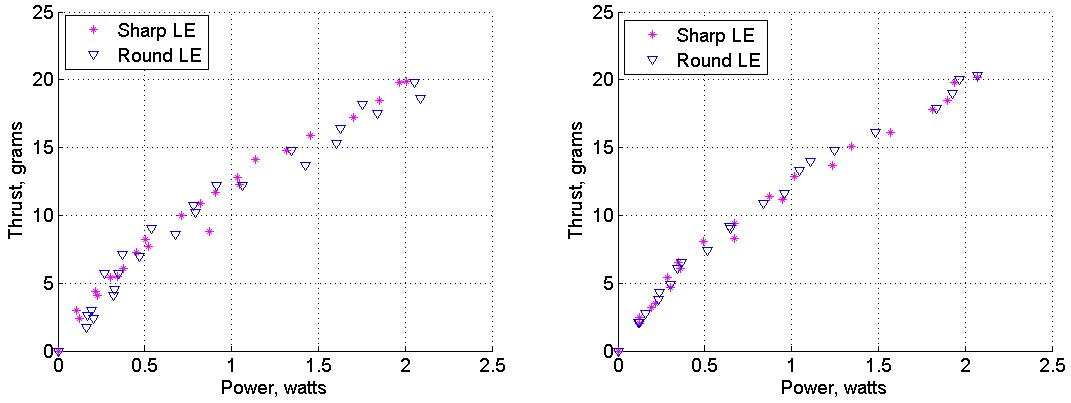

a) Rotor with 2.5% cambered airfoil *b) Rotor with 9% cambered airfoil*

Figure 4.14: Effects of leading edge shape on thrust versus power

4.2.5 Planform Taper

Previous studies [12] have suggested that the inclusion of 2:1 tip taper starting between .75R and .8R is beneficial for rotors operating at low Reynolds numbers. This phenomenon has not been thoroughly explored at these extremely low Reynolds numbers (below 30,000). Therefore experiments were performed to determine whether the taper, was beneficial in improving the power loading for the rotors.

For rotors with cambered plate airfoils where curvature is held constant, taper generally results in a reduction of the effective camber of the airfoil. It is easier to manufacture tapered blades with constant curvature than constant camber because a rectangular planform blade can simply be cut along its leading and/or trailing edge to make a tapered blade. Thus, a 2:1 taper ratio will also result in a 2:1 reduction in the camber. Furthermore, there are other geometric effects as a result of tapering the blades. A symmetric leading and trailing edge taper will result in a reduction of the camber but will not result in a geometric blade pre-twist, however, an asymmetric taper of either the leading edge or trailing edge will create a pre-twist of the blade as seen in Figure 4.15. A trailing edge taper will result in a wash-out (nose-down) twist while a leading edge taper will result in a wash-in (nose-up) twist.

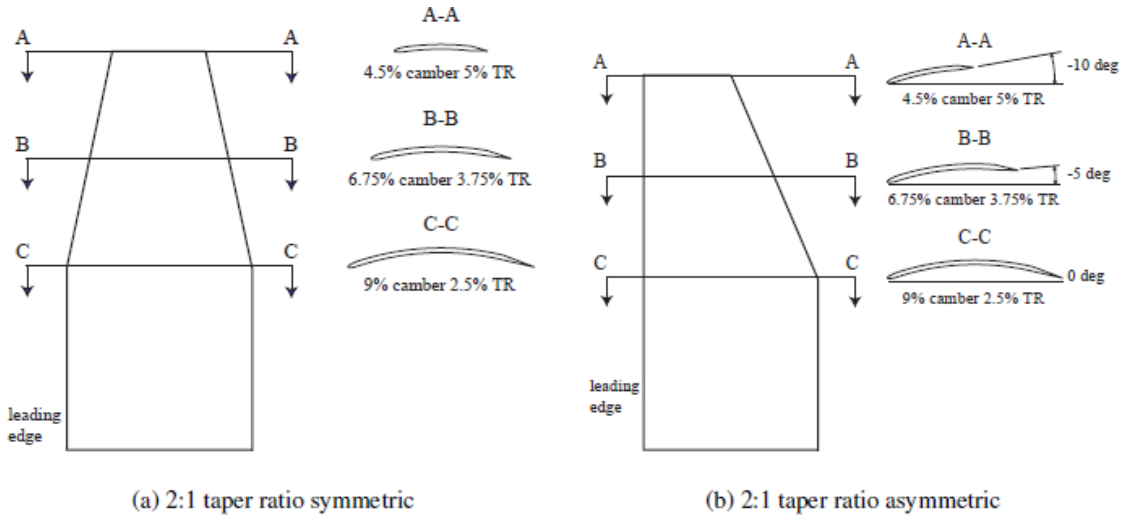

Figure 4.15: Geometric effects due to tapering a constant curvature rotor blade [12].

The current study examined the effects of symmetric planform taper to determine if symmetric taper offered any aerodynamic benefits. Symmetric taper of rotors with a 7.5% and 9% cambered plate airfoil was examined. The portion of the blade with taper was also varied and blades with full blade taper, and taper starting at .5R and .75R were examined. By introducing taper for the 9% cambered rotors, the thrust and power for a given rpm decreased; this is because of the reduced planform area. However, if thrust versus power is compared for the different rotors, as seen in Figure 4.10, there appears to be no change in the power loading. This suggests that at this scale, taper does not have a significant effect on power loading. While no aerodynamic benefits of symmetric taper could be seen, there is a hidden benefit of reducing the rotor weight by the removal of material, however, at the cost of rotor thrust for the same rpm.

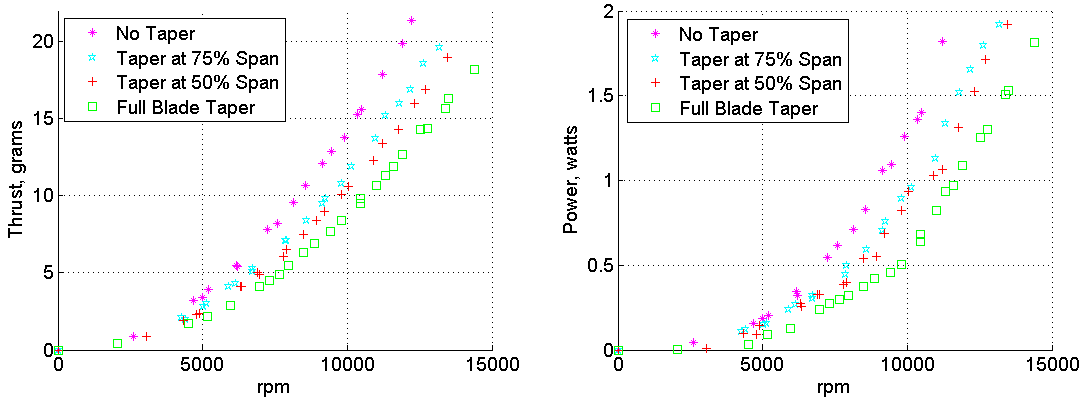

a) Thrust versus rpm *b) Power versus rpm*

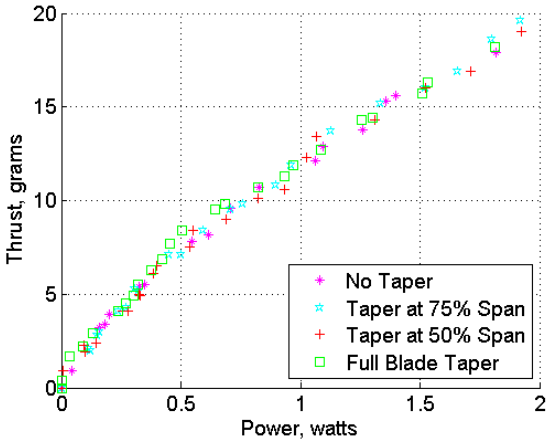

b) Thrust versus power

Figure 4.16: Effect of symmetric taper for rotors with a root airfoil of 9% camber.

No discernable trend could be determined for the thrust at a given power for the symmetrically tapered rotors. This is also reflected by examining the FM versus the thrust normalized by solidity for the different tapered rotors (Figure 4.17). At the quad rotor's operational thrust of 15 grams, all the rotors show a FM of around 0.6. These results differ from previous studies that showed that a tip taper is beneficial for both increasing the power loading and figure of merit. In these results, thrust was normalized by the blade solidity as the solidity of the blades varied from 0.13 to 0.17. Figure of merit cannot be

compared for blades of different taper unless thrust has been normalized by solidity or the blades have been designed to have the same thrust weighted solidity. Thrust weighted solidity is a means for generating an equivalent rectangular rotor blade that effects at the blade tip are more heavily weighted than stations further inboard.

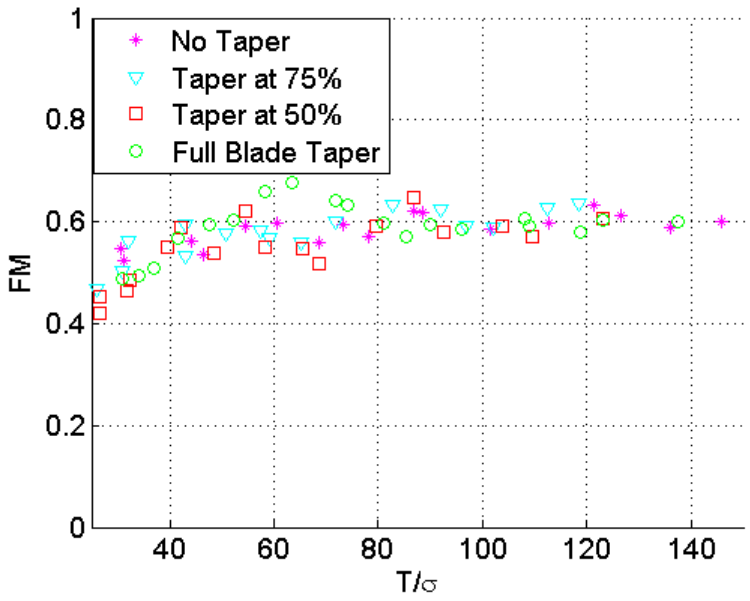

Figure 4.17: Figure of merit versus thrust for symmetric taper at different spanwise locations on the blade

To verify if there is any benefit to blade taper at this scale, a separate set of tests were done for a range of blade collectives and rotor speeds to determine if there was a combination of optimum speed and collective that might show the benefits of blade taper. Because the area of interest for the micro quad rotor is 15 grams of thrust, blade collectives of 16, 18, 20, 24, and 26 degrees were examined. Figure 17 shows results similar to those in Figure 4.16 as there appears to be no benefit to adding taper for the

micro rotors. However, there is a drop in performance of the rotors as taper is added, which is something that has not been seen before.

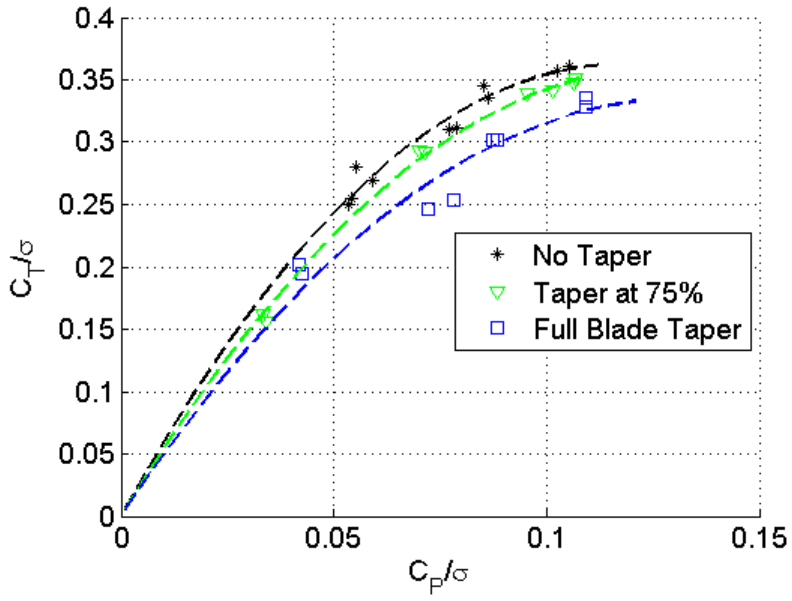

Figure 4.18: Normalized thrust versus power showing the results of tip taper and full blade taper on a micro rotor

4.3 Multiple Rotor Interference Effects

The effects of multiple rotors operating in close proximity to each other similar to the micro-quad are examined. A study by Griffiths and Leishman [28] used a free-vortex wake model to analyze the effects of rotor spacing to determine an induced power overlap factor. It was found that, as rotors are brought closer together, the induced power overlap factor actually goes below unity, suggesting that there is a region of rotor spacing that actually increase the performance of the rotors. It was postulated that when rotors are situated close to each other, but are not overlapping, there is actually a thrust and power benefit that is caused by part of one rotor operating in the tip-vortex induced upwash of

the other rotor. There is no experimental data to support this phenomenon. Also, this study was conducted at full-scale Reynolds numbers. Therefore, it was important for the design of the quad rotor to determine whether there are any changes in rotor performance, beneficial or detrimental, due to the multiple rotors operating in close proximity to each other.

4.3.1 Interaction of Two Rotors

The first set of experiments analyzed two rotors operating side-by-side in close proximity to each other. To accomplish this, a systematic study was carried out where a single rotor was measured in isolation and then an identical rotor was operated in the same plane and incrementally brought closer to the other. For this study, identical rotors, motors, and speed controllers were used to ensure ease of attaining equivalent rotational speeds between the two rotors, and as much the same operating conditions were maintained for both rotors. Thrust and power were measured on a single rotor only as it was assumed that the performance of the two rotors would be the same.

On a quad rotor helicopter, opposite rotors spin in the same direction and adjacent rotors spin in opposite directions of each other as seen in Figure 4.19. Therefore, the rotor tests were first done with two rotors spinning in the same direction, and then repeated for rotors spinning in opposite direction. This was done to see if there was also an affect due to relative direction of rotor rotation.

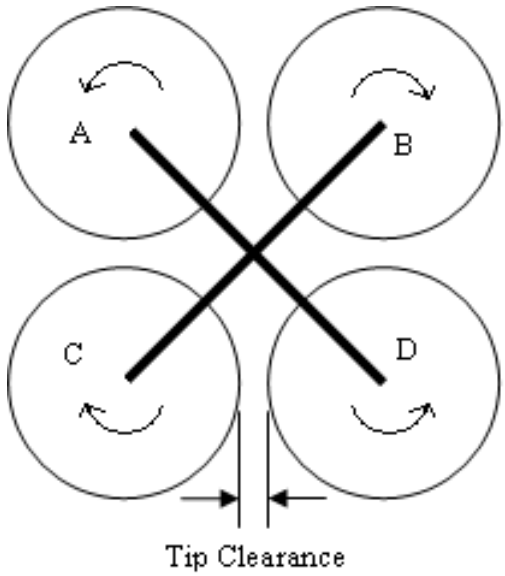

Figure 4.19: Quad rotor configuration and definition of rotor blade tip clearance used in rotor separation experiments

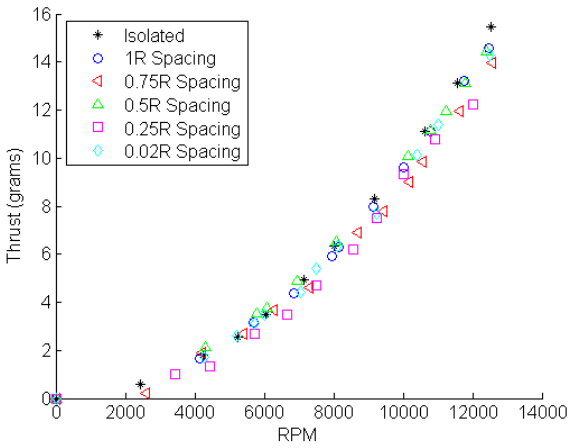

a)Thrust versus RPM

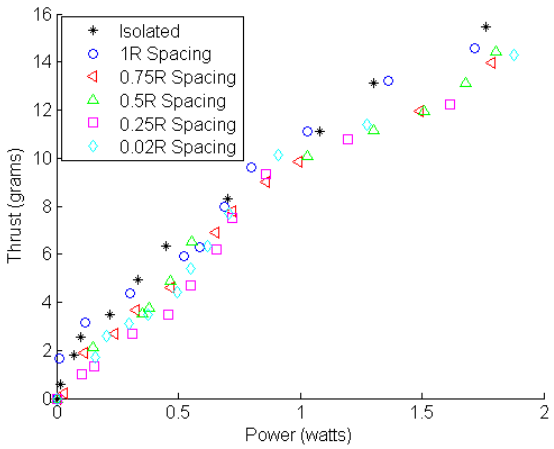

b) Thrust versus Power

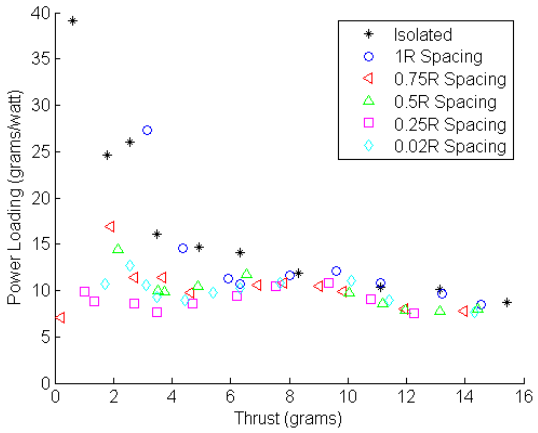

c) Power Loading versus Thrust

Figure 4.20: Effect of rotor spacing on rotors spinning in the same direction

Two methods of experimentation were performed to measure the effects of rotor spacing. The first method held the tip clearance constant and varied the rotor speed. Tip clearance was made non-dimensional by blade radius and was varied from 1 radius separation to .02 radius separation in steps of 0.25. Results for thrust versus rpm, thrust versus power, and power loading versus thrust are shown in Figure 4.20. Results for thrust versus rpm (Figure 4.20(a)) show that the variations in rotor spacing appear to have a slight effect on the thrust produced at a given RPM, but no clear trend could be identified. Examining the thrust versus power (Figure 4.20(b)), there appears to be a greater difference in the amount of thrust produced at a given power for different rotor spacing, and the trend seems to indicate that at a constant power, thrust decreases slightly as rotor spacing decreases. A better method for determining if the efficiency of the rotor is changing with rotor spacing is to look at the power loading (thrust/power) at different thrust levels as in Figure 4.20(c). At very low thrust levels, there appears to be some scatter but at higher thrust levels, results for all rotor spacing appear to converge. This indicates that for higher thrusts, aerodynamic efficiency does not change significantly with rotor spacing.

These tests were repeated multiple times to ensure that the results were repeatable. However, due to limitations with the servo tester, it was difficult to achieve the same rpm for all the measurements between tests. Therefore, a second method for measuring the effect of rotor spacing was used. This method held rotor speed constant and varied the tip clearance in order to get a clear picture of how thrust and power were directly affected by tip clearance. A separate test was also done with the rotors operating in slightly offset planes so that the rotors could be overlapped up to 40% radius.

Vinod and Baeder used CFD to predict the swirl velocity of the wake of small scale rotors with similar thrust coefficients as the current tests [29]. They found that the swirl velocity in the wake of the rotor stayed constant at 5 - 6% of the tip speed. If the interaction of the wakes of the micro rotors does affect rotor performance, the direction of swirl velocity could also have an effect. Therefore, two sets of experiments were completed to verify if there was an effect due to the relative direction of rotor rotation.

The first experiment analyzed rotors spinning in the same direction like rotors A and D in Figure 4.19, and the second experiment analyzed rotors spinning in opposite directions. Results showed that for varying rotor separation, there was no degradation in thrust or power for all operating conditions of the rotor. The power loading also showed that rotor spacing had no significant effect on rotor efficiency (Figure 4.21). Overall, there is a negligible effect of rotor separation on their performance.

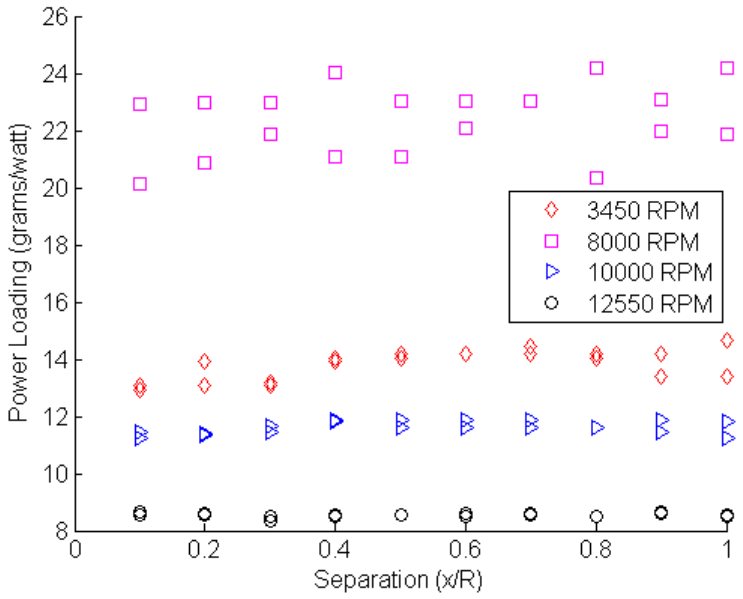

Figure 4.21: Effect of rotor separation on power loading for side-by-side rotors spinning in the same direction

A careful look into the variation of thrust and power due to rotor separation is accomplished by looking at a single operating condition. The operating condition of 5200 rpm with the zero separation and for an overlap of up to 40% of the rotor radius was examined. For the overlapping rotor case, the performance started to drop off with a reduction in thrust by up to 5%. Although it is easy to see that there is a drop-off in the thrust, variations in the power are insignificant (Figure 4.22).

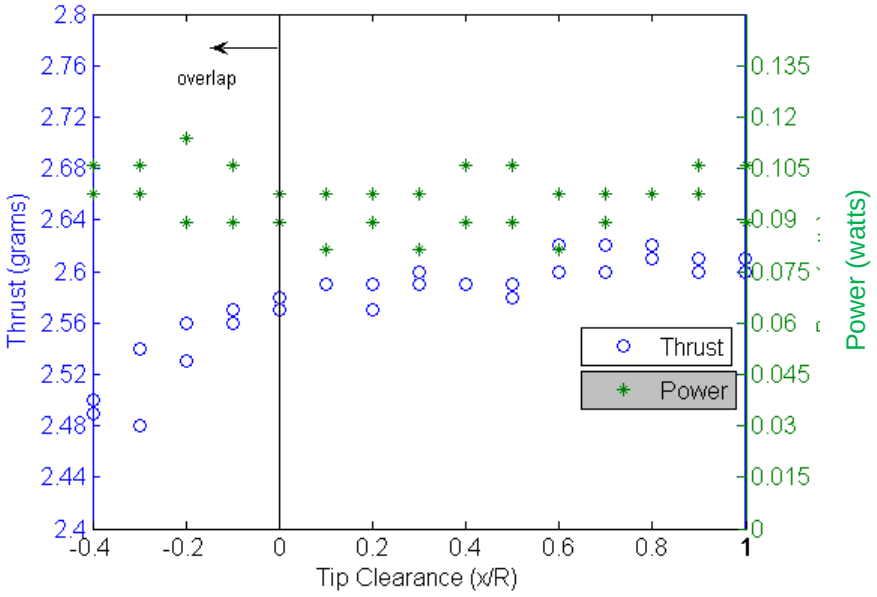

Figure 4.22: Effect of thrust and power on rotor separation at 5200 rpm

These experiments were also repeated for rotors that spun in opposite directions, which is similar to the case of rotors adjacent to each other on the quad rotor (like rotors A and B in Figure 4.19). It was not expected that these tests would be significantly different from the tests done with rotors spinning in the same direction because although the tips of the rotors do not pass each other in opposing directions, the tip vortices still rotate in opposite directions and should continue to follow the slipstream wake. Any difference that might occur would most likely be due to swirl effects due to the direction of rotor rotation.

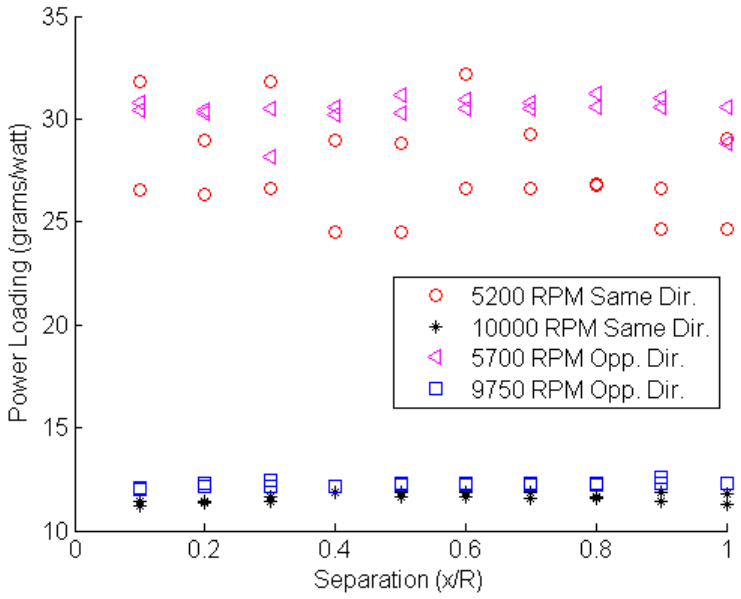

Figure 4.23: Power loading for rotors spinning in the same and opposite direction.

The experimental results for the rotors spinning in opposite directions agreed with the previously attained results for rotors spinning in the same direction. Both thrust and power remained relatively constant as rotor separation was reduced. Figure 4.23 shows a comparison between results obtained for rotors spinning in the same direction and opposite directions. It is agreed upon that overlapping rotors exhibit degradation of lift and power as the sections of the rotors that overlap experience a significant increase in disk loading.

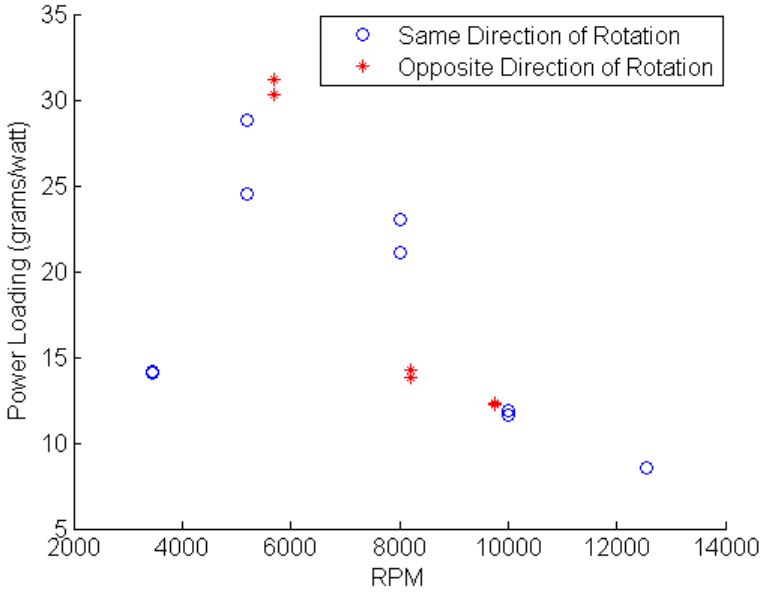

Figure 4.24: Power loading vs rpm for rotors spaced at 0.5 radius

Thrust and power measurements were also evaluated at similar rotational speeds to see if these change with the rotor's direction of rotation. Although it was seen that thrust and power did not change with rotor spacing as well as due to the direction of rotor rotation, the actual values of thrust and power may be different. Figure 4.23 shows that for at least two similar rotor rpm, the power loading stays the same, but this may not be the case for all operating conditions. Figure 4.24 shows how power loading changes with rpm for rotors spaced at 0.5 radius. The power loading for both directions of rotation appears to follow the same trend but at 8000 rpm, there appears to be a major difference. Further investigation into this region is necessary.

The use of smoke flow visualization was utilized to get a qualitative idea of how the rotors interact in close proximity to each other. The flow visualization showed when two rotors are operating side-by-side, they share a region of inflow but have two distinct

wakes as shown in Figure 4.25. This is seen even when rotor spacing is very close where tip clearance is 10% of the radius. Figure 4.25 shows two rotors operating side-by-side and spinning in opposite directions with a 10% radius tip clearance.

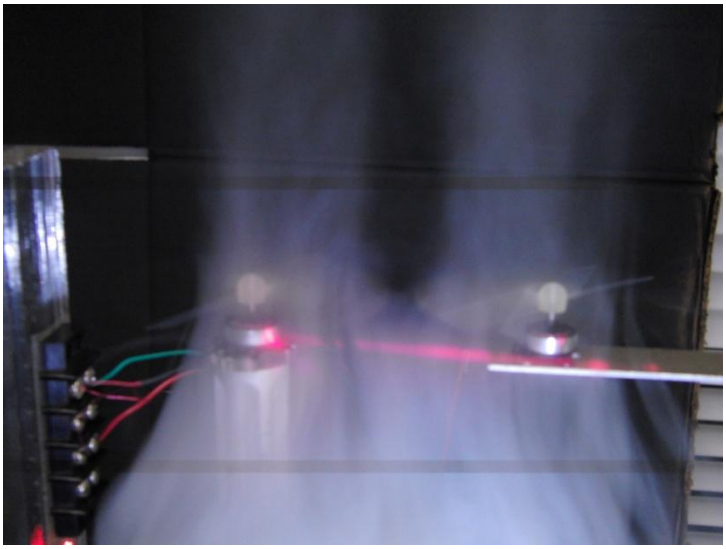

Figure 4.25: Two micro rotors operating side-by-side.

Figure 4.25 shows very clearly the two separate, contracting wakes of the rotors. Observations from the flow visualization suggest that there is a region between the rotors that experiences little momentum change and the wakes themselves continue to contract as in the isolated case. The flow visualization also provided clues as to the effect of rotors spinning in either the same direction or opposite direction as the swirl of the wake could also be seen. For rotors at this scale, inflow is about twice the value of a full-scale rotor and it was suspected when a second rotor was placed adjacent to an isolated rotor, the inflow velocity may be affected. However, initial results from the smoke flow tests showed that inflow was not significantly affected.

4.3.2 Interaction of Four Rotors

Measurements of the thrust and power were also done for the case where all four rotors were operating near each other as they would for the full quad rotor. The test setup simulated the current quad rotor design and all four rotors were spaced accordingly. Since rotor spacing was fixed, approximately 0.3R, the tests were compared to results for a single rotor operating in isolation over a range of RPM (Figure 4.26). The experiment shows that there is a slight decrease in rotor thrust when influenced by the addition of three other rotors operating side-by-side and in close proximity. This decrease in thrust is on the order of 1 gram, and occurs at the highest operating rpm which would translate to a total decrease of 4 grams of thrust over all four rotors on the microquad. For hover, this translates to a total decrease in thrust of approximately 7%. A comparison of the power between the single and quad rotor were also done but no distinguishable trend existed between the two tests.

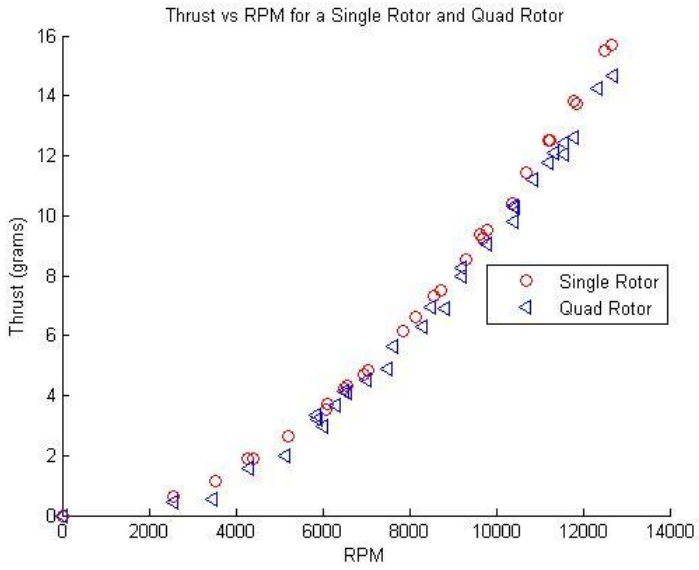

Figure 4.26: Thrust versus rpm comparing a single rotor against quad rotor

4.4 Brushless Motor Testing

Brushless motors work as the mechanical source of power for the rotor blades as they convert the electrical energy of the batteries into mechanical power. There is an efficiency associated with any conversion of power from one type to another. The efficiency of the rotors was discussed in terms of power loading which was defined as the amount of thrust per unit power the rotors were capable of producing. For the brushless motors, efficiency is determined by the percentage of electrical power that is converted into mechanical power through torque and rotational speed.

4.4.1 Motor Test Setup

In order to accurately determine the efficiency of the brushless motors, a specialized setup was used that included a motor dynamometer and a three-phase precision power analyzer. Layout of the test setup is shown in Figure 4.27.

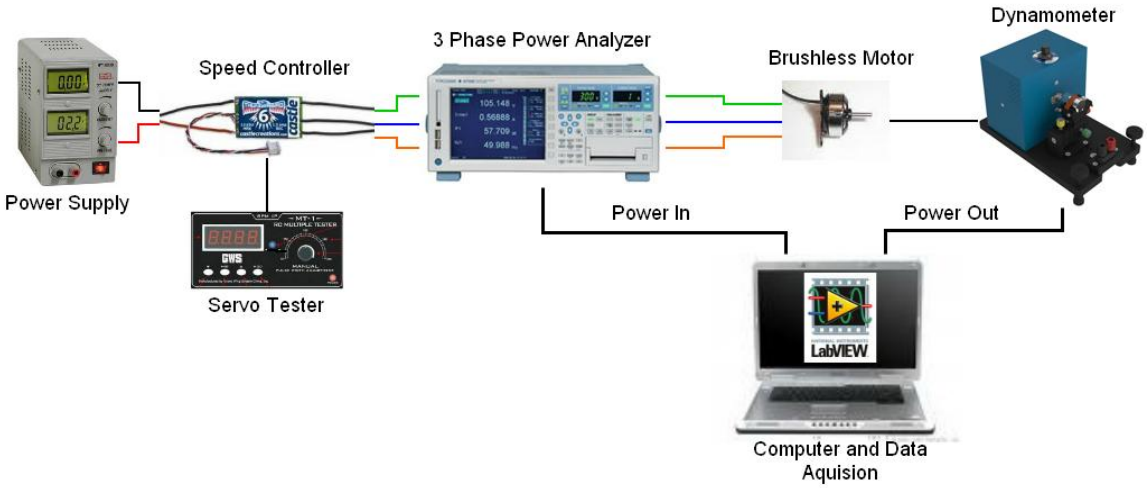

Figure 4.27: Brushless motor test setup

The setup utilized the same motor, speed controller, and servo tester that were used for all rotor testing. Test data was acquired by first setting the free rotor speed – the speed of the motor with no applied torque. As discussed in Chapter 2, the rotor refers to the rotating portion of the motor while the stator is the fixed part. The Labview software then collected a baseline of the torque required to spin the rotor casing and rpm and then used a ramp brake to apply a load on the motor. This load was increased, thus increasing the torque and decreasing the rpm. Once the rpm had reached a pre-set value, the brake slowly decreased the load on the motor until it had reached its free speed again. This ramp up/down method then allowed the software to analyze the hysteresis curve to eliminate the effects of rotor inertia. When applying torque to the motor, decreasing its speed, the inertia of the rotor applies a slight resistive force countering the speed decrease. The opposite occurs when the resistive force is released as the rotor speed "lags" behind as the rotor rpm increases. Thus, a slight hysteresis is seen when performing the tests. This relative magnitude of this hysteresis can be reduced by applying and releasing the braking force slowly.

The Yokogawa WT-3000 precision power analyzer measured the three phase power from the speed controller going into the brushless motor, and a Magtrol MicroDyne hysteresis dynamometer was used to measure the rotational shaft power output of the motor. These signals were fed into the computer and were simultaneously read and synched to provide the voltage and amperage of each phase as well as the electrical power going into the motor as well as the torque, rpm, and mechanical output of the motor. Efficiency was calculated based upon the ratio of output power to the input power. The dynamometer is highly accurate with the ability to measure rotational speeds as high as 100,000 rpm and

torques up to 4 mN-m, having a toque measurement accuracy of less than 0.04 mN-m and a speed measurement accuracy of 0.02% of the reading. The power analyzer is equally accurate with a basic power measurement accuracy of 0.02%. This provides highly accurate measurements of both the electrical and mechanical power going into and coming out of the motor respectively.

4.4.2 Brushless Motor Test Results

The free speed of the motor is based upon the input signal coming from the speed controller. This speed controller deciphers the PWM signal coming from the servo tester that acts as a throttle for the motor. Thus, a PWM signal with a shorter width will result in a lower free rotor speed and visa versa. Motor tests were performed at varying rotor speeds for two different brushless motors– an AP03 7500kv and an AP03 4000kv brushless motor. These two brushless motors have the same number of poles and stators, but the 4000kv motor has more coil windings than the 7500kv motor and should thus have a higher torque. Manufactures use the “kv” rating as a theoretical free rotor speed per volt for the motor. This speed is not necessarily accurate, but does give an indication as to whether the motor is high speed, low torque or low speed, high torque.

A brushless electric motor will exhibit linear behavior with respect to torque and rpm. As torque increases, rpm will decrease in a linear fashion as seen in figure 23. The slope of the torque/rpm curve indicates whether the motor is designed for high speed or high torque. A steep negative slope, as seen with the AP03 4000kv motor, indicates that it is designed for torque as a higher torque does not significantly decrease rotation speed as with the AP03 7500kv motor. Figure 4.28 also gives an indication to the power required

as power is the product of torque and rpm. Over most of the range of this figure, the AP03 4000kv motor is capable of achieving the same torques at a lower rpm and thus, a lower power.

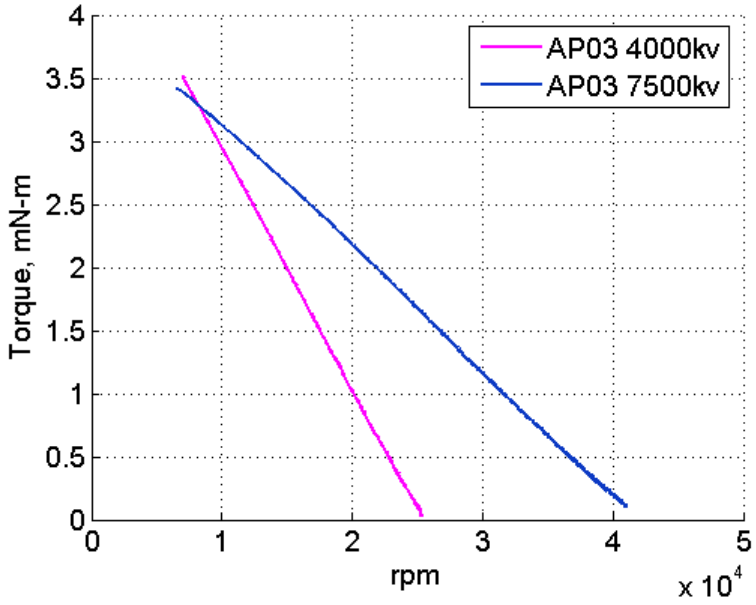

Figure 4.28: Linear variation of torque and rpm for two brushless motors

As previously discussed, the motor's efficiency is a function of many aspects of its design including number of poles, stators, coil windings, winding style, etc. The motor's efficiency is also a function of its "throttle" setting or free rotor rpm setting. These free rotor speeds are achieved through variation of the PWM signal going into the speed controller. A PWM signal with a 1 ms delay would correspond to a "closed throttle" while a signal with a 2 ms delay would correspond to 100% or full "open throttle". Figure 4.29 and Figure 4.30 show the variation of motor efficiency with "throttle" setting for both motors with settings shown in percentage of full. Low throttle settings correspond to

low maximum efficiencies and the motor's overall maximum efficiency corresponds to a full throttle setting.

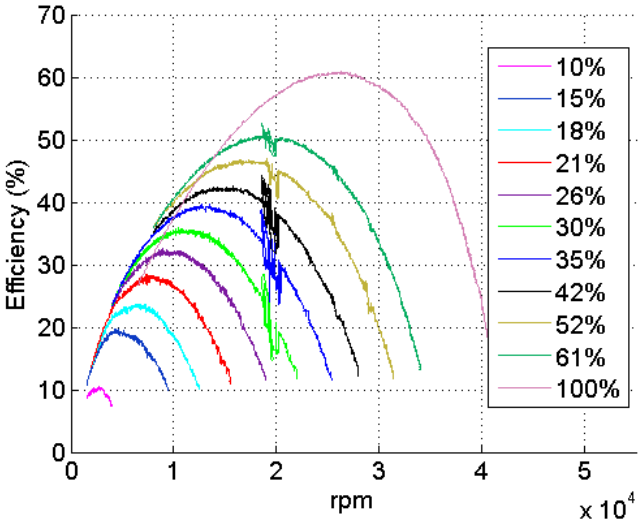

Figure 4.29: Efficiency versus rpm at different throttle settings for an AP03 7,500 kv brushless motor

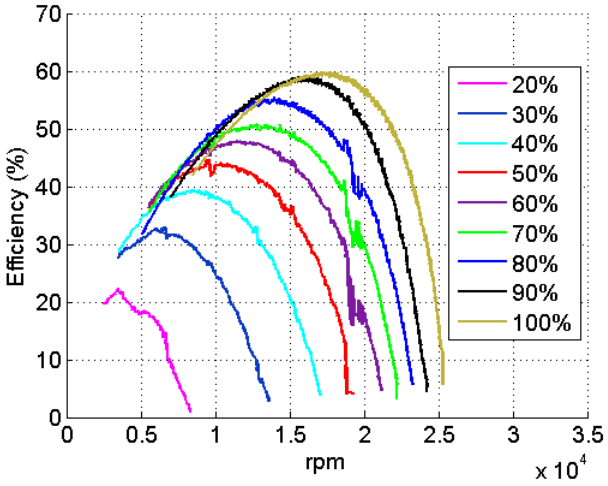

Figure 4.30: Efficiency versus rpm at different throttle settings for an AP03 4,000 kv brushless motor

For the brushless motors, max power is most easily seen by plotting the torque and rpm on a log-log graph. Figure 4.31 clearly shows that the 4,000 kv rated motor outputs a lower power than the 7,500 kv rated motor at the same torque.

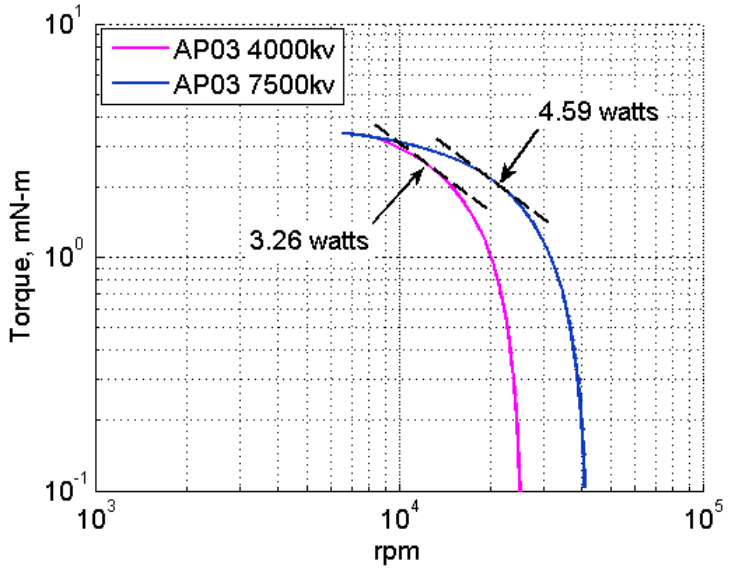

Figure 4.31: Torque versus RPM showing location of max power for two brushless motors

The 7,500 kv and 4,000 kv motor both exhibit similar maximum efficiencies of around 60%. However, the speed at which maximum efficiency occurs for the 4,000 kv motor is nearly 35% lower than the 7,500 kv motor. As was seen from the torque versus rpm lines for these two motors, it is expected that the 4,000 kv motor, operating at the lower rpm for the same torque, is able to achieve maximum efficiency at a lower power as well. This is the case for these two motors as seen in Figure 4.32. At a lower shaft power, the AP03 4,000 kv motor is capable of attaining efficiency near equivalent to the 7,500 kv motor. This is because torque is linearly related to the input current and because both motors are

operating at the same input voltage, the 4,000 kv motor uses less input power for the same torque and thus operates at an equivalent efficiency at the lower power.

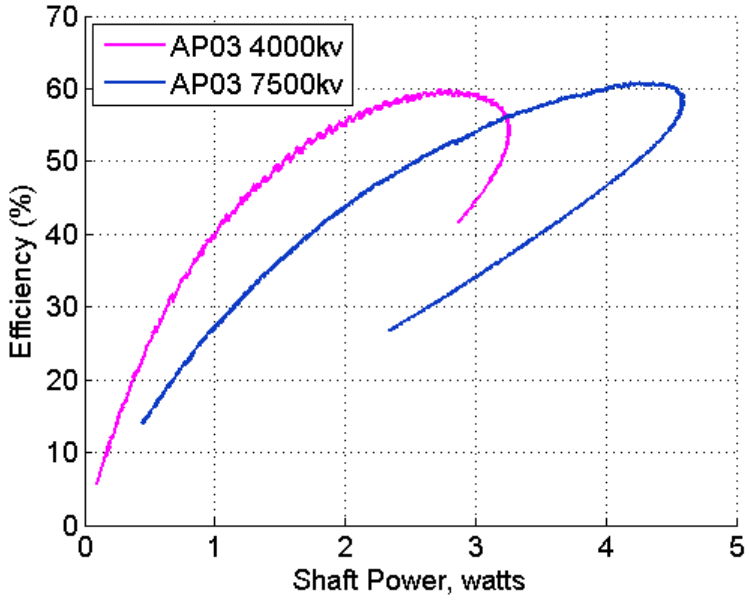

Figure 4.32: Motor efficiency versus shaft power for two different motors

From the figure, it can be seen that at a particular shaft power, there can be two associated efficiencies. This phenomenon is because the shaft power is directly related to the torque and rpm. There are two different torques and rpms that correspond to a single shaft power. Torque can be high and rpm low or rpm cam be high and torque low. However, efficiency will be higher for one combination over the other.

It is also seen that the motor is operating at a lower shaft power corresponding to a lower rpm. Therefore, the torque at which the maximum efficiency occurs is the same for both motors as seen in Figure 4.33. The torque stays the same for both these motors because the only difference between them is the number of coils in each stator. The 4,000 kv motor uses a thinner gauge wire and has more coil windings, thus, allowing it to operate

at the same torque as the 7,500 kv motor but at a much lower rpm. This figure also shows that the motor with the lower *kv* rating is capable of maintaining higher efficiency values at higher torques which is also expected since the motor is designed for torque.

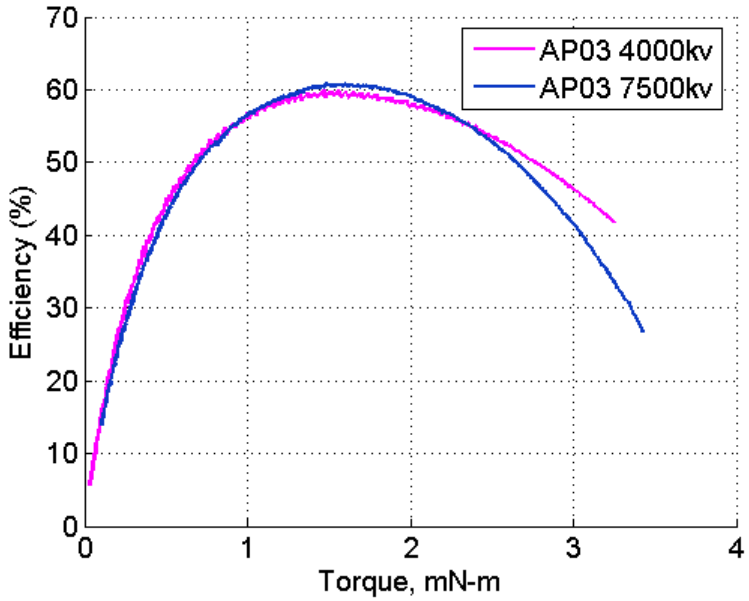

Figure 4.33: Efficiency as a function of torque for two brushless motors

It is difficult to see exactly how the motor efficiency changes as rpm and torque are changing since torque and rpm are coupled. Therefore, it is more useful to examine the efficiency at different rotational speeds with lines of constant torque. This is normally accomplished by applying a constant torque and then changing the PWM input until the desired rpm is reached. However, the dynamometer makes it easy to obtain complete performance curves and then find the points of constant torque in post processing. Figure 4.34 shows the efficiency variation between the two motors for constant torque.

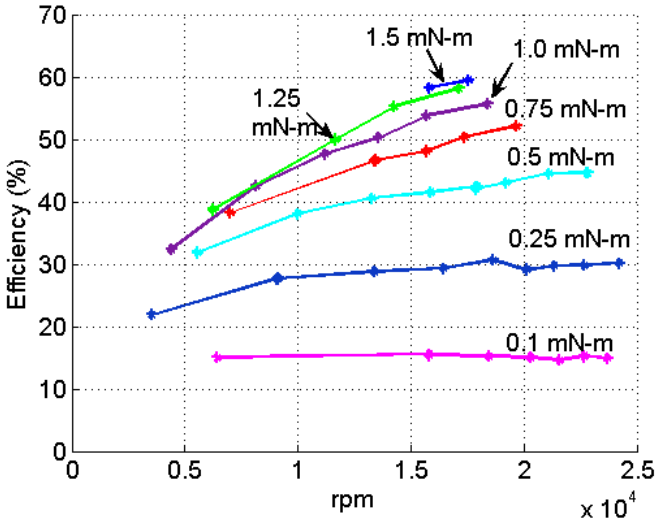

a) AP03 4,000 kv brushless motor

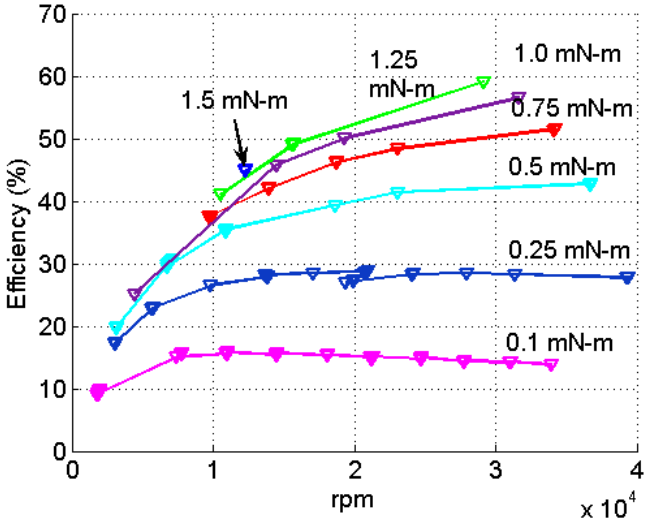

b) AP03 7,500 kv brushless motor

Figure 4.34: Efficiency versus rpm at constant torque for two brushless motors

Here it can be seen that at a given torque, the 4,000 kv motor is able to reach a higher efficiency. These plots will become useful in coupled rotor/motor pairing as the rotor's

torque and rpm at its operating thrust can be plotted as a point on this graph and the efficiency at which the motor will operate can be easily determined

4.5 Coupled Rotor and Motor Tests

In the previous section, the efficiencies of the individual components (rotor and motor) that constitute the propulsion system for the micro quad were examined. A rotor study was performed to examine how thrust and power changed for different rotor designs as well as determine the efficiencies of various designs in terms of rotor power loading. Brushless electric motors were tested to examine efficiency of the motors with torque and rotation speed. By coupling these two tests into one and measuring the electrical input power to the system and the aerodynamic output power from the rotors, estimates of the complete propulsion system efficiency were obtained. For these experiments, voltage and current were measured from the power supply before the motor speed controller and torque and rpm were measured at the rotor. Although these tests include the unknown efficiency of the speed controller and servo tester power electonics, power electronics for these systems have very high efficiencies and thus any power loss at the speed controllers was neglected.

In order to determine how overall propulsion system efficiency is affected by various rotor designs, efficiency was measured for the rotors during the rotor study at the beginning of the chapter. Efficiency was defined as the percentage of input electrical power that was converted to aerodynamic power at the rotor by measuring the rotor's torque and rpm. Although examining the propulsion system efficiency at a particular thrust might initially seem to be the best method for determining the best rotor for the

particular motor, it is important to remember that one rotor might be operating at a higher power than another. Therefore, there are two parameters that are important and must be maximized – overall propulsion system efficiency and rotor power loading. This phenomenon is easily illustrated by examining the propulsion system efficiency for rotors with different cambered airfoils.

In Figure 4.35, it can be seen that for an operating thrust of 15 grams, the most efficient rotor appears to be either the 5% cambered or 9% cambered rotors and the least efficient rotor is the 7.5% cambered rotor. It was found previously that the 7.5% cambered rotor had the best power loading. However, each of these rotors is operating at a different power and, therefore, examining the propulsion system efficiency against thrust is misleading as it does not provide any indication of the power consumed by the system. Examining the propulsion system efficiency against power loading is a more reliable method. By examining the propulsion system efficiency against rotor power loading as seen in Figure 4.36(a), it can be seen that the rotor with the 5% cambered airfoil is actually the most efficient rotor at all operating conditions. This rotor has a higher efficiency at a particular power loading which means that it requires the minimum amount of mechanical power from the motor to operate at a particular thrust as well as having a better overall propulsion system efficiency. To verify this is the case, a new parameter called electrical power loading can be used to evaluate which rotor gives the best efficiency for the system. Electrical power loading is the rotor thrust divided by the electrical input power to the system as can be seen in Figure 4.36(b).

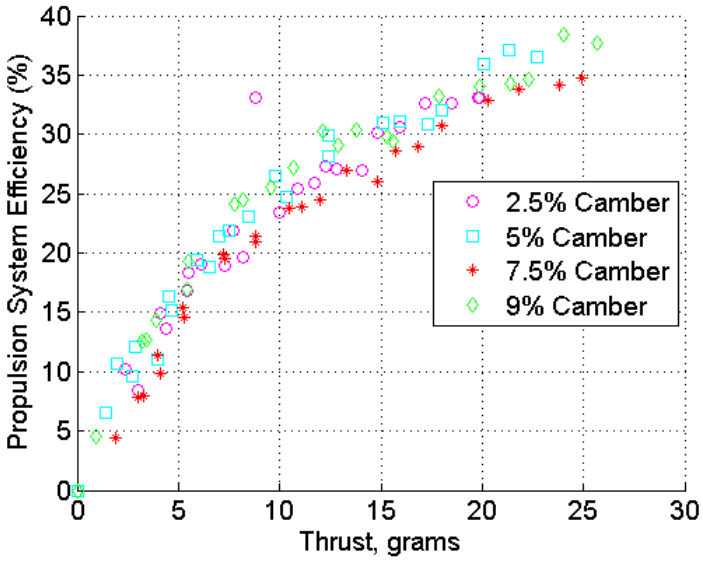

Figure 4.35: Overall propulsion system efficiency versus thrust for rotors with different airfoils

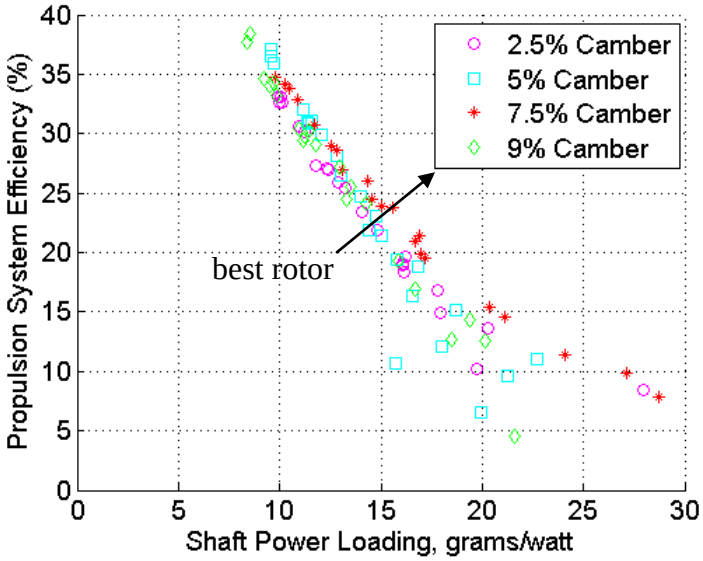

a) Propulsion system efficiency versus shaft power loading

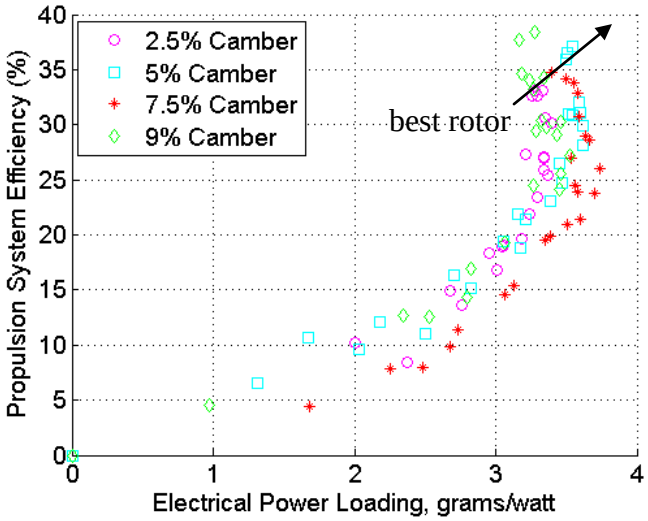

b) Propulsion system efficiency versus electrical power loading

Figure 4.36: Overall propulsion system efficiency for rotors with different airfoils

It is interesting to note that when examining propulsion system efficiency against shaft power loading, efficiency decreases as power loading increases. High power loadings occur when the rotors are operating at very low thrusts and powers and therefore the motors are operating at very low rpm. This combination results in low propulsive system efficiencies at high power loadings. The operating power loading for the micro rotors is generally between 10 – 15 grams/watt. This is also where we see the best propulsive system efficiency. However, if we examine the rotors using electrical power loading, more efficient rotors should result in a higher propulsion system efficiency which is reflected in Figure 4.36b. These results prove that although a particular rotor design might have the best aerodynamic performance, when incorporated into the system, the efficiency of the motor also plays a large role in the system's efficiency and the rotor with the best power loading might not provide the best propulsion system efficiency.

Once again, the effects of max camber location were examined (Figure 4.37). The results show that all of the rotors are capable of reaching a maximum propulsion system efficiency of near 35%. The rotors with max camber at the quarter or three quarters chord all have a lower power loading than the rotor with camber at the mid chord. Therefore, this confirms the results of the single rotor testing that optimum camber location occurs at the mid chord.

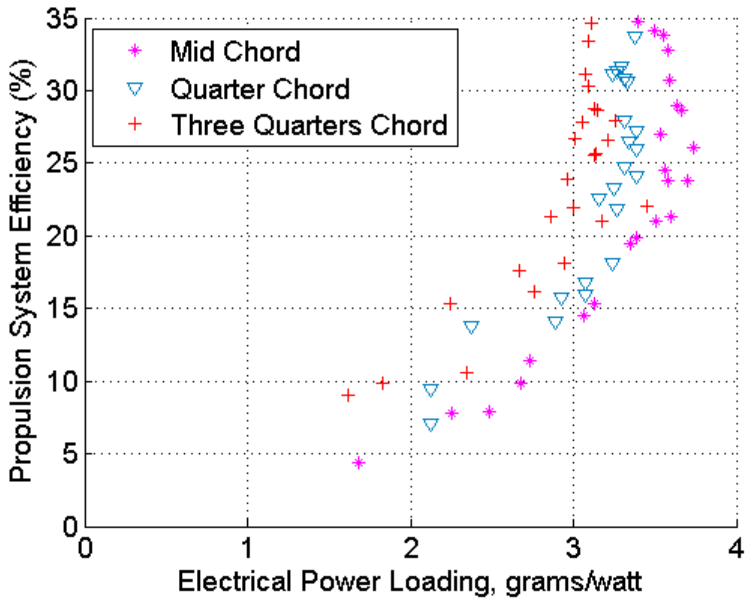

Figure 4.37: Effect of max camber location on propulsion system efficiency and electrical power loading

In the rotor study, it was seen that for symmetrically tapered rotors, there was no effect on power loading due to taper location when thrust was varied through rpm. Therefore, based upon power loading alone, a taped blade would have the same performance as a rectangular blade. However, when thrust was varied by collective, taper was shown to have a detrimental effect. Examining propulsion system efficiency for the symmetrically

tapered rotors, a trend emerges that shows that having blade taper over a larger portion of the blade radius would be detrimental in terms of efficiency versus electrical power loading. This is shown in Figure 4.38. However, taper starting at the .75R does appear to be beneficial in terms of electrical power loading. Here, the aerodynamic performance benefits that have been examined in previous studies [12] are reflected in the electrical power loading for the rotor where a 2:1 tip taper at 75% span has the best performance.

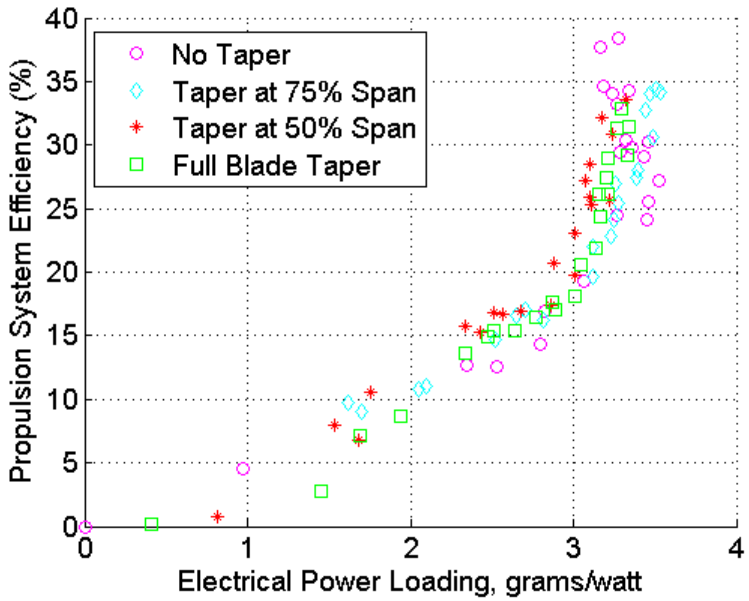

Figure 4.38: Overall propulsion system efficiency versus rotor electrical power loading

When collective was varied, taper was shown to be detrimental as thrust decreased for a given power. Plotting these results from those tests to determine if there is an overall benefit to the propulsion system as a whole results in a similar conclusion as was found in the rotor tests alone that no blade taper is most beneficial.

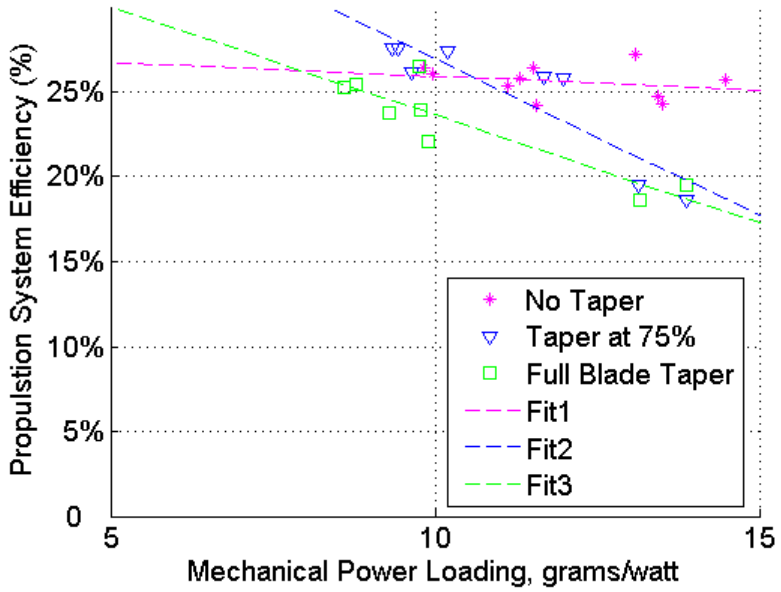

Figure 4.39: Propulsion system efficiency versus mechanical power loading for tapered rotors

The effect of number of blades was also examined to determine if propulsion system efficiency could be increased by changing the number of blades. The rotor with two blades was shown to have the best power loading and thus, best performance in the parametric study. By examining the propulsion system efficiency against electrical power loading, it can be easily seen that the rotor with two blades gives the best propulsion system efficiency and electrical power loading. Therefore, the two bladed rotor uses the least amount of electrical power for a given thrust and operates at a better motor efficiency than the rotors with one, three, or four blades.

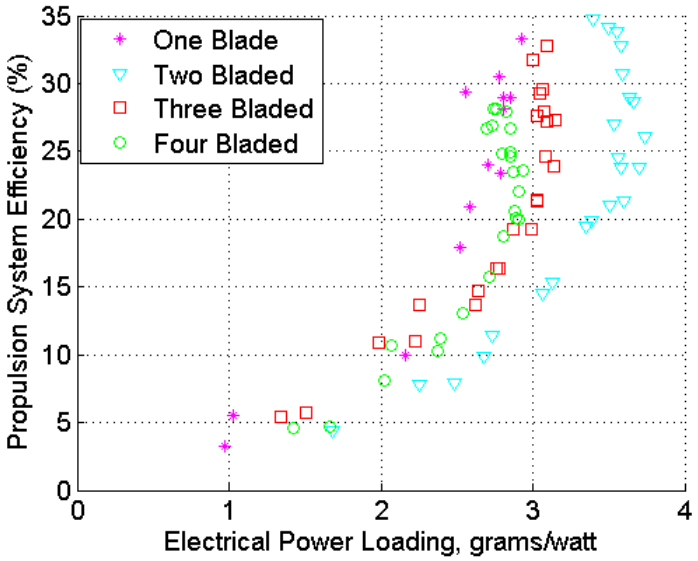

Figure 4.40: Propulsion system efficiency versus electrical power loading for rotors with different numbers of blades

4.6 Motor Rotor Pairing

All of these coupled motor and rotor tests reflected the results that were seen in the single rotor tests at the beginning of the chapter. These results show which rotors offer the best power loading and propulsion system efficiency. However, these tests do not indicate how to increase the propulsion system efficiency. The efficiency in all of these experiments remained low and at the operating condition where the rotor were producing 15 grams of thrust, rotor efficiency was near 30%. As was previously discussed, these low propulsion system efficiencies are the underlying reason for the low endurance of many MAVs and particularly the micro quad rotor.

The brushless motors show the capability to reach efficiencies as high as 60%. If this efficiency could be reached, the endurance of the vehicle would also double. However, this might not be realizable, as maximum efficiency of the motors only occurs at their full

throttle setting, which would not allow the vehicle margins for maneuvers, climb, or payload. Therefore, it may only be realizable to operate the micro quad rotor at throttle settings between 50% and 75%. This would reduce the maximum attainable efficiency to around 50%.

As was seen in the brushless motor experiments, two main parameters affect the efficiency of the motor – the operating torque and rpm. In the rotor tests, it was seen that the parameters that most affected the power loading of the rotors infuenced their performance over the entire range of rotational speeds. Therefore, the torque and rpm of the rotors is mainly influenced by the rotor collective. With fore knowledge of the rotor's torque and rpm at its operating thrust, and the motor performance curves, a method for proper rotor and motor pairing can be used for propulsion system design.

In the coupled rotor and motor tests, the AP03 7,500 kv motor was used as it is currently incorporated in the micro quad rotor. A rectangular rotor with a 7.5% cambered plate airfoil was plotted on the motor constant torque curves as seen in Figure 4.41. It shows that at the rotor's operating torque and rpm, the motor will operate at an expected efficiency of around 37%. If the same rotor was to be used with the AP03 4,000 kv motor, there would be an expected efficiency increase of nearly 10% as is illustrated in Figure 4.42. This 10% increase in motor efficiency, using the same rotor, would not be known if selecting a motor solely based upon its *kv* rating.

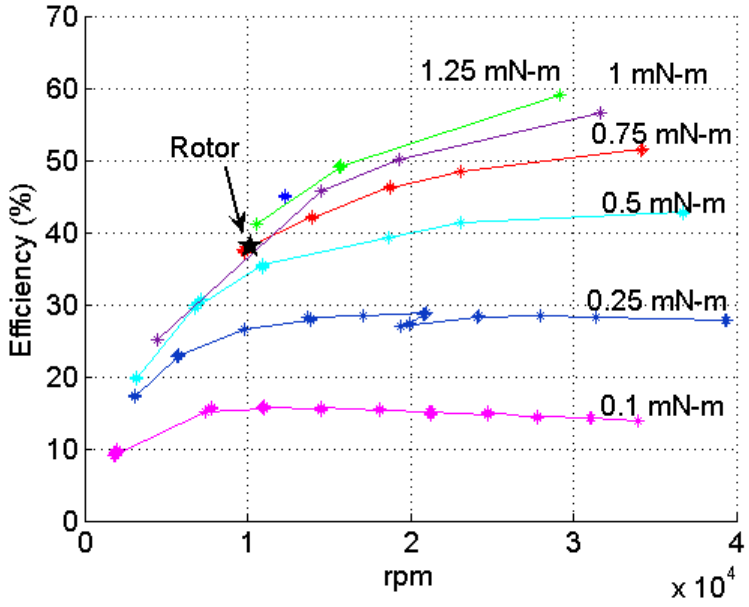

Figure 4.41: Expected motor operating efficiency with a rectangular rotor with 7.5% cambered airfoil

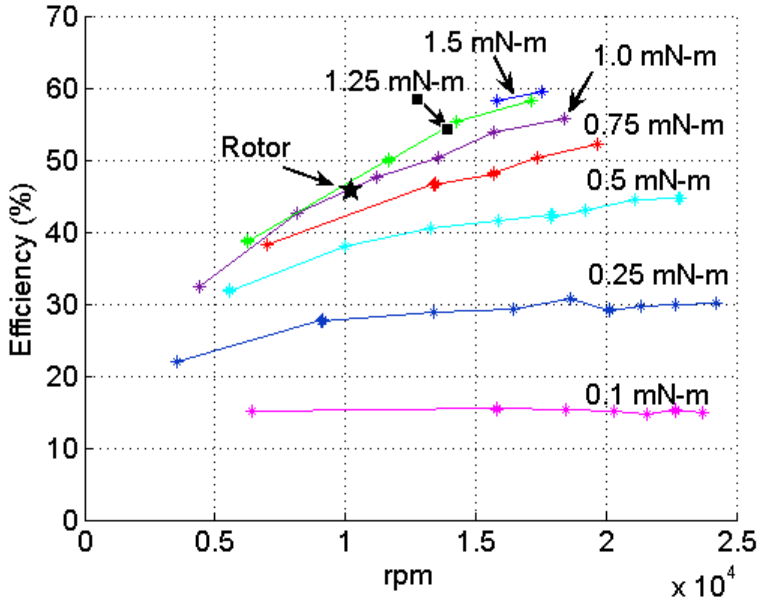

Figure 4.42: Expected motor operating efficiency with a rectangular rotor with 7.5% cambered airfoil

These plots of motor efficiency provide valuable insight into proper motor rotor selection and it becomes much easier to design a rotor to maximize propulsion system efficiency when the motor efficiency curves are known. Thus, for a high speed and low torque motor such as the AP03 7,500 kv, a rotor that operates at 20,000 rpm with a torque of 1.0 mN-m would be beneficial, where rotor that operates at 15,000 rpm and 1.25mN-m of torque would be more beneficial for the AP03 4,000 kv motor.

4.7 Summary

The individual rotor tests were used to determine how parameters such as airfoil shape, max camber location, leading edge shape, number of blades, and planform taper affect the rotor efficiency through figure of merit and power loading. It was seen that the rotor alone with a 7.5% cambered plate airfoil demonstrated the best overall performance both in terms of power loading and FM. Max camber location at the mid chord was also shown as having the best performance indicating that it minimized the adverse pressure gradient along the chord. The use of a two bladed rotor was also found to be optimum both in terms of power loading and weight savings. The results of the experiments for rounded and sharp leading edged blades showed no indication that a sharp leading edge was better than a curved leading edge. The results of the planform taper location were also surprising as they indicated that non-tapered blades were more beneficial than tip taper, half blade taper, or full blade taper. These results indicate that at this scale, rotor blade performance is quite dependent on Reynolds number as the results do not correlate with experiments carried out at higher Reynolds numbers.

Rotor blade separation experiments were also performed to determine if there was a beneficial or detrimental effect due to multiple rotors operating in close proximity to each other. Tandem rotor tests appeared to be unaffected by tip clearance even at very close rotor spacings (within 10% radius.) Rotors that were in close proximity to one another and were spinning in the same direction had identical performance to rotors that spun in opposite directions. Rotor thrust was only affected when rotors started to overlap as would be expected due to the significant increase in rotor inflow, thus reducing the aerodynamic angle of attack, that would occur on the overlapped portion of the lower rotor. Experiments where all four rotors were operating next to each other in the same configuration as on the micro quad rotor showed a negligible decrease in rotor thrust that would not be expected to have a significant impact on the endurance of the micro quad rotor.

The experiments done on the brushless motor offer a great deal of insight into the design of these motors. Generally designers opt for rotors with higer kv ratings as they operate at higher rotational speeds for a given input voltage. However, for two brushless motors with the same number of poles and stators and only a different wire gauge and coil windings show nearly identical maximum efficiencies. The 4,000 kv rated motor is capable of attaining higher efficiencies at lower rotational speeds than the 7,500 kv motor. The 4,000 kv motor was also determined to operate at a lower power for the same efficiency as the higher rated brushless motor.

Coupled rotor and motor tests showed different results than the single rotor tests. A rotor with 5% cambered airfoil was found to have a higher propulsion system efficiency and electrical power loading than the 7.5% cambered rotor. Also, a rotor with tip taper at 75%

span was also found to have better propulsion system efficiency than a rectangular planform. The operating torque and rpm were then plotted on the motor efficiency curves and it was found that the motor with the lower kv rating would potentially increase the operating efficiency of the motor by 10%. This would also have an effect on the overall propulsion system efficiency and would likely lead to an increase in the overall system efficiency by 10% as well. This method of plotting the rotor operating torque and rpm on the motor efficiency curves could be a beneficial method for selecting a particular motor for use with a specific rotor. It would also be beneficial for rotor design as rotors can now be designed to operate at a particular torque and rpm in an attempt to maximize both their power loading as well as the motor's operating efficiency.

Chapter 5

Conclusions and Future Work

In recent years, micro air vehicles have become a major field of research. This stems from the fact that MAVs can be used for a wide variety of military and civilian applications that can include surveillance, reconnaissance, search and rescue, terrain and environment mapping, perimeter control, etc. The main advantage of these vehicles is their small size, which makes it possible for them to covertly fly into areas that have previously been inaccessible by traditional means of surveillance. Therefore, they are an ideal solution for going inside of buildings, caves, or other confined environments. Because of their small size, low mechanical complexity, and low cost, they are man portable and require little or no infrastructure and can be piloted by an individual or flown autonomously. This makes them more useful and practical than larger UAVs.

There are many types of MAVs that include fixed-wing, rotary-wing, and flapping-wing vehicles. Rotary-wing MAVs tend to be the most practical and useful for most proposed missions because of their hover and low-speed flight capabilities. However, most of the current MAV technology is not mature enough for mass deployment as key technical barriers still needs to be overcome. Many of these barriers stem from the need for compactness and small size and important components such as batteries, motors, and rotors become constrained by size and weight. This usually leads to the lightest or smallest components being chosen for a particular design without providing enough

attention to the efficiencies of these subsystems, which finally determines the endurance of the vehicle. Therefore, most of the challenges in MAV design are issues related to power storage, propulsion system efficiency, performance, and stability and controls.

Many of today's hover capable MAVs (rotary-wing) have very low endurance (less than 10 min) and unless endurance can be increased, their applications will be severely limited. Designing an efficient propulsion system is a major challenge at these scales. The aerodynamic efficiency of rotors is directly linked to airfoil choice, but at the low Reynolds numbers at which these vehicles operate (below 100,000) lift-to-drag ratios are low [30]. Brushless motor technology at these small scales is also restricted and efficiencies are lower than larger industrial brushless motors (say, 20% – 30%). This may be often linked to manufacturing issues and these small motors are often assembled by hand with lower tolerances in coil winding, magnet spacing, and rotor/stator separation, which leads to reduced maximum efficiency (around 60%). These motors are powered by batteries and although new advancements in lithium polymers have increased their energy density, the propulsion system still constitutes a significant portion of the total vehicle mass.

In the current study, the propulsion system for a micro quad rotor was analyzed to address the issues associated with its low endurance. Quad rotors are highly maneuverable and have a high payload capability, and offer good stability characteristics and, therefore, quite suited for many of the missions described above. However, design of their propulsion system is severely lacking. Endurance is compromised by the need for four motors and rotors and the vehicle requires more power.

5.1 Quad Rotor Design

Quad rotors have many applications due to their compact size, high agility, and superior flight stability. The current micro quad rotor was designed to meet the requirements of the Army's MAST CTA and there were constraints on its size and weight. Currently the quad rotor is built using the lightest weight materials, smallest motors, and modified commercial off-the-shelf rotors. The current vehicle uses modified commercial off-the-shelf rotors that are trimmed down to a 34 mm radius. Rotors manufactured using the stereolithography rapid prototyping process has been used on early phases of the development of the vehicle, but the structural properties of this material tend to change over time. The current study has identified the parameters that make the propulsion system more efficient. By utilizing the knowledge gained from this study new rotors can be developed that are specifically designed for use with the motors. The final rotor design can then be manufactured using either a plastic injection molding or CNC milling process instead of using the rapid prototyping process.

5.2 Rotor Analysis

An aerodynamic analysis based upon the blade element momentum theory was coupled with a structural analysis (FEM) in order to predict rotor performance. The BEMT used airfoil table lookup for thin flat and cambered plates because the airfoils at low Reynolds numbers analyzed (below 30,000), do not exhibit linear lift curve slopes. The structural analysis was used to compute blade bending and torsional deformations and to include their effects on thrust and power for the micro rotors. Following are the specific conclusions drawn from the analysis:

1. The combined BEMT and FEM analysis proved to be a viable method for analysis for micro rotors. The analysis was able to capture the effects due to airfoil shape, and planform taper, and provide the correct trends for twist. As was shown for previous studies, cambered plate airfoils offer the best performance at the Reynolds numbers at which the micro rotor operate and airfoils with 7.5% camber had the best performance both in terms of power loading and figure of merit.
2. Lift and drag coefficients are sensitive to Reynolds number and it is, therefore, important to capture these effects. The addition of the airfoil table lookup increased the predictive accuracy of the analysis. The analysis was validated for many cases, and experimental results for airfoil camber and planform taper were correlated. The current airfoil coefficient tables were obtained using CFD studies (because the data within the desired Reynolds number range was lacking.) The analysis shows the potential to accurately predict rotor performance and, therefore, with a more complete set of airfoil tables, preferably obtained through wind tunnel testing, would increase the predictive accuracy of the analysis further.
3. The coupled aeroelastic analysis of the rotor in hover was able to accurately capture the bending and torsion effects on thrust and power for flexible rotors and aided in the design of rotors.

5.3 Single Rotor Tests

An experimental parametric study was conducted to determine how power loading was affected by different rotor designs. The study examined the effects of airfoil shape, maximum camber location, number of blades, leading edge shape, and planform taper

location. These experiments were performed for varying rotational speeds at a fixed pitch as needed for the quad rotor. The following conclusions were drawn from the experimental study:

1. For rectangular rotors with a radius of 34 mm and a chord of 9.4 mm, the optimal collective pitch of the blades occurs at 18 degrees. This allows a significant portion of the blades to operate at their best lift to drag ratio, thus maximizing power loading (thrust/power).
2. The choice of the airfoil has the greatest impact on the performance of the rotor. A flat plate airfoil, has the lowest performance, while a 7.5% cambered plate airfoil has the greatest overall performance. Increasing the camber from 0% to 7.5% increases thrust for a given power and increases the power loading. However, increasing the camber from 7.5% to 9% causes the power to increase more than the increase in thrust and results in a decreased power loading. These results agree with past studies where the optimal camber was found to be between 6% and 9%.
3. Max camber location for small rotors with cambered plate airfoils is usually placed at the mid chord location. The study examined the effects of placing the maximum camber at two other locations – the quarter chord and the three quarter chord. The rotor with the maximum camber located at the mid chord showed slightly better performance than the rotors with maximum camber at other locations. This may be due to favorable pressure recovery due to viscous effects at mid chord.

4. Rotors with different numbers of blades were tested to determine the optimal number of blades at this scale. The rotors with three and four blades had similar power loadings, with the two-bladed rotor exhibiting the best power loading. A single bladed rotor was also tested. However, a single bladed rotor requires a counter mass to balance the rotor. This counter mass does not contribute to the lift but creates sufficient drag causing a decrease in the power loading. A single bladed rotor, although of the lightest weight, would not be a viable option for the micro quad rotor.
5. Previous experimental and CFD studies have shown the benefit of having a sharp leading edge for airfoils at these low Reynolds numbers. The current study examined the effect of a rounded versus sharp leading edge for rotors with 2.5% camber and 9% camber. For both rotors, there was no distinguishable effect on power loading due to leading edge shape.
6. Previous parametric studies on small scale rotors at higher Reynolds numbers have shown that there is a benefit to a 2:1 planform taper starting at 75% – 80% of the blade radius. The current study examined the effects of a 2:1 taper starting at 75%, 50% and over the entire blade span. Two sets of experiments were performed for both varying rpm and varying collective respectively. The experiments utilizing fixed pitch rotors and varying rotational speed did not show a significant effect due to planform taper location. However, the experiments utilizing a fixed rotational speed an varying collective showed a slight decrease in performance for rotors with taper. The reason for these results to differ from past

studies on small scale rotors may be because of the much lower Reynolds numbers at which the present rotors operate.

5.4 Multiple Rotor Interference Effects

No other studies appear to have examined the effects of multiple rotors operating in close proximity to each other such as the case with the micro quad rotor. Analytical studies using free-wake analysis methods have been performed at higher Reynolds numbers, which suggest that there may be a specific rotor separation that results in a benefit to thrust and/or power. The following are conclusions drawn through the experiments on rotors operating in tandem:

1. Rotors on the micro quad rotor helicopter operate in close proximity to each other. Rotors on opposite sides of the quad rotor spin in the same direction, while adjacent rotors rotate in opposing directions. In the experiments, two cases were studied – two rotors spinning in the same direction and two rotors spinning in opposite directions. The study found no decrease in the power loading when the tip clearance between rotors was changed from one radius of clearance to 10% radius clearance for both the cases. Smoke flow visualization studies showed that each rotor has its own independent wake and there was no interaction between two wakes.
2. It is known that when rotors overlap each other, the disk loading on the lower rotor is increased and power loading decreases. The study examined the effect of rotors overlapping by up to 40% of their radius and found that thrust decreased as more of the rotor area was overlapped causing a decrease in power loading.

3. An experiment was performed were all four rotors were configured as they would be on the micro quad rotor. The results from the rotor interaction experiments indicate that there is no significant penalty due to placing the rotors in close proximity. Over the operating range of the rotors, the maximum thrust penalty of 6% of total thrust is only seen when all four rotors are operating in close proximity to each other and there is no distinguishable penalty in power.

5.5 Brushless Motor Experiments

The brushless motors are an equally important part of the propulsion system. Although the rotors actually create the thrust required for the vehicle to hover, the brushless motors need power to overcome the rotor torque to achieve the desired speed. If the motors are operating at a torque and rotational speed that result in poor motor efficiency, then using the most efficient rotors will still result in low vehicle endurance. The brushless motors were characterized using a hysteresis dynamometer that measured the mechanical output power of the motors and a three phase precision power analyzer measured the electrical input to the motor. Efficiency for the brushless motor was then determined at various torque and rpm values. Conclusions from the motor tests follow:

1. Although the brushless motors that were tested had two different *kv* rating, they had an equal number of stators and magnets. The brushless motor with the lower *kv* rating was able to achieve the same torques as the higher *kv* motor and, therefore, did so at a lower input power. However, torque and rpm are directly related to input current and voltage respectively, and so the overall efficiency of

the two motors was the same. The torque at which the maximum efficiency occurred also was the same between the two motors

2. For brushless motors, maximum efficiency is a combination of the torque and rpm. The maximum efficiency decreases as throttle setting is decreased. Generally, the point at which maximum efficiency occurs for any given throttle setting is about 50% of the free rotor speed of the motor.
3. The brushless motors use a pulse width modulated signal sent through a speed controller as a form of throttle setting. The maximum efficiency of the motor only occurs when the motor is running at full throttle. As the throttle setting is decreased, both the torque and rpm at which the max efficiency occurs decreases and maximum efficiency decreases as well.
4. An interesting aspect of the motor's performance was determined where at a particular shaft power, there were two different associated efficiencies. This phenomenon occurs because there are two different combinations of torque and rpm that correspond to a particular shaft power. Maximum efficiency will only occur at a particular torque and rpm for a given input power.

5.6 Coupled Rotor and Motor Tests

The main propulsion system of the micro quad rotor consists of both the rotor and motor. The battery supplies the power and the speed controller regulates the power input to the motor. The efficiency of the speed controller and associated electronics were not considered as they consume relatively little power compared to the motor and rotor. Therefore, rotor and motor were tested together and the propulsion system efficiency was defined as the percentage of electrical input power that was converted to input power at

the rotors. The following are the main conclusions derived from the coupled rotor and motor experiments:

1. Rotor airfoil shape was tested to determine the amount of propulsion system efficiency change. The rotor with the 5% cambered airfoil performed the best and was capable of reaching the maximum propulsion system efficiency of about 37%. This generally occurred at low rotor power loadings which corresponded to the maximum thrust. This result showed that the 5% cambered rotor, although having a lower power loading than the 7.5% cambered rotor, operated at a lower motor power and higher motor efficiency and thus resulted in better propulsion system efficiency.
2. A method for pairing the proper rotor with a particular brushless motor was demonstrated. Using the known torque and rotational speed of the rotor at its operating thrust, the corresponding motor efficiency can be determined from the efficiency curves. This allows the designer to see which motor would be better suited for a particular rotor as well as provides data that can be used in the process of designing the rotors. Therefore, during the process of design, the rotors can be designed to produce a given thrust at specific torque and rpm that corresponds to the motor's best efficiency.
3. The micro quad rotor incorporated the AP03 7,500 *kv* brushless motor. This design choice was based on the misconception that a higher *kv* motor offered better performance over lower *kv* motors. The current study did not find this to be the case and results from brushless motor tests indicate that the AP03 4,000 *kv* motor would be a better design choice for the vehicle as it requires 29% less

power than the current motor for the same torque. The current rotors operate at rotational speeds from 8,000 – 9,000 rpm. This is found to be in a range of very low efficiency for the higher *kv* motors and would be more well suited for the lower *kv* motors.

5.7 Contribution to the State of the Art

There has been a lot of research in rotor design and optimization for MAVs. The BEMT analysis has been used successfully by other researchers for designing rotors for different types of rotary wing MAVs. The current BEMT analysis has been formulated with the addition of a structural analysis with bending and torsion degrees of freedom. This allows for the analysis of flexible rotors and the effects of blade deformation on rotor thrust and power to be determined. However, efforts to increase vehicle endurance through rotor aerodynamics alone has not been entirely successful and the endurance of many of these vehicles is still low (less than 10 min).

Isolated rotor studies were performed that examined airfoil shape, number of blades, leading edge shape, max camber location, and blade taper. Although many of these aspects of rotor design parameters have been previously studied, the experiments showed some results that differ from tests performed at higher Reynolds numbers. It has been generally accepted that using a sharp leading edge on thin cambered plate airfoils at low Reynolds numbers was more beneficial over a blunt or rounded leading edge. However, the current study found that there was little difference between the performance of rotors with a sharp or rounded leading edge in terms of power loading and thus, this has little effect on the efficiency of the system. Previous studies have also shown benefits to

utilizing 2:1 planform taper at the tip of the rotor. The current study found that the addition of taper had no effect when thrust was varied through rpm, like on the quad rotor, and power loading was decreased when thrust was varied through collective.

It was speculated that multiple rotors operating close to each other could lead to significant interference effects, which could be beneficial or detrimental to rotor performance. In the current study, rotor tests were performed for multiple rotors spinning in the same direction as well as opposing directions and it was determined that there was no effect due to rotor spacing. Four rotors were also spun in close proximity to each other as they would on the actual vehicle and the reduction in thrust was only marginal. Therefore, multiple rotors can be spun in close proximity to each other with very little tip clearance and in future iterations of the vehicle design, the rotors can be placed in even closer proximity to each other without having an effect on vehicle endurance or payload capability. This will lead to an even smaller size vehicle and will reduce weight further.

No other study has characterized the brushless motors at this scale or examined the parameters that affect motor efficiency. Measurements of the input voltage, current, output torque, and rpm were taken at a wide range of motor throttle settings in order to determine how efficiency is affected over a variety of operating conditions. Most of the brushless motors at these small scales are assembled by hand and therefore have lower tolerances in magnet spacing, coil winding, or stator/magnet spacing compared to large-scale motors. This leads to reduced maximum efficiencies and can be a major issue in propulsion system design for the micro quad rotor. Therefore, characteristics of these motors became extremely important. It was found that the brushless motors, although having different *kv* ratings, were manufactured with the same number of stators and

magnets but with different gauges of wire and numbers of coil windings. This had no effect on the achievable torque of the motors or their maximum efficiency, but only changed the rotational speed and thus, the input power at which maximum efficiency was attained. The relationship between torque and rpm provides an indication as to the motor's torque producing capability. Torque versus rpm line with a lower slope indicate that the motor is designed for high rotational speeds and low torque while a steep slope indicates that the motor is designed for high torque and low operational speed.

Contribution to the state of the art was further enhanced by coupled testing of the rotor and motor. Measuring the propulsion system efficiency and rotor power loading together allowed for the best rotor and motor combination to be analyzed. The effect of different rotor parameters on the propulsion system efficiency has not been studied before. The rotor's operating torque and rpm can be used to predict what the motor performance will be. The motor efficiency curves can likewise, be used to aide in the design of new rotors and these new rotors can be designed to operate at the motor's best efficiency while still providing margins for maneuvering flight.

5.8 Recommendations for Future Work

There are several areas that further research needs to be performed in order to complete or improve upon the knowledge gained by the present study. The current study focused on identifying the key parameters that mainly affect propulsion system efficiency for a micro quad rotor. The rotors were tested to identify the design features that had the greatest influence on power loading. The most comprehensive of these tests focused on multiple rotor interference effects and the thrust and power changes due to rotor

separation. The motor experiments examined how two motors with the same number of stators and magnets but with different numbers of coil windings affected motor torque, rpm, and efficiency. Coupled rotor and motor tests were also completed to identify rotor parameters that increased propulsion system efficiency. It was seen that parameters that affected rotor power loading do not necessarily result in gains in propulsion system efficiency. Further examination of parameters including twist could expand upon the understanding gained by the present research.

Although the rotor analysis showed good agreement with experiments, further enhancement of the analysis is possible. In order to improve the accuracy of the analysis further, better airfoil tables need to be developed with more data at intermediate Reynolds numbers corresponding to lower rotational speeds at airfoil sections further inboard on the blade. In past studies, these tables have been developed though CFD techniques and it may be more beneficial to create a more sophisticated CFD-CSD analysis for the purposes of rotor design. The aeroelastic analysis could be further enhanced though a better non-linear structural model with the inclusion of the lag and extension degrees of freedom and the inclusion of any couplings to properly model blade deformations.

Although rotor design and optimization has been extensively researched for small rotors at higher Reynolds numbers (around 60,000), some of the results from the present study do not reflect the trends found in earlier studies. The present research found that for rotors at this scale, there was no significant effect due to rotor leading edge shape on its performance. Two dimensional airfoil research has indicated that a sharp leading edge is beneficial while a blunt or rounded leading edge results in flow separation, lower lift, and higher drag. The findings in the current research could be explored in more depth though

the use of simple flow visualization techniques and Particle Image Velocimetry (PIV) to obtain a clear picture of what is happening at the rotor leading edge and the effects of leading edge shape. Taper was also not found to be beneficial where as past research has shown performance benefits with a 2:1 planform taper at the tip. Varying collective and rpm for all the blades tested will provide a clearer picture of how each parameter affects blade performance.

The present research focused on two similar brushless motor designs and identified how throttle setting, torque, and rpm affected the motor's efficiency. A parametric study on motor designs may provide a more comprehensive understanding of the parameters that affect efficiency for motors at this scale. However, the lack of availability of brushless motors at this size would require motors to be made in-house which would be a long and laborious process. The main parameters that could be varied would include number of stators, magnets, coil windings, and wire material. Other parameters that may be more difficult to test would include stator/motor gap, winding style, and different types of ferrous and non ferrous cores. These tests would significantly expand the knowledge base and understanding of how brushless motor efficiency at this scale is affected. This parametric study could then be used to develop mathematical motor models where the various motor parameters discussed above could be used as inputs to predict the motor efficiency at different torques and rpm.

The combined rotor and motor tests examined the same parameters as in the single rotor tests. The parameters that had the greatest effect on power loading were then studied for their effects on propulsion system efficiency. The different rotors' operating torques and rpm were then shown to correlate with the single motor tests and predictions of the

motor's efficiency at the rotor's operating conditions could then be determined. The present study only examined the effects of various designs on propulsion system and motor efficiency, but no specific rotor was developed for use with a particular motor. Future research in this area could use the current analysis and research to develop a comprehensive design tool for the purposes of coupled rotor/motor design by coupling the rotor aeroelastic analysis with the motor model. Such a design tool could use a multi-objective numerical optimizer that would simultaneously attempt to maximize both the rotor power loading and motor efficiency at the rotor's operating thrust. Such a comprehensive analysis would require a more complete set of airfoil tables for the table lookup, as well as an empirical model of the brushless motor so that estimates of the efficiency based upon the torque and rpm could be determined.

To thoroughly examine the propulsion system, other factors need to be considered that include battery, speed controller, and associated electronics. In this study, the two main components that have the greatest effect on efficiency – the rotor and the motor, were considered. However, characterization of the power output from different types of lithium-ion, lithium-polymer, and other batteries could be used to determine the type of batteries that would perform the best under the quad rotors operating conditions. Characterization of different speed controllers would also provide information on the efficiency of different types of speed controllers from different manufactures. Thus, to properly examine the propulsion system for the entire vehicle, every aspect from the batteries to the rotors must systematically be examined to determine the most efficiency propulsion system.

Bibliography

[1] McMichael, J. M., and C. M. S. Francis USAF (Ret.). "Micro Air Vehicles Towards a New Dimension in Flight." *U.S. Department of Defense Weapons Systems Technology Information Analysis Center (WSTIAC) Newsletter* 1, No. 13 (June-July 2000). *Http://www.darpa.mil/tto/MAV/mav Auvsi.html*. 7 Aug. 1997. Web.

[2] Pereira, Jason L. *Hover and Wind-Tunnel Testing of Shrouded Rotors for Improved Micro Air Vehicle Design*. Thesis. University of Maryland, College Park, 2008. *Digital Repository at the University of Maryland*. Feb. 2011.

[3] Pines, D. J., and F. Bohorquez. "Challenges Facing Future Micro-air-vehicle Development." *Journal of Aircraft* 43.2 (2006): 290-305. *AIAA Electronic Library*. Web. May 2011.

[4] "Unmanned Aircraft Systems." *AeroVironment, Inc. (AV) : Unmanned Aircraft Systems, Electric Vehicle Charging Systems, Power Cycling & Test Systems*. AeroVironment, Inc, 2011. Web. Jan. 2011. <http://www.avinc.com/>.

[5] Felipe Bohorquez, Darryll Pines, and Paul D. Samuel, *Small Rotor Design Optimization Using Blade Element Momentum Theory and Hover Tests*, Journal of Aircraft, Vol. 47, No. 1, pp. 268-283, 2010

[6] Hrishikeshavan, Vikram, and Inderjit Chopra. *Performance and Rotor-Based Control of a Shrouded Rotor MAV in Edgewise Flow*. Proc. of American Helicopter Society' Specialists' Meeting on Unmanned Rotorcraft and Network Centric Operations, Phoenix, AZ. AHS International, Jan 2011. Print.

[7] Benedict, Moble. *Fundamental Understanding of the Cycloidal-rotor Concept for Micro Air Vehicle Applications*. Thesis. University of Maryland, College Park, 2010. *Digital Repository at the University of Maryland*. Web. Feb. 2011.

[8] Chopra, Inderjit. *"Hovering Micro Air Vehicles: Challenges and Opportunities*. Proc. of AHS International Meeting on Advanced Rotorcraft Technology and Safety Operations (HeliJapan), Ohmiya, Japan. Nov. 2010. Print.

[9] Nice, Erik B. *Design of a Four Rotor Hovering Vehicle*. Thesis. Cornell University,, 2004. Print.

[10] Schmitz, F. W. *Aerodynamics of Model Aircraft Wing Measurements I*. Rep. Issued by Ministry of Aircraft Production, 1983. Print. R.T.P. Translation No 2460.

[11] Laitone, E. V. "Wind Tunnel Tests of Wings at Reynolds Numbers below 70 000." *Experiments in Fluids* 23.5 (1997): 405-09. Print.

[12] Bohorquez, Felipe. *Rotor Hover Performance and System Design of an Efficient Coaxial Rotary Wing Micro Air Vehicle*. Thesis. University of Maryland, College Park, 2007. *Digital Repository at the University of Maryland*. Web. Aug. 2010.

[13] Bawek, Dean, and Inderjit Chopra. *Design, Control, and Performance Verification of a Quadrotor MAV*. Proc. of American Helicopter Society' Specialists' Meeting on Unmanned Rotorcraft and Network Centric Operations, Phoenix, AZ. AHS International, Jan 2011. Print.

[14] Friedman, Chen, and Inderjit Chopra. *Towards Obstacle Avoidance and Autonomous UAV Operation*. Proc. of AHS International Meeting on Advanced Rotorcraft Technology and Safety Operations (HeliJapan), Phoenix, AZ. AHS International, Jan 2011. Print.

[15] United States of America. Army Research Laboratory. *Micro Autonomous Systems and Technology (MAST) Collaborative Technology Alliance (CTA) Final Program Announcement (PA)*. By Joseph Mait. 1 Sep. 2006. Print. W911NF-06-R-0006.

[16] Samuel, Paul. "Daedalus Flight Systems, LLC." *DFS*. 2010. Web. Sept. 2010. <http://daedalusflightsystems.com/>.

[17] C.Gencer, and M. Gedikpinar. "Modeling and Simulation of BLDCM Using MATLAB/SIMULINK." *Journal of Applied Sciences* 6.3 (2006): 688-91. Print.

[18] Miller, D., G. Gremillion, B. Ranganthan, J. S. Humbert, P. Samuel, S. Zarovy, M. Costello, and A. Mehta. *Challenges Present in the Development and Stabilization of a Micro Quadrotor Helicopter*. Proc. of Presented at the Institute of Navigation GNC Challenges for Miniature Autonomous Systems Workshop. October 2010. Print.

[19] Bouabdallah, S., P. Pierpaolo, R. Siegwart. *Design and Control of an Indoor Micro Quadrotor*. Proc. of IEEE International Conference on Robotics and Automation, 2004.

[20] Mehta, A., and K. Pister. *WARPWING: A Complete Open Source Control Platform for Miniature Robots*. Proc. of Presented at the IEEE/RSJ International Conference on Intelligent Robots and Systems, Taipei, Taiwan. October 2010. Print.

[21] Pillay, Pragasen, and Ramu Krishnan. "Modeling, Simulation, and Analysis of Permanent-Magnet Motor Drives, Part II: The Brushless DC Motor Drive." *IEEE Transactions of Industry Applications* 25.2 (1989): 274-79. Print.

[22] Mueller, Thomas J. "Development and Operation of UAVs for Military and Civil Applications." *Aerodynamic Measurements at Low Reynolds Numbers for Fixed Wing Micro-Air Vehicles*. Proc. of RTO AVT Course, Rhode-Saint-Genese, Belgium. RTO EN-9, 1999.

[23] Sun, Quanhua, and Iain D. Boyd. “Flat-plate aerodynamics at very low Reynolds number.” *Journal of Fluid Mechanics* 502 (1999): 199-206.

[24] "3D Printing and Rapid Prototyping." *Objet Geometries Ltd*. 2011. Web. <http://www.objet.com/>.

[25] Leishman, J. Gordon. *Principles of Helicopter Aerodynamics*. Cambridge: Cambridge UP, 2006.

[26] Harrington, Robert D. *Full-Scale-Tunnel Investigation of the Static-Thrust Performance of a Coaxial Helicopter Rotor*. Tech. no. 2318. Langley, VA: National Advisory Committee for Aeronautics, 1951.

[27] Meirovitch, Leonard. *Fundamentals of Vibrations*. Long Grove, IL: Waveland, 2010.

[28] Griffiths, Daniel A., and J. Gordon Leishman. *A Study of Dual-Rotor Interference and Ground Effect Using a Free-Vortex Wake Model*. Proc. of 58th Annual Forum of the American Helicopter Society, Montreal, Canada. American Helicopter Society, 2002.

[29] Lakshminarayan, Vinod K. *Computational Investigation of Micro-Scale Coaxial Rotor Aerodynamics in Hover*. Thesis. University of Maryland, 2009. College Park

[30] Schroeder, Eric J., and James D. Baeder. *Using Computational Fluid Dynamics for Micro-Air Vehicle Airfoil Validation and Prediction.* Proc. of 23rd AIAA Applied Aerodynamics Conference, Toronto, Ontario Canada. American Institute of Aeronautics and Astronautics, Inc, June 2005.